Evidence within Sediment of Historical Cyanobacterial Blooms on the Southwestern Shores of Lake Superior in Wisconsin, USA

A Thesis

SUBMITTED TO THE FACULTY OF THE UNIVERSITY

OF MINNESOTA

BY

Jordan Taylor Bremer

IN PARTIAL FULFILLMENT OF THE REQUIREMENTS FOR THE DEGREE OF

MASTER OF SCIENCE

Dr. Kathryn M. Schreiner, Dr. Byron A. Steinman

2024

Acknowledgements

I would like to express my sincere, heartfelt gratitude to the following individuals who have played a crucial role in the completion of this thesis:

Advisors: My primary advisor, Dr. Kathryn M. Schreiner, and my co-advisor, Dr. Byron A. Steinman, for their insightful input and expertise, invaluable guidance, support, and encouragement throughout this journey.

Committee Members: Dr. Kathryn M. Schreiner, Dr. Byron A. Steinman, Dr. Robert W. Sterner, and Dr. Melissa A. Mauer-Jones for their constructive feedback and thoughtful contributions that enriched the quality of this work.

UMN-Duluth Chemistry Department: The collective support and resources provided by the entire UMN-Duluth chemistry department, especially Carrie Misuraco, Jennifer Johnson, Bonnie Christensen, and Steve Berry, have been instrumental in the success of this research. Faculty such as Dr. Luke Busta and Dr. Jacob Wainman, have personally made an impact on my career here at UMN-Duluth.

Funding: This research was made possible through the generous support of the USGS - NECASC. Their financial assistance has been instrumental in carrying out the experiments and analyses essential to this thesis.

Field and Laboratory Assistance: Special thanks to Julia Agnich, Neil Weberg, Dr. Robert Brown, Dr. Ted Ozersky (UMN-Duluth) and Dr. Joseph Carlin (CSU-Fullerton) for their valuable insights and advice, which significantly contributed to the development and refinement of this work.

Graduate Students: I want to acknowledge the contributions of fellow graduate students who have generously shared their expertise and time. In particular, Emma C. MacNeill, Erin E. Bergen, Payton K. Kittaka, Jake D. Zunker, Andy P. Kasun, Reane N. Loiselle, Shannon Christiansen and Bennett Hanson have been instrumental in various aspects of this research.

Undergraduate Assistant: I extend my appreciation to Lily Karg for her dedication and hard work in assisting with the practical aspects of this project. Her enthusiasm and commitment have been truly commendable.

Support System: A special mention goes to my therapists, Dr. Donald C. Mattson and Dr. Ian T. White; my friends, Nathan J. Castetter, Jacob M. Miner, Christopher J. Cerny, and Juuso I. N. Mittentag-Helviö; the Mittentag Clan, the Bergen family, and my own family. Their unwavering support and guidance have been the cornerstone of my resilience and determination.

I extend my heartfelt thanks to each and every individual mentioned above. Your contributions have made a lasting impact on this thesis and, by extension, on my academic and personal growth.

Dedications

Dear Lily,

In the world of academia, some friendships are forged in the *crucible* of shared dreams, struggles, and aspirations. Though you have seen me as your “Fearless Leader,” you, my “Faithful Undergrad,” have walked beside me in this journey of academic pursuit and have been quite the guiding star at times. Your unwavering support, encouragement, and friendship have been an *anchor* (a bag of rocks) during the challenging voyage of completing this thesis.

Together, we explored uncharted *sediments*, delved deep into the realms of knowledge and unfamiliarity, and yet you stood by me through it all. The very long lab days and nights, the endless data analyses, and the many, many moments of uncertainty. Your belief in my abilities and your willingness to lend an empathetic ear turned my academic struggles into shared triumphs.

This thesis is not only a testament of my dedication to the subject, but also a *biomarker* of the hardships and resulting *bond* we share because of it. This thesis bears **your** fingerprints, your *pigments*. Your wisdom, patience, and camaraderie have made this journey not only bearable but also memorable.

As I embark on this new chapter in my life, I want to express my profound gratitude to you, Lily. Your friendship has been a source of strength and a constant reminder of the importance of community and collaboration in the pursuit of knowledge. So, no matter where life takes you, just remember I will always be a *QC* to your *QA*. I hope that one day our paths will cross again, so until then, I will *cyano* you later.

With heartfelt appreciation,
Jordan

Abstract

Reconstruction of historical environments and phytoplankton communities, specifically past cyanobacteria blooms prior to their first recorded appearances within the southwestern region of Lake Superior, was accomplished through investigating elemental and biomarker compositions preserved within sediment cores of Siskiwit Bay, Wisconsin, USA. Carotenoids and other phytoplankton pigments, paleo-tracers of algal and bacterial communities, were measured using high-performance liquid-chromatography. To further investigate the origin of organic matter, particularly for algal inputs, stable isotope carbon-13 abundances, carbon and nitrogen content were measured via elemental analysis isotope ratio mass spectroscopy. Radiocarbon dating and gamma spectroscopy were utilized to reconstruct the historical environment as far back as 5,400 years prior to 2021. Loss-on-ignition and X-ray fluorescence analyses were employed to generate lithological and geochemical core profiles by measuring the composition of elements and organic matter. Along with visual identification, these analyses identified sand layers at 1,205 to 2,270 calendar years before present (cal year BP), and 2,560 to 3,490 cal year BP. Cyanobacterial-associated pigment concentrations were in high concentrations around 10 cal year BP, representing the cyanobacterial bloom seen in 2012, and 470 cal year BP, an uncharted record. Diatom-indicating pigments have been in higher concentrations compared to cyanobacteria-indicating pigments since 170 cal year BP, consistent with the fact that diatoms are a dominant phytoplankton group in Lake Superior. Between 192 and 786 cal year BP, shifting pigment concentrations are indicative of a transitional period between cyanobacteria and diatoms. Prior to 790 cal year BP, phytoplankton pigments point to a cyanobacteria-dominated environment.

Keywords: Cyanobacteria, Phytoplankton Pigment Biomarkers, Carotenoids, High-Performance Liquid-Chromatography, Radiocarbon Dating, Gamma Spectroscopy, X-Ray Fluorescence, Loss-on-Ignition, Elemental Analysis Isotope Ratio Mass Spectroscopy

Table of Contents

Acknowledgements i
Dedications ii
Abstract iii
List of Tables vi
List of Figures vi
List of Equations vi
Chapter 1. Introduction and Background 1
1.1 Cyanobacteria in Lake Superior 1
1.2 Cyanobacteria 3
1.3 Sedimentary Elemental Composition and Stable Isotopes 8
1.4 Carotenoid Pigments 10
1.4.1 Introduction 10
1.4.2 Functionality 11
1.4.3 Carotenoids in Sediment 15
1.4.4 Application of Analytical Methods 17
1.5 Geochronology 17
1.6 Mineralogical Sediment Tracers 25
1.7 Study Sites 26
1.8 Goals and Hypotheses 28
Chapter 2. Historical Cyanobacterial Blooms in Siskiwit Bay - Lake Superior, Wisconsin, USA 31
2.1 Introduction and Background 31
2.2 Methods 34
2.2.1 Site Description 34
2.2.2 Sample Collection 34
2.2.3 Sample Processing 36
2.2.4 Bulk Density 37
2.2.5 Bulk Element and Isotope Analysis 38
2.2.6 Loss on Ignition 39
2.2.7 Geochronology 39
2.2.8 Pigment Analysis 41
2.2.9 X-Ray Fluorescence Analysis 42

2.3 Results ... 44
2.3.1 Sediment Age and Depositional Rates ... 44
2.3.2 Elemental Composition ... 45
2.3.3 Siskiwit Lake Bloom Phytoplankton Pigment Content ... 54
2.3.4 Siskiwit Bay Bloom Phytoplankton Pigment Content ... 56
2.3.5 Mineral Elemental Content ... 66
2.4 Discussion ... 69
2.4.1 Overall Trends ... 69
2.4.2 Unit A (3,490 to 5,400 cal year BP) ... 71
2.4.3 Unit B (1,200 to 3,490 cal year BP) ... 72
2.4.4 Unit C (2021 to 1,205 cal year BP) ... 74
2.5 Conclusions ... 76
Chapter 3. Appendix ... 78
3.1 The Organic Geochemical Record of Siskiwit Lake, Wisconsin, USA ... 78
3.1.1 Sample Collection ... 78
3.1.2 Sample Processing ... 78
3.1.3 Bulk Element and Isotope Analysis ... 79
3.1.4 Results ... 80
3.1.5 Discussion and Conclusion ... 81
3.2 Supplementary Data ... 86
3.2.1 Sample Collection ... 86
3.2.2 Phytoplankton Pigments Standard Curves ... 87
3.2.3 Siskiwit Bay Phytoplankton Pigments ... 88
3.3 Standard Operating Procedures ... 91
3.3.1 Sediment Core Sampling ... 91
3.3.2 Sediment Core Extrusion ... 93
3.3.3 Freeze-drying Sediment ... 94
3.3.4 Loss on Ignition (LOI) ... 95
3.3.5 Fumigation (for EA-IRMS Analysis) ... 98
3.3.6 Sample Preparation for EA-IRMS Analysis ... 100
3.3.7 Pigment Extraction from Sediment ... 101
3.3.8 HPLC and Analysis ... 103
References ... 107

List of Tables

Table 1. Studied phytoplankton pigments. 20
Table 2. Sample collection information. 35
Table 3. Carbon and Nitrogen EA-IRMS Standards. 39
Table 4. Phytoplankton pigments of Siskiwit Lake cyanobacterial bloom 43
Table 5. Siskiwit Bay linear sediment accumulation rates 45
Table 6. Phytoplankton pigment contributions of Siskiwit Lake bloom 51
Table 7. Detailed information of each sediment core 86

List of Figures

Figure 1. Study site locations 2
Figure 2. Microscopy images of microalgae samples from 2021 Siskiwit Lake bloom.....3
Figure 3. Diagram of diatoms 7
Figure 4. Primary sources of organic material 10
Figure 5. Chlorophyll-a, -b, and carotenoids absorbance spectra 12
Figure 6. Water sampling locations on Siskiwit Lake 36
Figure 7. Siskiwit Bay sediment core age model 47
Figure 8. Carbon and Nitrogen content of Siskiwit Bay 48
Figure 9. Primary source of organic matter of Siskiwit Bay sediment 49
Figure 10. Siskiwit Bay stratigraphic column 52
Figure 11. Siskiwit Bay sediment and mass accumulation rates 53
Figure 12. Pigment concentrations from the Siskiwit Lake cyanobacterial bloom 54
Figure 13. Siskiwit Bay individual phytoplankton pigments (µg/gOC) 61
Figure 14. Siskiwit Bay phytoplankton pigments by source types 62
Figure 15. Summary of Siskiwit Bay phytoplankton pigments by section 63
Figure 16. Pigment peaks in upper layers of the Siskiwit Bay sediment core 64
Figure 17. Pigment accumulation rates within the Siskiwit Bay sediment core..........65
Figure 18. Siskiwit Bay residual minerogenic content and elemental data 67
Figure 19. Siskiwit Bay elemental ratios from XRF 68
Figure 20. Sediment core sampling location on Siskiwit Lake. 79
Figure 21. Carbon and Nitrogen content of Siskiwit Lake 83
Figure 22. Primary source of organic matter of Siskiwit Lake 84
Figure 23. Phytoplankton pigment standard individual concentration curves 87
Figure 24. Siskiwit Bay individual phytoplankton pigments (ng/g Dry sediment) 90

List of Equations

Equation 1. Bulk Density 38
Equation 2. Stable Carbon Isotope Values 38

Chapter 1. Introduction and Background

1.1 Cyanobacteria in Lake Superior

On July 14th and 15th, 2012, for the first time in recorded history, a mass of thick, floating algae was observed along the shorelines west of the Wisconsin Apostle Islands in Lake Superior (Sterner et al., 2020; Figure 1). This bloom was an accumulation of cyanobacterial biomass, formed through growth, migration, and physical-chemical processes such as residence times, mixing, temperature, pH, nutrient inputs, salinity, and trace metal content (Paerl, 1996; Tromas et al., 2017). Cyanobacteria, the first organisms known to have produced oxygen and found in almost every type of aquatic system (Whitton and Potts, 2012), are a large and diverse phylum of photoautotrophic prokaryotes that have unique combinations and concentrations of specific pigments. Some cyanobacteria species, under certain conditions, will reproduce quickly to bloom-sized levels and produce toxins which are dangerous to animals and humans, causing liver, digestive, and neurological diseases when ingested (Huisman et al., 2018; Sterner et al., 2020). These blooms are known as harmful algal blooms (HABs). During the 2012 bloom, the National Park Service (NPS) took water samples and identified the dominant algal taxon *Dolichospermum lemmermannii* (formerly, *Anabaena lemmermannii*) (Figure 2; Sterner et al., 2020), with zero toxins found or measured. Similar blooms of the same dominant taxon subsequently occurred every year since 2016 (Sterner et al., 2020; Lafrancois & Reinl, 2024). Though this was the first record of such a large bloom occurring in Lake Superior, throughout the other Great Lakes cyanobacterial blooms are much more common (Conroy et al., 2014; Kane et al., 2014; Paerl, 2017; McKindles et al., 2020).

Certain cyanobacteria species are known to be always toxic, and some species may only be toxic in the correct circumstances. Types of cyanobacteria that produce toxins are *Microcystis aeruginosa, Dolichospermum circinalis, Dolichospermum flos-aquae, Aphanizomenon flos-aquae,* and *Cylindrospermopsis raciborskii* (Perri et al., 2015; Huisman et al., 2018). In Lake Superior, toxicity measurements of the cyanobacterial blooms to date have indicated the presence of one potentially toxic substance (Anabaenopeptin A) at a very low concentration (Sterner et al., 2020).

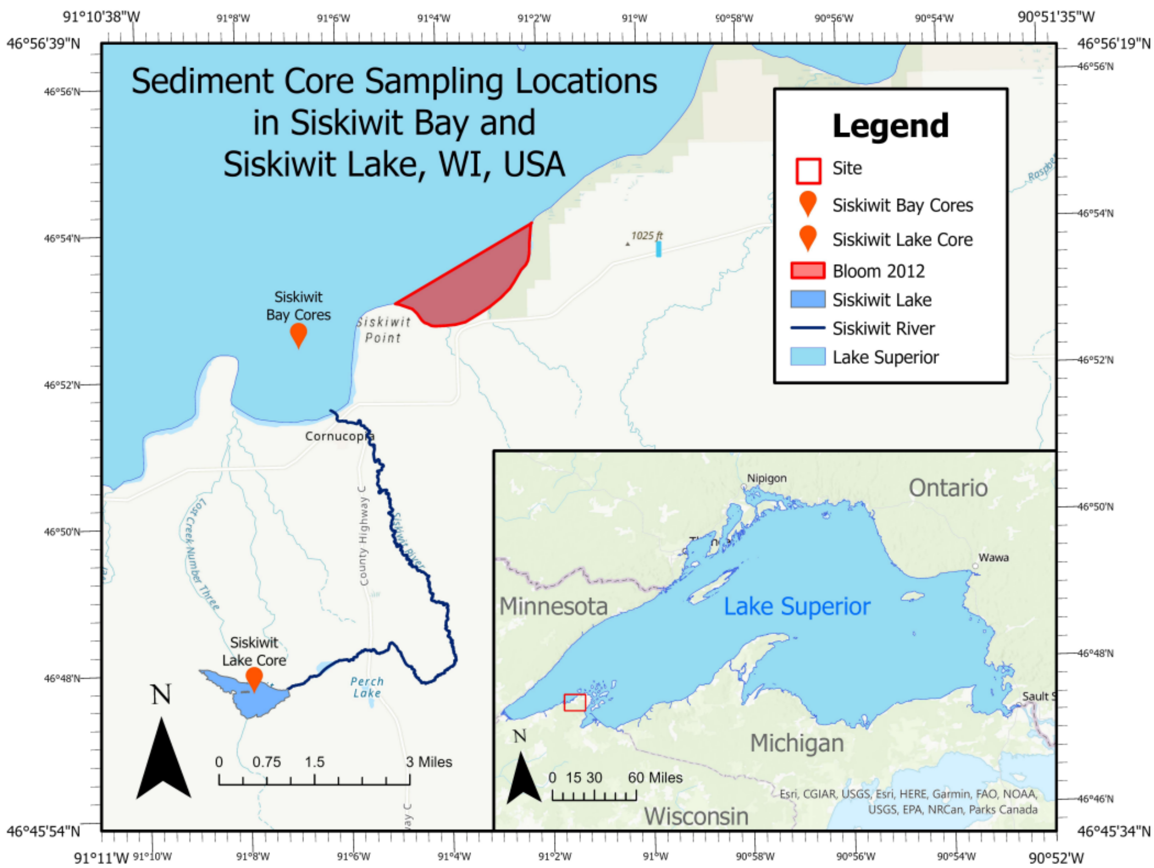

Figure 1. ***Study site locations.*** *The southern shoreline of Lake Superior at Cornucopia, Wisconsin, USA. Orange pinpoints and corresponding labels show the study areas. The red-shaded area indicates the location of the first recorded cyanobacteria bloom (2012). Siskiwit Bay's hydrologic connection to Siskiwit Lake, a potential source of cyanobacteria to Lake Superior, is highlighted in dark blue (Siskiwit River).*

From the first recording of cyanobacterial blooms in 2012, questions have been raised about whether these are new occurrences and what may be influencing the size and frequency of these blooms. While in Lake Erie large toxic cyanobacterial blooms are known to be driven by phosphorus inputs from the agricultural Maumee basin (Kane et al., 2014), Lake Superior's watershed contains minimal agricultural activity, so cyanobacterial blooms are likely not caused by anthropogenic nutrient inputs (National Oceanic and Atmospheric Administration (NOAA), 2010).

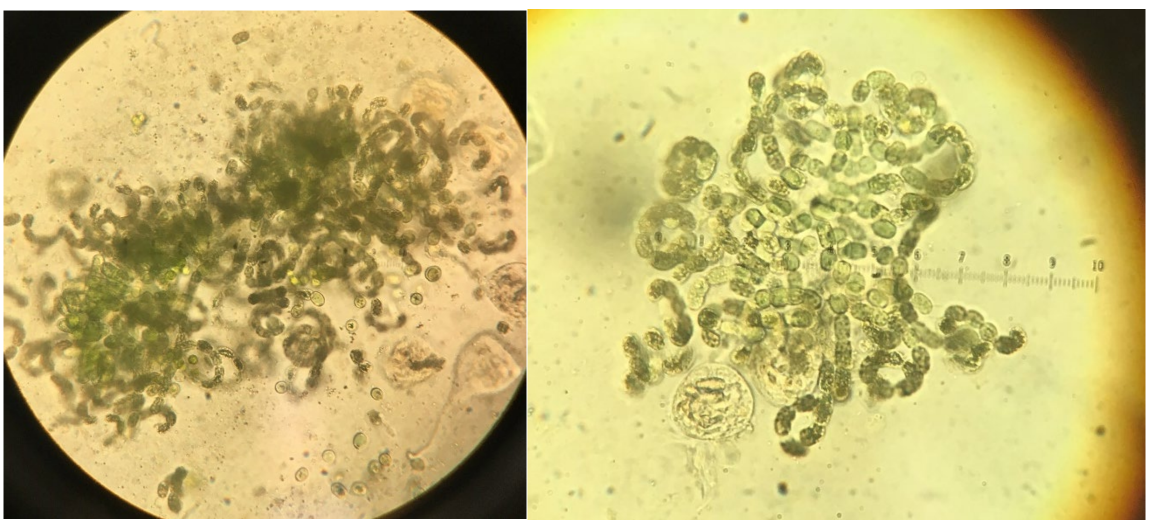

Figure 2. *Microscopy images of microalgae samples taken from the surface water of the 2021 Siskiwit Lake bloom. Microscopic examination suggested the samples belonged to the Dolichospermum genus; likely D. circinale or D. lemmermannii, the latter of which has previously been identified in Lake Superior blooms. Images provided by Kaela Natwora and Cody Sheik of the Large Lakes Observatory.*

1.2 Cyanobacteria

Cyanobacteria are oxygen-producing bacteria that can form dense and sometimes toxic blooms in freshwater and marine environments (Huisman et al., 2018). Large blooms, even if they do not produce toxins, can threaten ecosystem functioning and degrade water quality for recreation, drinking water, fisheries, and human health. Depending on the size of the bloom, photosynthesis of aquatic plants within the water body can be hindered by lack of sunlight. This in turn affects fish and other aquatic species that feed on these plants by decreasing the amount of available vegetation to eat. Additionally, these blooms can further affect the freshwater environment when they decompose, depleting oxygen in the water column through microbial degradation, causing fish and invertebrate die-off (Huisman et al., 2018). Particular cyanobacterial species can produce a deterring taste, odor, and thick scum on the surface of a water body, which can ultimately interfere with the recreational function of lakes and the use of reservoirs for drinking water.

Additionally, as water temperature increases, it will absorb less oxygen thus lowering oxygen concentration in the water column and create anoxic or hypoxic zones. Cyanobacterial communities can adapt to anoxic and hypoxic zones more readily than competing diatom communities, allowing them to reproduce and dominate the habitat (Panigrahi et al., 2013). So, as temperatures are projected to increase 2.1-4.0°C for the Great Lakes Basin by 2040-2069 (Zhang et al., 2020), cyanobacterial communities are as well. Furthermore, with the predicted increase in precipitation of up to 16.5% by 2040-2069 (Zhang et al., 2020), the water column organic matter and nutrient content will be directly increased, stimulating respiration, and reducing oxygen concentrations further (Panigrahi et al., 2013).

Some of the common cyanobacterial bloom-forming genera include *Aphanizomenon*, *Cylindrospermopsis*, *Dolichospermum*, *Microcystis*, *Nodularia*, *Planktothrix* and *Trichodesmium* (Huisman et al., 2018). For this study, *Dolichospermum* and *Microcystis* will be specifically targeted because of their previous and frequent observed presence within the Great Lakes (Conroy et al., 2014; Hobbs et al., 2021; Reinl et al., 2020; Salmaso et al., 2015; Sheik et al., 2022; Sterner et al., 2020). *Dolichospermum lemmermannii* was identified as the most abundant phytoplankton species in the 2016, 2017, and 2018 blooms (Reinl et al., 2020; Sheik et al., 2022; Sterner et al., 2020), while one of the most dominant cyanobacteria in the Great Lakes region is *Microcystis* (Conroy et al., 2014).

Dominant cyanobacteria genera in a bloom are controlled by the synergistic effects of nutrient supplies, light, temperature, water residence times, and biotic or food chain interactions (Paerl, 2017). Driven by nutrient over-enrichment, anthropogenically caused hydrologic modifications, and global climate change, cyanobacteria blooms have surged in biomass production and accumulation in Lake Superior (Reinl et al., 2020; Sheik et al., 2022; Sterner et al., 2020). Though, some have found that bloom magnitude, severity, and duration in inland waterbodies, defined by trends in chlorophyll-a, have not been widespread for hundreds of lakes in the US (Wilkinson et al., 2022). Near the southern shore of Lake Superior, the increased occurrence of cyanobacterial blooms is theorized to be due to enhanced nutrient loading from the surrounding watersheds and the warming climate (Sterner et al., 2020). Lake Superior has had documented increases in water temperature of about 2-3°C since 1973 (Austin and Colman, 2007; O'Reilly et al., 2015; Van Cleave et al., 2014), which promotes growth by lengthening the duration of the bloom season (Huisman et al., 2018; Paerl, 2017; Rigosi et al., 2014).

Lake Superior, due to its cold temperatures and low nutrient concentrations, has historically been dominated by diatom communities (Munawar and Munawar, 1978; Reavie et al., 2014).Diatoms are divided into two groups that differ by shape of the siliceous portions of their cell walls, or frustules: centric diatoms have cells that are radially symmetric while pennate diatoms exhibit bilateral symmetry (Figure 3). Diatoms are considered a high-quality food for benthic primary consumers, while cyanobacteria are thought to be a lower-quality food because of their lower nutritional value to zooplankton and benthic filter feeders (Basen et al., 2011, 2012, 2013; Hedberg et al., 2021; Pillsbury et al., 2021). Therefore, a shift to more cyanobacteria-dominated primary producers can cause significant ecological changes, including alterations to benthic species composition and production. Climate change and eutrophication, which have both been recorded in Lake Superior (Baustian et al., 2020; O'Beirne et al., 2017; O'Reilly et al., 2015; Zhang et al., 2020), reduce diatom growth and promote cyanobacterial growth (Huisman et al., 2018; Paerl, 2017; Rigosi et al., 2014; Hedberg et al., 2021). With a larger cyanobacterial population, this leads to enhanced benthic bacterial production and oxygen depletion within the water column (Andersson et al., 2015).

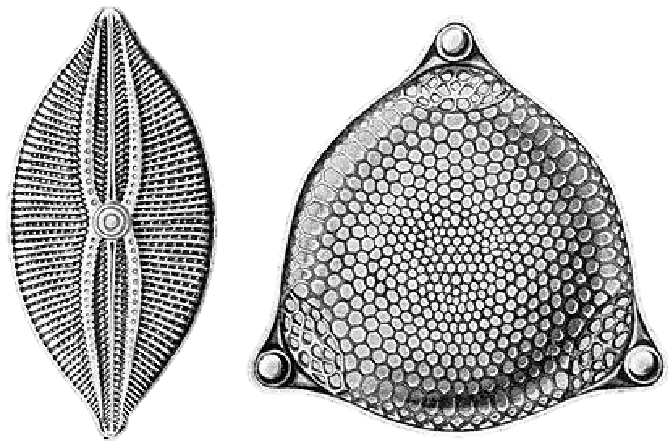

Figure 3. Diagram of diatoms. *Selections from Ernst Haeckel's 1904 Kunstformen der Natur, showing pennate (left) and centric (right) frustules.*

Aside from cyanobacteria, there are other types of phytoplankton commonly found in the Lake Superior Wisconsin shoreline. The phytoplankton community composition is predominated by Bacillariophyta (multiple genera; pennate and centric diatoms) and Cryptophyta (principally *Komma*; algae). The nearshore community includes Chrysophyta (principally *Dinobyron*; golden algae), Chlorophyta (principally *Golenkinia*; green algae) and lesser amounts of Euglenophyta (principally *Strombomonas*; unicellular flagellates) (Munawar and Munawar, 1978; Reavie et al., 2014; Sterner et al., 2020). Picocyanobacteria (0.2 to 2 μm), which are common throughout freshwater, brackish, and marine environments (Fahnenstiel et al., 1986) and are present in great abundance in Lake Superior (Fahnenstiel et al., 1986; Sterner 2010). Comparatively, in Lake Erie the phytoplankton communities are composed of centric diatoms in the spring, until the summer season when cyanobacteria dominate. In Lake Michigan and Lake Huron, centric diatoms, pennate diatoms, and chrysophytes make up most of the phytoplankton community (Reavie et al., 2014).

1.3 Sedimentary Elemental Composition and Stable Isotopes

In the benthic zone of water bodies, sediments consist of mineral grains, plant and animal remains, and other types of organic matter. Benthic zones, or the floor of the lake, are composed of accumulated sunken organic matter, while littoral zones, or the area bordering the shore, has more light penetration and hence more thriving aquatic plants (The Nature Conservancy, 2005). Thus, sediment composition is highly dependent on the location and surrounding environment, making it a historical archive of events through time (Schnurrenberger et al., 2003).

The analysis of bulk elemental characteristics of organic matter can provide insights on the general composition and source of the organic matter within aquatic sediments (Meyers, 1994; Bianchi et al., 2011). Due to the distinctive differences in chemical makeup of terrestrial plants and aquatic plants, the atomic carbon-to-nitrogen (C:N) molar ratios of the organic matter in sediments can provide insight on terrestrial or aquatic sourcing. Terrestrial plants produce carbon-rich biopolymers for structural support, which results in a higher C:N molar ratio (Meyers and Ishiwatari, 1993). Algae have C:N ratios between 4 and 10, while vascular land plants have C:N ratios of greater than or equal to 20 (Meyers, 1994).

To further investigate the origin of organic matter, particularly for algal inputs, stable isotope carbon-13 ($\delta^{13}C$) abundances can be paired with C:N molar ratios to better differentiate between sources. While the C:N ratio distinguishes between algae and land plants, the addition of $\delta^{13}C$ can assist in differentiating between the types within those categories (Prahl et al., 1980; Meyers, 1994; Meyers and Ishiwatari, 1993; Figure 4). Terrestrial plants using the C3 Calvin-Benson photosynthetic pathway produce organic matter with depleted $\delta^{13}C$ signatures ranging between -16 to -25‰ (Meyers and Ishiwatari, 1993). In comparison, terrestrial plants using the C4 Hatch-Slack photosynthetic pathways produce more enriched $\delta^{13}C$ signatures ranging from -2 to -12‰ (Meyers and Ishiwatari, 1993).

To generally determine organic matter and carbonate content within sediments, Loss on Ignition (LOI; Bengtsson & Enell, 1986; Dean, 1974; Heiri et al., 2001; Santisteban et al., 2004) can be applied. Organic matter is oxidized to carbon dioxide and ash at temperatures between ~200 and 550ºC. Further evolution of carbon dioxide from carbonate mineral forms occurs at temperatures between approximately 900-1,000°C. Weight losses associated with water and carbon dioxide evolutions may be correlated to water content, and organic matter and carbonate content (Bengtsson & Enell, 1986; Dean, 1974; Heiri et al., 2001; Rosenmeier, 2005; Santisteban et al., 2004).

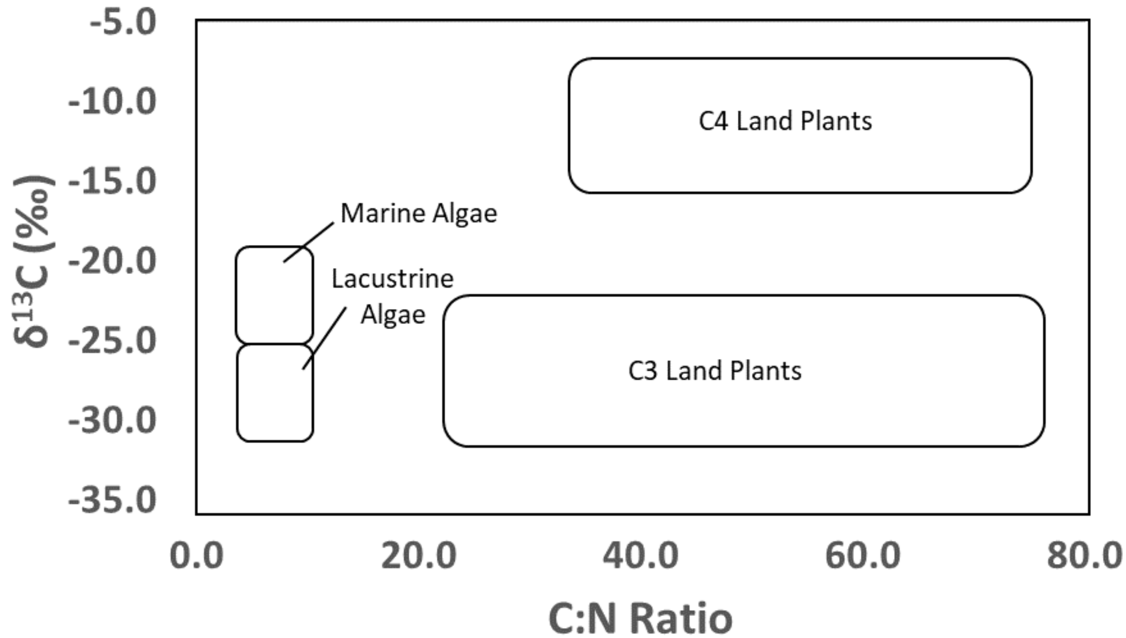

Figure 4. *Carbon to nitrogen (mol to mol) ratios together with stable isotope ($\delta^{13}C$) values can distinctively identify primary sources of organic material in the core location, ranging from C4 land plants, C3 land plants, marine algae, and lacustrine algae. Adapted from Meyers, 1994.*

1.4 Carotenoid Pigments

1.4.1 Introduction

Carotenoid pigments can be used as biomarkers to determine past phytoplankton community as well as the environmental conditions surrounding these organisms, such as over-stimulation of UV radiation. Carotenoid pigments are synthesized by all photosynthetic organisms as well as several non-photosynthetic bacteria and fungi (Egeland, 2016), and make up the largest class of naturally occurring pigments, with more than 750 natural carotenoids identified to date (Egeland, 2016; Hirschberg and Chamovitz, 1994). Carotenoids are generally hydrophobic isoprenoid compounds that are synthesized and accumulated in protein complexes within the photosynthetic membrane, and because of their hydrophobic nature, their bioavailability can be limited (X. Chen et al., 2021; Hirschberg and Chamovitz, 1994). Most carotenoids are composed of a C_{40} hydrocarbon backbone made from eight C_5 isoprenoid units that contain a series of conjugated double bonds (Hirschberg and Chamovitz, 1994). From this backbone, carotenoids are structured into two separate main groups: xanthophylls and carotenes. Carotenes such as beta-carotene (Table 1) do not contain oxygen atoms and are either linear or cyclized molecules containing one or two end rings (Hirschberg and Chamovitz, 1994), and tend to be orange pigments (Hirschberg and Chamovitz, 1994; Vallentyne, 1957). Xanthophylls such as zeaxanthin (Table 1) are oxygenated derivatives of carotenes and tend to be yellow pigments (Hirschberg and Chamovitz, 1994; Vallentyne, 1957).

1.4.2 Functionality

In photosynthetic organisms, carotenoid pigments have two major functions: carotenes are an accessory pigment for light harvesting, while xanthophylls work to prevent photooxidative damage (Table 1; Egeland, 2016; Hirschberg and Chamovitz, 1994). Carotenoids will extend an organism's optical collection window by increasing the number of peak absorption wavelengths beyond chlorophyll-a's peak absorption wavelengths of 430 nm (blue) and 663 nm (red) (Guidi et al., 2017; Table 1; Figure 5), increasing absorption efficiencies. Additionally, carotenoids assist in adaptation capabilities of phytoplankton not only by assisting in harvesting light but also in transferring more energy to chlorophyll during the photosynthesis process (Trees et al., 2000). Carotenoids also protect the cell against photooxidation processes in the photosynthetic apparatus that are caused by the excited triplet states of chlorophyll. Carotenoid molecules with π-electron configuration of nine or more carbon-carbon double bonds absorb the energy of the triplet state chlorophyll, which then prevents the formation of harmful singlet-state oxygen radicals (Hirschberg and Chamovitz, 1994).

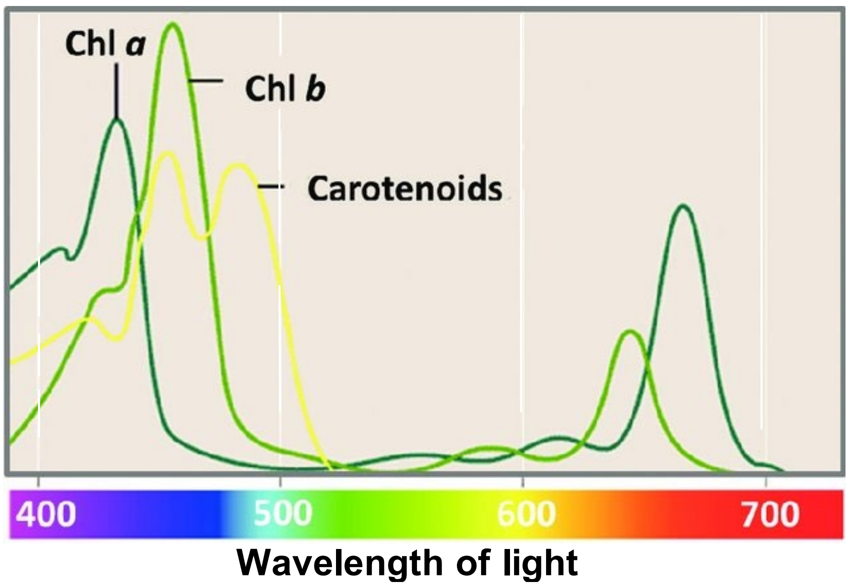

Figure 5. *Chlorophyll-a, -b, and carotenoids absorbance spectra. Adapted from Guidi et al., 2017.*

From a biomarker perspective, carotenoid pigments can be used to reconstruct the presence of different types of phytoplankton since diverse phytoplankton groups have differing pigments. For example, zeaxanthin (Table 1) can be produced in aurearenophytes, brown seaweeds/golden algae, eustigmatophytes (Egeland, 2016), and higher plants all around the world (Bianchi and Canuel, 2011), but when specifically looking in a freshwater system, zeaxanthin is more uniquely found in cyanobacteria (Bianchi and Canuel, 2011; N. Chen et al., 2001; Egeland, 2016; Hirschberg and Chamovitz, 1994; Jeffrey et al., 1997; Schlüter et al., 2018; Schreiner et al., 2013; Tóth et al., 2015; Trees et al., 2000). Similarly, canthaxanthin and echinenone (Table 1) are produced in eustigmatophytes or yellow-green algae (Egeland, 2016), but they are also unique ketocarotenoids (carotenoids containing a ketone) of freshwater cyanobacteria (Bianchi and Canuel, 2011; Egeland, 2016; Hertzberg et al., 1971; Hirschberg and Chamovitz, 1994; Schlüter et al., 2018; Tóth et al., 2015). Myxoxanthophyll (Table 1), while found in some non-photosynthetic and photosynthetic bacteria (Hirschberg and Chamovitz, 1994), has also been used as a unique indicator for cyanobacteria within freshwater (Egeland, 2016; Hertzberg et al., 1971; Hirschberg and Chamovitz, 1994; Pagels et al., 2015; Schlueter et al., 2018; Toth et al., 2015). Aphanizophyll (Table 1) is a unique type of xanthophyll in *Aphanizomenon* (Hirschberg and Chamovitz, 1994), a specific species of cyanobacteria (Hirschberg and Chamovitz, 1994; Schlüter et al., 2018). Non-accessory pigments, such as chlorophyll-a its degradation product pheophytin-a (Table 1; Bianchi and Findlay, 1991), and β-carotene (Table 1), can be indicators of the total productivity (Schreiner et al., 2013) since they are produced by all algae (Bianchi and Canuel, 2011; Egeland, 2016; Jeffrey et al., 1997; Schreiner et al., 2013), including cyanobacteria (Tóth et al., 2015). Additionally, picocyanobacteria pigment production pathways are not well known enough to determine when one pigment (or a collection) is directly related to picocyanobacteria versus cyanobacteria, for example both phytoplankton create zeaxanthin Bianchi et al., 2000). This study cannot determine which phytoplankton type contributed more than the other, so pigments associated to ‘cyanobacteria’ will also include influences from picocyanobacteria. In addition, due to the size of picocyanobacteria, they are less likely to make it down the water column and deposit into sediments.

Additionally, the pigments diatoxanthin and diadinoxanthin (Table 1) are unique to and biomarkers of diatoms within the freshwater environment (Bianchi & Canuel, 2011; N. Chen et al., 2001; Egeland, 2016; Munawar & Munawar, 1978; Reavie et al., 2014; Schreiner et al., 2013; Trees et al., 2000), even though they are produced in small amounts in green algae, euglenophytes, golden-brown algae, silicoflagellates, xanthophytes, pelagophytes, and aurearenophytes (Egeland, 2016) in other types of habitats. Fucoxanthin (Table 1) is unique to and an indicator of diatoms (Bianchi and Canuel, 2011; N. Chen et al., 2001; Egeland, 2016; Schreiner et al., 2013; Trees et al., 2000) and dinoflagellates (Bianchi and Canuel, 2011; Schlüter et al., 2018) in freshwater environments, though it is also produced in brown seaweed (Bianchi and Canuel, 2011; Egeland, 2016), golden algae, aurearenophytes, and silicoflagellates (Egeland, 2016). In this study location, alloxanthin (Table 1) is a general indicator for cryptophytes (Bianchi and Canuel, 2011; Schreiner et al., 2013), though it is also produced in green algae and cryptomonads (Egeland, 2016) in other habitats. Neoxanthin (Table 1) is a general indicator of green algae within this study, but it is also produced in green algae, land-plants (Bianchi and Canuel, 2011; Egeland, 2016; Trees et al., 2000), prasinophytes, and euglenophytes (Egeland, 2016) in other habitats. Chlorophyll-b (Table 1) is an indicator for green algae (Trees et al., 2000; Bianchi and Canuel, 2011) as well, even though it is also produced in chlorophytes like euglenophytes (Schlüter et al., 2018) and higher plants (Bianchi and Canuel, 2011). Violaxanthin (Table 1) is also a unique biomarker of green algae (Bianchi and Canuel, 2011; Trees et al., 2000), despite its production in some diatoms, prochlorophytes, aurearenophytes, brown seaweeds, golden algae, eustigmatophytes (Egeland, 2016), and chlorophytes including euglenophytes (Schlüter et al., 2018). Within this study location, violaxanthin would be more prominently found from diatom production. More detailed information about each of the pigments used in this study can be found in Table 1.

Commonly known cyanobacteria do not synthesize carotene-like structural pigments other than β-carotene. Hence, β-carotene is normally the only cyclic carotene present (Hertzberg et al., 1971; Hertzberg and Liaaen-jensen, 1971; Hirschberg and Chamovitz, 1994). However, they can produce some unique types of xanthophylls, such as 2-hydroxy-derivatives and glycosides, and aphanizophyll in Aphanizomenon. Glycosylated carotenoids are also very common in cyanobacteria (Hirschberg and Chamovitz, 1994). Glycosylation substantially increases the water solubility, bioavailability, photostability and biological activities of carotenoids (X. Chen et al., 2021). The molecular structures of some common cyanobacterial carotenoids are shown in Table 1 (Hertzberg et al., 1971).

1.4.3 Carotenoids in Sediment

Although pigments are known to be susceptible to a variety of pre- and post-depositional decay processes, such as photo-oxidation, chemical- and microbial-mediated oxidation herbivory, and enzymatic metabolism during senescence (Bianchi and Findlay, 1991; Vallentyne, 1957; Watts and Maxwell, 1977; Egeland E, 2016), pigments can be very useful as molecular fossils when they are preserved or unaltered upon deposition into lakebed sediment. When pigments are preserved, they can be extracted, identified, and studied to reconstruct past environmental conditions or events (Meyers, 2003). Ideally, biomarkers are resistant to degradation within the water column and depositional bed, have a unique molecular structure that is easily detectable, and are derived from singular known or identifiable source (Bianchi et al., 1997, 2011; N. Chen et al., 2001; Granado-Lorencio et al., 2017). In fact, unaltered carotenoids have been recovered from both freshwater and marine sediments that are more than 20,000 years old (Vallentyne, 1957; Watts and Maxwell, 1977). Additionally, limnological surveys show that fossil pigment concentration in sediment is an accurate predictor of algal production (Leavitt, 1993).

Chlorophylls and carotenoids can be isolated and extracted from aquatic sediments in order to reconstruct paleoenvironments and tell of the past phytoplankton communities (Heathcote et al., 2023; Leavitt, 1993; Leavitt & Hodgson, 2001; Picard et al., 2022; Vallentyne, 1957). In addition, pigment analysis can focus on carotenoids characteristic of cyanobacteria (zeaxanthin), all cyanobacteria (echinenone), filamentous or colonial cyanobacteria (myxoxanthophyll), Nostocales (canthaxanthin) and some specific N_2-fixing cyanobacteria (aphanizophyll) (Heathcote et al., 2023). Freshwater biomarker pigments in combination with secondary evidence, such as DNA extraction, have been used to reconstruct cyanobacterial abundance and toxicity through time (Heathcote et al., 2023; Picard et al., 2022).

For example, an 8,000-year record using fossil cyanobacterial pigments was created from sediment cores from the Baltic Sea proper, specifically Ancylus Lake (freshwater; Bianchi et al., 2000). In the study, it was found that by creating depth profiles of zeaxanthin, which ranged from undetectable or very low values to 2.1 μmol/g C, that the presently predominating nitrogen limitation of phytoplankton was not man-induced but rather had been naturally occurring over some 7,000 years (Bianchi et al., 2000). Additionally, pigment biomarkers were used to document the changes in hypoxia events over 100 years within the Louisiana shelf sediment (N. Chen et al., 2001). There, it was found that zeaxanthin and fucoxanthin to be the dominant carotenoids within the sediment, indicating that cyanobacteria and diatoms were the most likely dominant species of phytoplankton within that region (N. Chen et al., 2001).

1.4.4 Application of Analytical Methods

Carotenoid pigments, as useful paleo-tracers of algal and bacterial communities (Bianchi et al., 2000; N. Chen et al., 2001) can be measured in a few different ways, including thin layer chromatography (Hirschberg and Chamovitz, 1994), gas chromatography–mass spectroscopy (Brocks et al., 2005) and high-performance liquid-chromatography (HPLC) with fluorescence or UV detection (N. Chen et al., 2001). Using an HPLC has the advantage of higher sensitivity, better resolution, speed, and reproducibility (Van Leeuwe et al., 2006). Furthermore, artifactual results are minimized since the separation is achieved in a dark and oxygen-free environment (Van Leeuwe et al., 2006).

1.5 Geochronology

Geochronology of Lake Superior surface sediment is done primarily using alpha spectroscopy and gamma spectroscopy measurements of ^{210}Pb activities (Klump et al., 1989; Appleby, 2001; Smalley, 2013). With a half-life of 22.26 years, the radioactive isotope ^{210}Pb is widely used for dating recently deposited sediments, generally within the last 150 years (Appleby, 1998, 2001; Appleby and Oldfield, 1983; Smalley, 2013). There are two major models for calculating ^{210}Pb dates under sediment accumulation rates that vary: the constant rate of ^{210}Pb supply (CRS) and the constant initial concentration (CIC) (Appleby & Oldfield, 1983). The CRS model can account for changes in the sedimentation rate, while the CIC model is utilized where sedimentation rates are relatively constant. The CIC model also requires knowledge of the annual flux of atmospheric ^{210}Pb.

^{210}Pb is a naturally occurring radioisotope and part of the ^{238}U decay series. When ^{226}Ra (half-life of 1,622 years) decays to ^{222}Rn (half-life of 3.83 days), fractionation occurs as some amount of radon gas escapes the sediment matrix into the atmosphere, while remaining ^{222}Rn within the sediment decays quickly, with a 3.8-day half-life, *in situ* through several other short-lived daughter nuclides to, finally, ^{210}Pb. ^{210}Pb can then be sourced from atmospheric deposition when atmospheric ^{222}Rn decays, referred to as unsupported or excess ^{210}Pb (Appleby, 1998; Appleby and Oldfield, 1983), as well as when trapped ^{222}Rn in the sediment decays, referred to as supported ^{210}Pb (Appleby, 1998; Appleby and Oldfield, 1983). Over time the influx of unsupported ^{210}Pb is often assumed to be constant (Robbins and Ed, 1975; Smalley, 2013), and is deposited through wet and dry deposition to the lake surface, attaches to particles, travels through the water column, and finally gets deposited in bottom sediments. The supported ^{210}Pb is generally near equilibrium with ^{226}Ra, and accordingly, ^{226}Ra activity is sometimes used to determine the amount of supported ^{210}Pb in a sample (Smalley, 2013).

Typically paired with ^{210}Pb dating is the radioisotope ^{137}Cs, which is not naturally occurring and was introduced into the atmosphere through detonations of nuclear weapons. The first nuclear detonations occurred in 1945, allowing radioactive debris particles to enter the stratosphere and disperse globally. The amount of fallout varied spatially with factors such as precipitation and latitude. These detonations were constrained by two major political events: the signing of a moratorium, or temporary prohibition, in 1958 that lasted until 1961, and the signing of the Limited Test Ban Treaty in 1963 (Smalley, 2013). Significantly reducing the number of nuclear weapon detonations worldwide (Appleby, 2001; Smalley, 2013), this led to the highest rates of ^{137}Cs isotope deposition in sediments in 1963-1964 (half-life of 30 years; Appleby, 2001; Smalley, 2013), and a globally ubiquitous age marker in sediments.

Table 1. *A list of the studied pigments, their structure, indicator organism, and reference material associated with them.*

Pigment	Structure	Organism	Citation
Carotenoids			
Alloxanthin	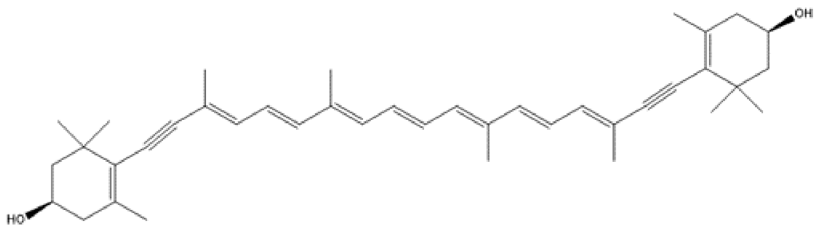	Cryptophytes	(Bianchi & Canuel, 2011; Schreiner et al., 2013)
		Green Algae, Cryptomonads	(Egeland E. 2016) (Pinckney 1998)
Aphanizophyll	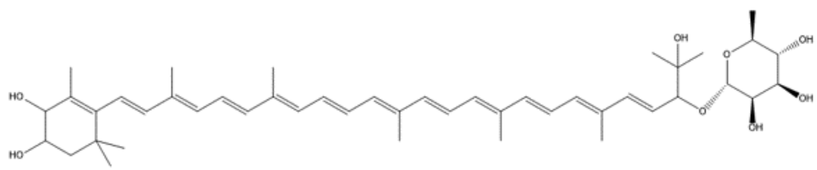	Cyanobacteria	(Hirschberg & Chamovitz, 1994; Schlueter et al., 2018)
Beta-Carotene*	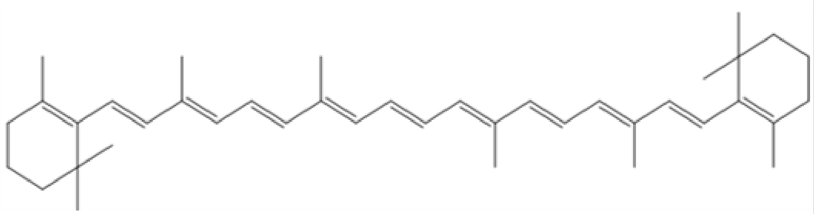	All algae	(Bianchi & Canuel, 2011; Schreiner et al., 2013)

*Beta-Carotene is the only carotene studied. The other pigments are xanthophylls.

Pigment	Structure	Organism	Citation
Canthaxanthin	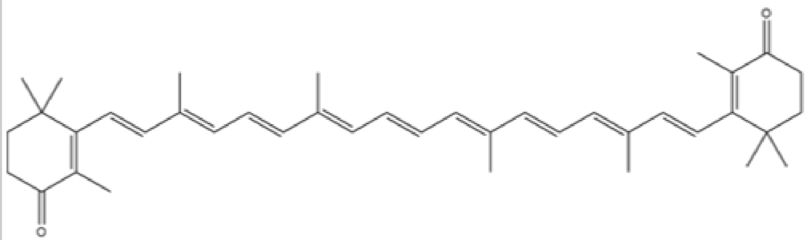	Cyanobacteria	(Bianchi & Canuel, 2011; Egeland, 2016; Hertzberg et al., 1971; Hirschberg & Chamovitz, 1994; Schlueter et al., 2018; Toth et al., 2015; Pagels et al., 2021)
		Eustigmatophytes	(Egeland E. 2016)
Diadinoxanthin	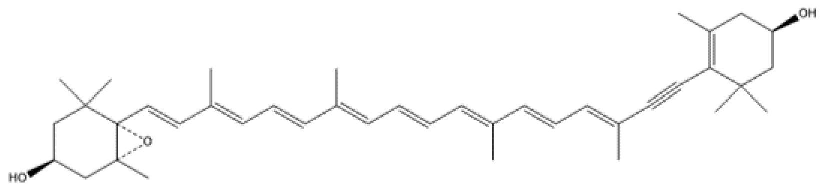	Diatoms	(N. Chen et al., 2001; Schreiner et al., 2013; Trees et al., 2000; Bianchi & Canuel, 2011; Egeland E. 2016)
		Dinoflagellates	(Bianchi & Canuel, 2011)
		Green Algae, Euglenophytes, Golden-brown algae, Silicoflagellates, Xanthophytes, Pelagophytes, Aurearenophytes	(Egeland E. 2016)
Diatoxanthin	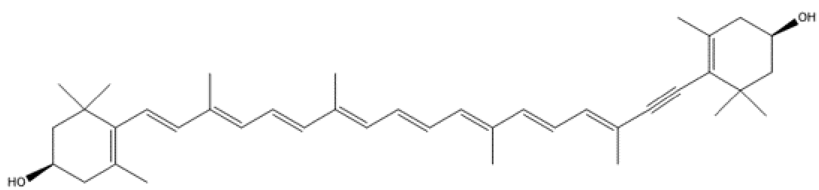	Diatoms	(N. Chen et al., 2001; Schreiner et al., 2013; Trees et al., 2000; Egeland E. 2016)
		Green Algae, Euglenophytes, Golden-brown algae, Silicoflagellates, Xanthophytes, Pelagophytes, Aurearenophytes	(Egeland E. 2016)

Pigment	Structure	Organism	Citation
Echinenone	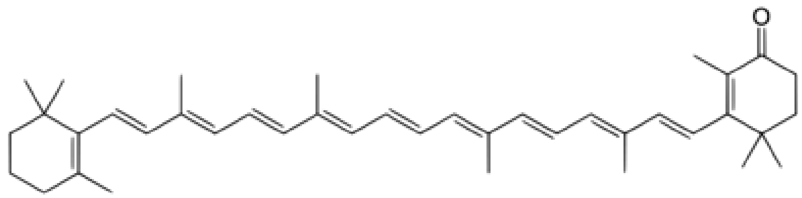	Cyanobacteria	(Bianchi & Canuel, 2011; Egeland, 2016; Hertzberg et al., 1971; Hirschberg & Chamovitz, 1994; Schlueter et al., 2018; Toth et al., 2015)
Fucoxanthin	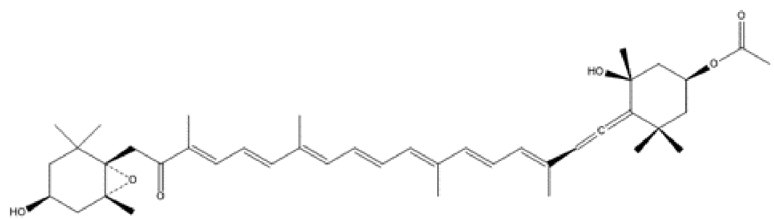	Diatoms, Brown Seaweed	(N. Chen et al., 2001; Schreiner et al., 2013; Trees et al., 2000; Bianchi & Canuel, 2011; Egeland E. 2016; Schlueter et al., 2018; Pinckney 1998)
		Dinoflagellates	(Bianchi & Canuel, 2011; Schlueter et al., 2018)
		Golden Algae, Aurearenophyes, Silicoflagellates	(Egeland E. 2016)
Myxoxanthophyll	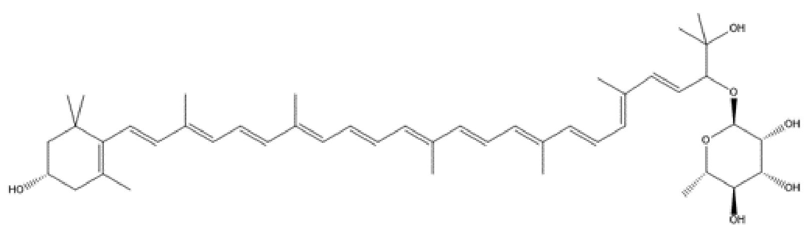	Cyanobacteria	(Egeland, 2016; Hertzberg et al., 1971; Hirschberg & Chamovitz, 1994; Pagels et al. 2015; Schlueter et al., 2018; Toth et al., 2015)

Pigment	Structure	Organism	Citation
Neoxanthin	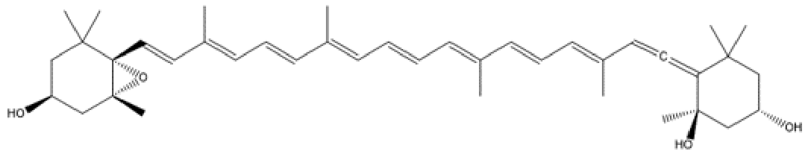	Green algae	(Trees et al., 2000; Bianchi & Canuel, 2011; Egeland E 2016)
		Plants, Prasinophytes, Euglenophytes	(Bianchi & Canuel, 2011; Egeland E. 2016)
Violaxanthin	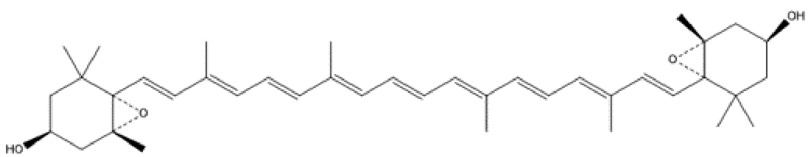	Green algae	(Bianchi & Canuel, 2011)
		Diatoms, Prochlorophytes, Aurearenophyes, Brown Seaweeds, Golden Algae, Eustigmatophytes	(Egeland E. 2016; Pinckney, 1998;Schlueter et al., 2018)
Zeaxanthin	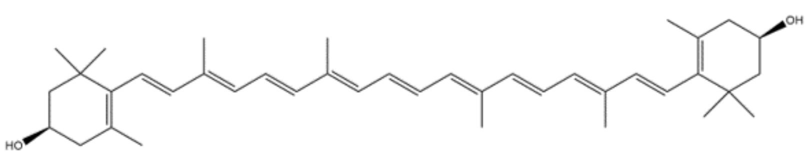	Cyanobacteria	(N. Chen et al., 2001; Jeffrey et al., 1997; Schreiner et al., 2013; Trees et al., 2000; Bianchi & Canuel, 2011; Egeland E. 2016; Hirschberg et al. 1994; Schlueter et al., 2018; Toth et al., 2015)
		Higher plants	(Bianchi & Canuel, 2011)
		Aurearenophyes, Brown Seaweeds/ Golden Algae, Eustigmatophytes	(Egeland E. 2016)

Pigment	Structure	Organism	Citation
Chlorophylls and Chlorophyll Degradation Products (Pheopigments)			
Chlorophyll-a	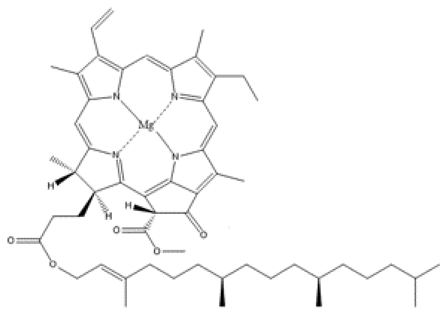	Photosynthetic microalgae	(Bianchi & Canuel, 2011)
		Cryptomonads, Diatoms, Euglenophytes, Golden-Brown Algae, Aurearenophyes, Brown Seaweeds, Eustigmatophytes, Xanthophytes	(Egeland E. 2016; Jeffrey et al., 2011; Pinckney 1998)
Chlorophyll-b	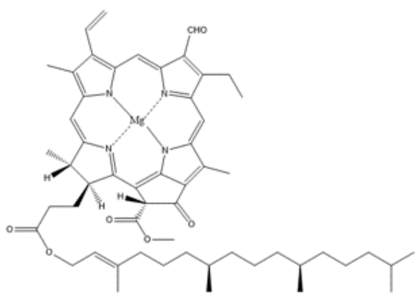	Green algae, higher plants	(Trees et al., 2000; Bianchi & Canuel, 2011)
		Euglenophytes	(Egeland E. 2016)
Pheophytin-a	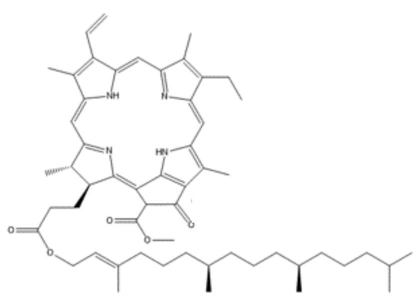	Zooplankton feces, sediments	(Bianchi and Canuel, 2011)

1.6 Mineralogical Sediment Tracers

Within the freshwater lake sediment application, Titanium (Ti), Potassium (K), Silicon (Si), and Aluminum (Al) are common elements measured and utilized in recreating paleoclimates. These element's compositions can be measured using x-ray fluorescence (XRF), which is a rapid, non-destructive, and a high-resolution geochemical analysis (Davies et al., 2015) that utilizes the emission of secondary x-rays from a material that had been excited with primary, high-energy x-rays (Streli et al., 1999). Later, the compositions and ratios of elements can then be used to interpret past environmental and climatic changes through time.

Ti is a lithogenic element that is a widely used mineral element in lake sediment studies (Davies et al., 2015). Ti resides in resistant minerals and is quite conservative in most geochemical environments, making it a stable and abundant element that can be a baseline for normalizing other element profiles to background minerogenic inputs (Davies et al., 2015). Ti is often applied as an indicator of allochthonous inputs from the catchment (Boës et al., 2011; Cohen, 2003). Ti can be used to normalize Si and K to interpret past environmental or climatic events. Si is a lithogenic element that is an indicator of detrital inputs (Boës et al., 2011) such as sand layers. K, another indicator of detrital inputs (Boës et al., 2011; Davies et al., 2015), is often used to represent overall vegetation cover versus drought conditions within the past (Foerster et al., 2012). When the terrain is stabilized by more extensive vegetation cover, K would be preferentially leached away through chemical weathering, resulting in lower sedimentary K inputs. On the other hand, high K can represent drought conditions (Davies et al., 2015; Foerster et al., 2012). Al, abundant and stable, can be associated with terrestrial silts and clays that are Al-enriched (Davies et al., 2015). Al:Si ratios can present the fraction of clay to sand within the sediment make up when deposited on the lakebed (Davies et al., 2015).

1.7 Study Sites

Lake Superior, located north of Minnesota, Wisconsin, and Michigan, is the largest freshwater lake in the world by surface area, and the third largest by volume behind Lake Baikal and Lake Tanganyika. Due to its volume of 12,115 km^3 and its surface area of 82,100 km^2, Lake Superior has a water residence time of approximately 173 years, making it the slowest of the Great lakes to respond to contaminant or excess nutrient loading (Quinn, 1992; Smalley, 2013). The maximum depth in Lake Superior is 405 m, or 1,332 feet (Munawar and Munawar, 1978). The area of the Lake Superior Basin watershed is approximately 125,000 km^2, of which nearly 2% is developed (Hollenhorst et al., 2011), 1% agriculture, and 97% natural land cover. Using both of the both the Canadian (Ontario Provincial Land Cover data) and US (National Land Cover Data) land cover data (State of the Great Lakes, 2022), the natural land cover can be broken down to 76% is forest land (Hollenhorst et al., 2011), 1.5% grassland, 15% forested wetland, 4.4% wetlands, and 0.2% barrens (State of the Great Lakes, 2022). Runoff from the Lake Superior Basin, which was 60.75 cm/year on average from 1948-1999, accounts for approximately 43% of all water input into Lake Superior (Lenters, 2004).

The ~100 km southern shoreline of Lake Superior that stretches from the Duluth-Superior Harbor to the northeastern terminus at the Apostle Islands region is known as the Western Arm (Sterner et al., 2020). The Western Arm has become increasingly subject to extreme precipitation events delivering large amounts of sediment and nutrients to the nearshore in the past decade (Cooney et al., 2016; Reinl et al., 2020; Walsh et al., 2014). Further, since 1991-2014, there has been an estimated 30% increase in heavy precipitation events above the 1901-1960 average (Walsh et al., 2014). Extreme storms provide large fluxes of nutrients and organic material to the lake (Cooney et al., 2016; Reinl et al., 2020), providing an excess of nutrients for phytoplankton, like Cyanobacteria, to reproduce and grow exponentially. Two 500–1000-year rainfall events that created unusually high runoff from the south shore of Lake Superior in 2012 and 2018 (Cooney et al., 2016; Reinl et al., 2020; Sterner et al., 2020) were followed by cyanobacterial blooms varying in size and duration (Sterner et al., 2020). Additionally, cyanobacterial blooms are generally associated with higher water temperatures (Paerl, 2017), and Lake Superior has been warming at the fastest rate of the Laurentian Great Lakes (based on maximum summer surface temperature; Austin and Colman, 2007), approximately 2.5°C from 1979-2006 (0.11 ± 0.06 °C yr^{-1}). This may also be contributing to the observable emergence of cyanobacterial blooms (Reinl et al., 2020; Sterner et al., 2020). Within the Western Arm resides Siskiwit Bay (Figure 1). Embayment's such as Siskiwit Bay provide a protective barrier to the lakebed sediment, preserving it from most small and medium-sized storms or wave-initiated resuspension events. Siskiwit Bay is situated at the mouth of the Siskiwit River, which originates from Siskiwit Lake 7.25 km south of the Bay. Because Siskiwit Lake has experienced very frequent cyanobacteria blooms, it is theorized that the blooms noted in the Lake may have contributed to the blooms in the Bay (Reinl et al., 2020).

1.8 Goals and Hypotheses

Alone among the Laurentian Great Lakes, Lake Superior had not been known to exhibit cyanobacterial blooms until 2012. Lake Erie, being shallow and warm watered, is known to have frequent cyanobacterial blooms, and eutrophication is one of their primary drivers (Kane et al., 2014). In contrast, the emergence of localized blooms in Lake Superior is surprising, given the lake's cold, oligotrophic, and increasing nitrate and low phosphate concentrated waters (Sterner et al., 2007, 2020). 2012 was the first time cyanobacterial blooms were recorded along the southern shore of western Lake Superior. Siskiwit Bay and Siskiwit Lake, WI (Figure 1) are the focus of this study, especially since Siskiwit Lake experiences semi-regularly occurring cyanobacterial blooms each summer season, and is hydrologically connected through the Siskiwit River to Siskiwit Bay, Lake Superior (Reinl et al., 2020). However, it is currently unknown if there were cyanobacterial blooms prior to 2012 and if there were, the frequency at which they have been throughout history. Anthropogenic activity often causes changes in phytoplankton abundance and community composition, making it the main suspect in these recognized events. By looking into the sediment and the biomarkers of past phytoplankton that lie within it, a reconstruction of phytoplankton community changes over time can be produced. These changes can be correlated with historical events to provide further context for present day events.

Therefore, this study aims to identify and analyze the evidence of historical algal communities, specifically past cyanobacteria blooms, prior to their first recorded appearances within the southwestern region of Lake Superior. Trends in pigment composition and concentration in sediments, specifically cyanophyte or cyanobacteria markers, can provide information about past surface water and benthic algal communities. By looking into the sediment and the biomarkers of past phytoplankton that lie within it, a reconstruction history can be compiled and hence present changes within the phytoplankton communities over time. These changes will be correlated with historical events to provide further context for present day events.

<u>Question 1</u>: Can specific phytoplankton pigments be used to reconstruct historical blooms in Lake Superior's western arm?

> Hypothesis 1: Phytoplankton pigments extracted from water column particulates in the location of a current cyanobacterial bloom in the study area can be correlated to preserved historical pigments analyzed from sediment cores and used to identify past productivity 'highs', such as cyanobacterial blooms.

<u>Question 2</u>: What is the make-up of the phytoplankton community in the western arm of Lake Superior now, and how has it changed over the historical period?

> Hypothesis 2: Diatoms are and have historically been the dominate phytoplankton within Lake Superior, but cyanobacteria will outcompete diatoms during recorded bloom years, with more frequent blooms or productivity observed in recent years.

Chapter 2 of this thesis discusses results of bulk and stable isotope composition, age modeling, x-ray fluorescence, and the carotenoid pigment analysis of the Siskiwit Bay sediment. It is written and formatted for publication in a scholarly journal, and because of this, the introductory information and some parts of the methods section may be redundant with Chapter 1. Chapter 3 discusses the results of bulk elemental and stable isotope composition of Siskiwit Lake. Additionally, Chapter 3 contains detailed descriptions of the pigment extraction method and calculations, other data collected in this project, and other analyses not included in the main manuscript.

Chapter 2. Historical Cyanobacterial Blooms in Siskiwit Bay - Lake Superior, Wisconsin, USA

2.1 Introduction and Background

On July 14th and 15th, 2012, for the first time in recorded history, a mass of thick, floating algae was observed along the shorelines west of the Wisconsin Apostle Islands in Lake Superior (Sterner et al., 2020; Figure 1). This bloom, mainly *Dolichospermum lemmermannii* (formerly, *Anabaena lemmermannii*) (Figure 2; Sterner et al., 2020) was an accumulation of cyanobacterial biomass, formed through growth, migration, and physical-chemical forces (Tromas et al., 2017). Similar blooms of the same dominant taxon subsequently occurred in 2016, 2017, and 2018 (Sterner et al., 2020). Though this was the first record of such a large bloom occurring in Lake Superior, throughout the other Laurentian Great Lakes cyanobacterial blooms are relatively common (Conroy et al., 2014; Kane et al., 2014; Paerl, 2017). Based on occurrences in other freshwater lakes, some cyanobacterial species are known to be toxic (Perri et al., 2015; Huisman et al., 2018). In Lake Superior, toxicity measurements to date have indicated the presence of one potentially toxic substance (Anabaenopeptin A) at a very low concentration (Sterner et al., 2020).

From the first recordings of these blooms in 2012, questions have been raised about whether these are new occurrences and what may be influencing the size and frequency of these blooms. While in Lake Erie large toxic cyanobacterial blooms are driven by phosphorus inputs from the agricultural Maumee basin (Kane et al., 2014), Lake Superior's watershed contains minimal agricultural activity, so cyanobacterial blooms are likely not driven by anthropogenic nutrient inputs (National Oceanic and Atmospheric Administration (NOAA), 2010). Dominant cyanobacteria genera in a bloom are controlled by the synergistic effects of nutrient supplies, light, temperature, water residence times, and biotic or food chain interactions (Paerl, 2017). With nutrient over-enrichment, anthropogenically caused hydrologic modifications, and global climate change, cyanobacteria blooms can surge in biomass production and accumulation. Near the southern shore of Lake Superior, the increased occurrence of cyanobacterial blooms is theorized to be due to enhanced nutrient loading from the surrounding watersheds and from the warming climate (Sterner et al., 2020). There have been multiple extreme precipitation events delivering large amounts of sediment and nutrients to the nearshore in recent years (Cooney et al., 2016; Reinl et al., 2020; Walsh et al., 2014), providing an excess of nutrients for phytoplankton, including cyanobacteria, to reproduce and grow exponentially (Sterner et al., 2020). Lake Superior has also experienced an increase in water temperature of about 2-3°C since 1973 (Austin and Colman, 2007; O'Reilly et al., 2015; Van Cleave et al., 2014), which has further promoted growth and lengthened the duration of the blooms (Huisman et al., 2018; Paerl, 2017; Rigosi et al., 2014).

Lake Superior, due to its cold temperatures and low nutrient concentrations, has historically been dominated by diatom communities (Munawar and Munawar, 1978; Reavie et al., 2014). Diatoms are considered a high-quality food for benthic primary consumers while cyanobacteria are thought to be a lower-quality food because of their absence of sterols causes constraint in carbon transfer efficiency from cyanobacteria to zooplankton and benthic filter feeders (Basen et al., 2011, 2012, 2013; Hedberg et al., 2021). Therefore, a shift to more cyanobacteria-dominated primary producers can cause significant ecological changes, including alterations to benthic species composition and production. Climate change and eutrophication, which have both been recorded in Lake Superior (Baustian et al., 2020; O'Beirne et al., 2017; O'Reilly et al., 2015; Zhang et al., 2020), reduce diatom growth and promote cyanobacterial growth (Huisman et al., 2018; Paerl, 2017; Rigosi et al., 2014; Hedberg et al., 2021). With greater cyanobacterial dominance in the primary producer community, this leads to enhanced benthic bacterial production and oxygen depletion within the water column (Andersson et al., 2015).

Alone among the Laurentian Great Lakes, Lake Superior was not known to exhibit cyanobacterial blooms until 2012. In Lake Erie, however, eutrophication is one of the primary drivers of blooms (Kane et al., 2014). In contrast, the emergence of localized blooms in Lake Superior is surprising, given the lake's cold, oligotrophic, and stoichiometrically unbalanced (Nitrogen:Phosphorus) waters (Sterner et al., 2007, 2020). 2012 was the first time cyanobacterial blooms were recorded along the southern shore of western Lake Superior. These bloom events expose knowledge gaps of any prior cyanobacterial blooms to 2012 and the frequency at which they have been throughout history, especially as compared to the observed record.

This study aims to address these knowledge gaps by identifying and analyzing biomarker evidence of historical algal communities, specifically past cyanobacteria blooms, prior to their first recorded appearances within the southwestern region of Lake Superior. Historical trends in pigments, specifically cyanophyte or cyanobacteria markers, will provide information about historical surface water and benthic algal communities. These historical changes in algal community makeup will be correlated with historical events to provide further context for present day events.

2.2 Methods

2.2.1 Site Description

Two “major” cyanobacterial blooms, defined as a bloom lasting more than one day in one location, occurred on July 14 – 15, 2012 on the shorelines from Cornucopia, Wisconsin to Little Sand Bay (~20 km) in Lake Superior and on August 9, 2018 within Mawikwe Bay, the Sea Caves area (Sterner et al., 2020; Reinl et al., 2020), and at the nearby Cornucopia Beach in Siskiwit Bay (Figure 1; Sheik et al., 2022). An additional 48 blooms have been observed on the shorelines of Superior-Duluth to the Sea Caves of the Apostle Islands in Wisconsin since the 2012 bloom (Lafrancois & Reinl, 2024). Embayment’s such as Siskiwit Bay provide a protective barrier to the lakebed sediment, preserving pigment deposition in sediment from storm or wave-initiated resuspension events. Siskiwit Bay is situated at the mouth of the Siskiwit River, which originates from Siskiwit Lake 7.25 km south of the Bay. Because Siskiwit Lake has experienced very frequent cyanobacteria blooms, it is theorized that the blooms noted in the Lake may have contributed to the blooms in the Bay (Reinl et al., 2020).

2.2.2 Sample Collection

To investigate the existence of historical cyanobacterial blooms in Lake Superior’s Western Arm, surface water samples were collected in multiple places around Siskiwit Lake on June 8th, 2021, during a cyanobacteria bloom (Table 2). Surface water grab samples were taken from the Siskiwit Lake Boat Launch, Siskiwit Lake Campground, and both the Left and Right sides of the Dock (Figure 6).

Three sediment cores were collected from Siskiwit Bay (Table 2) on September 28th, 2021, using an Aquatic Instruments Hammer Corer with 2-5/8 in diameter polycarbonate core barrels. Out of these three cores, one (88 cm) would be used for an XRF analysis, another (126 cm) for ^{210}Pb and ^{14}C dating, and finally one for bulk elemental and isotopic concentrations, pigment analysis and ^{14}C dating. Sediment packages for coring were previously identified via CHIRP data collection on September 15th, 2021, with a SB-424 Full Spectrum Sub-Bottom Tow Vehicle (EdgeTech Discover Sub-Bottom 4.09) aboard the R/V Kingfisher. The three long cores ranged from 65 cm to 126 cm in length. One of these cores was analyzed by x-radiograph analysis, while the two others were visually inspected; all were determined to have an undisturbed sediment-water interface.

Table 2. *Sample locations, type of sample(s) and brief sample method, and its coordinates.*

Location Name	Type	Latitude, Longitude
Siskiwit Lake Boat Launch	Water Sample - Grab	N46.796225°, W091.122498°
Siskiwit Lake Campground	Water Sample - Grab	N46.798355°, W091.129682°
Siskiwit Lake Dock - Left	Water Sample - Grab	N46.796185°, W091.122516°
Siskiwit Lake Dock - Right	Water Sample - Grab	N46.796188°, W091.122575°
Siskiwit Bay	3 Sediment Cores	N46.877250°, W091.113200°
Siskiwit Lake Deep Spot	1 Sediment Core	N46.793920°, W91.129940°

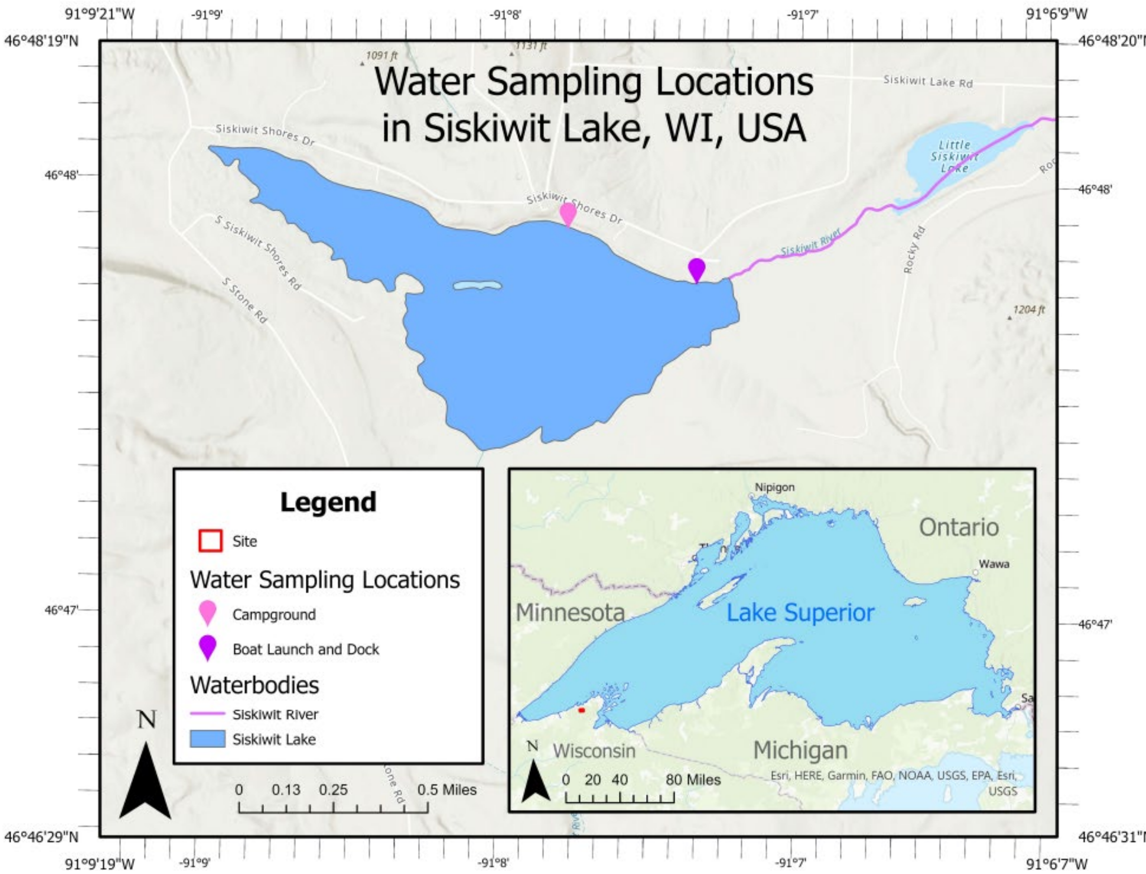

Figure 6. *Water sampling locations on Siskiwit Lake at Cornucopia, Wisconsin, USA, during cyanobacterial bloom on June 8th, 2021. Pink (campground) and purple (boat launch and dock) pinpoints display exact locations. Siskiwit Lake, as a potential source of cyanobacteria to Lake Superior, is hydrologically connected to Siskiwit Bay by the waterway highlighted in purple (Siskiwit River). Sample locations include: Siskiwit Lake Boat Launch, Siskiwit Lake Campground, and both the left and right sides of the dock.*

2.2.3 Sample Processing

The Siskiwit Lake surface water samples were vacuum filtered using pre-combusted 23 mm glass fiber filters of 0.2 µm pore size to capture particulates. These filters were then frozen, freeze-dried, pre- and post-weighed, and ground into homogenous mixtures using a ball mill. Between samples, the vessel and ball bearings were rinsed with deionized water, then wiped with a lint-free KimWipe, then rinsed with methanol to ensure no sample transfer.

Using a tray fitted to the top of the core barrel and a spatula, two Siskiwit Bay sediment cores were extruded into 1 cm samples down the entire core length (65 cm and 126 cm, respectively) and stored in 24 oz polyethylene Nasco WHIRL-PAKs. Between each centimeter section, the extruder tray and spatula were wiped dry with paper towel to minimize contamination between samples. All extruded samples were frozen at -20°C within 12 hours of collection and then lyophilized to dryness with a LABCONCO Freezone-6 System. After lyophilization, samples were inspected visually for terrestrial organic matter, such as leaves and sticks, and these were removed for carbon-14 (^{14}C) dating. Samples were ground and homogenized with a mortar and pestle, weighed, and kept in pre-combusted glass scintillation vials, and stored at -20°C until further processing and analysis. The third core (89 cm) from Siskiwit Bay was split longitudinally down the core barrel with one half archived for X-ray fluorescence (XRF) analysis.

2.2.4 Bulk Density

Bulk density is a primary measurement of the water content within the sediment, meaning it can be highly dependent on deposition rates and compaction. It generally increases with depth and time as the pore water is expelled to the surface of the sediment from compaction. Bulk density for each sample depth was measured by dividing the sample’s mass by the sample’s volume, using Equation 1. Sample volume was determined by calculating cylindrical volume of each extruded sample, determined using a diameter of 2 5/8 inches or 6.6675 cm, and a height of 1 cm.

$$Bulk\ Density = \frac{Sediment\ Weight\ (grams)}{(\pi)\ (1\ cm)\ (3.33375\ cm)^2} \qquad \text{(Equation 1)}$$

2.2.5 Bulk Element and Isotope Analysis

Bulk elemental concentrations of carbon (%OC) and nitrogen (%N) were analyzed using a Costech 4010 Elemental Analyzer coupled to a Thermo Fisher Scientific - Finnigan Delta Plus XP isotope ratio mass spectrometer at the Large Lakes Observatory at University of Minnesota, Duluth. For %OC and its associated isotopes ($\delta^{13}C$), carbonates were removed from freeze-dried sediments using the HCl vaporization method (Harris et al., 2001). Stable carbon isotope values are reported in delta notation (Equation 2) relative to the Vienna Pee Dee Belemnite (VPDB) isotopic standard. Samples for N concentration (%N) analysis did not undergo fumigation and were weighed directly into 2x5 mm tin capsules and stored in a desiccator until analysis.

$$\delta^{13}C_{VPDB}(‰) = \left(\frac{R_{sample}}{R_{standard}} - 1\right) x\ 1000,\ where\ R = \frac{13C}{12C} \qquad \text{(Equation 2)}$$

Standards were analyzed every 10 samples to calculate instrument drift. The set of standards used were acetanilide, low-organic content soil (B-2153), sorghum flour (B-2159), and caffeine (Table 3). Precision (1σ) of the internal lab standards was approximately ± 0.8%OC, ± 0.2%N, and ± 0.3‰ for $\delta^{13}C$. Selected samples run in duplicate had measurements within this standard error.

Table 3. *The set of standards, acetanilide, low-organic content soil (B-2153), sorghum flour (B-2159), and caffeine, and their set values for organic carbon (%OC), carbon-13 isotope (‰ $\delta^{13}C$), and nitrogen (%N).*

Standards	%OC	‰ $\delta^{13}C$	%N
Acetanilide	71.1	-33.8	10.4
Low-Organic Content Soil [B-2153]	1.9	-22.9	0.1
Sorghum Flour [B-2159]	41.6	-13.7	N/A
Caffeine	49.5	-38.5	28.9

2.2.6 Loss on Ignition

Lake sediment organic matter and carbonate content were estimated by weight loss measurements in sediment samples subjected to sequential heating within a Cole-Parmer muffle furnace (Bengtsson & Enell, 1986; Dean, 1974; Heiri et al., 2001; Santisteban et al., 2004). The amount of organic matter within the sediment was then estimated by the measured weight loss after oxidizing the sample at 550°C (Bengtsson & Enell, 1986; Dean, 1974; Heiri et al., 2001; Santisteban et al., 2004). Carbonate content was calculated through the measured weight loss after heating the sediment to 1,000°C (Bengtsson & Enell, 1986; Dean, 1974; Heiri et al., 2001; Santisteban et al., 2004).

2.2.7 Geochronology

Surface sedimentation rates were determined from ^{210}Pb and ^{137}Cs analysis performed at California State University, Fullerton. Each dried sample was sealed in a petri dish for at least 21 days to allow the ^{226}Ra daughter isotopes to reach equilibrium. Samples were measured for at least 24 hours using gamma spectroscopy, thus measuring the gamma radiation emitted by the sediment. A self-absorption calibration was performed for each sample (Cutshall et al., 1983) to account for any activity blocked by the sediment in the sample before reaching the detector. Finally, the age model was created by combining ^{210}Pb and ^{137}Cs data into the BACON program with the PLUM package (Aquino-López et al., 2018), which provided specific ages for each sample depth.

Below the limit of ^{210}Pb dating (10 cm), terrestrial organic matter was picked from the cores for ^{14}C dating. Samples underwent a "standard acid-base-acid" wash technique (Abbott & Stafford, 1996) pre-treatment prior to combustion at Northern Illinois University. This process consisted of first soaking the samples in a weak acid (0.5 N HCl) to remove carbonates, then a weak base (0.5% KOH) to remove reactive organics, then a stronger acid (6 N HCl) to ensure carbonates were removed, and finally placement into sealed glass tubes where they were combusted to CO_2 gas. Following this, samples were analyzed for ^{14}C at the W.M. Keck Carbon Cycle Accelerator Mass Spectrometry facility at the University of California, Irvine. Sedimentation rates below the ^{210}Pb limit were then determined through interpolation of ^{14}C date differences downcore using the PLUM package within the program BACON (Aquino-López et al., 2018, 2020). These estimations stemmed from the Bayesian-Plum model, as it provided a distribution of ages based on a range of uncertainties for the depths between the measured ^{14}C depths. Together the three isotopes allowed other parameters, such as the sediment accumulation rates, to be calculated and to observe any changes within the phytoplankton community via their pigment biomarkers.

2.2.8 Pigment Analysis

Pigments were extracted from approximately 2 g dry weight samples of freeze-dried sediment or ground water filters with 5 mL of optima-grade acetone. Samples were suspended in acetone and then sonicated for 1 minute to break cell walls. Then, samples were stored at -20°C for 12 to 16 hours, centrifuged at 2,000 rpm for 5 minutes (G force of 454), and filtered using 0.22 µm NYLON 25 mm syringe filters to separate solid and liquid phases. Dissolved pigments were then blown down to dryness and reconstituted in 200 µL of Optima-grade acetone with 0.500 mg/L *trans*-β-Apo-8'-carotenal internal standard (Sigma Aldrich) prior to analysis on a ThermoScientific Dionex UltiMate 3000 UHPLC outfitted with photodiode array detector and fluorescence detector. Each injected sample was separated into individual pigments using the two mobile phases, (A) 70:30 (v:v) Methanol:Tetrabutylammonium acetate (TbAA) and (B) 100% Optima-grade Methanol, at a flowrate of 0.200 mL/min through an Agilent - Zorbax Eclipse Plus C8 HPLC column (2.1 x 100 mm, 95Å, 1.8-µm) and a VanGuard - Acquity UPLC BEH C8 HPLC guard column (2.1 x 5 mm, 1.7-µm). Each injection's flow gradient started with 95% mobile phase A and 5% B that lasted 11.5 minutes, then ramped up to 5% A and 95% B over the course of 15 minutes, held there for another 11.5 minutes, until it ramped back down to 95% A and 5%B, where it was then held for the remaining 6 minutes. *(See Appendix 3.3.7 for details).* The resulting elution order and method of identification of each pigment can be seen in Table 4. Pigment peak identification and quantification within sediment samples were performed through comparison to the internal standard and standard pigments (DHI Laboratories, Denmark). All actions were performed in dark or dim-light to reduce the amount of pigment degradation.

Pheophytin-a, a degradation product of chlorophyll-a, when used in summary with chlorophyll-a can be referred to as the sum of chlorophyll-a at the time of deposition. Pheophytin-a was ratioed to this past sum of chlorophyll-a to produce a relative percentage of chlorophyll-a degradation since deposition.

Additionally, accumulation rates of pigments (µg/yr) were calculated throughout the core in order to spot large depositional changes of pigment biomarkers. Though they are not able to detect annual changes in phytoplankton community composition, accumulation rates were calculated by taking total running average of pigments and dividing them into annual rates. In addition, measuring accumulation rates leave selective biases in rapid degradation of pigments in surface sediments, while organic matter-specific carotenoid concentrations are less biased because the degradation of bulk organic matter is partly compensating for carotenoid losses.

2.2.9 X-Ray Fluorescence Analysis

X-ray fluorescence analysis was performed on the split core at a 0.2-cm radiographic resolution and a 60-second dwell time. Elemental measurements were performed on a ITRAX Core Scanner (COX Analytical Systems, Molndal, Sweden) located at the Large Lakes Observatory, University of Minnesota, Duluth. The split-cores were wrapped with 4 µm Ultralene film for preservation and, prior to measurement, the surface sediment was smoothed to reduce the roughness of the surface. Scans were conducted at a voltage of 10 kV, yielding count intensities for elements Al, Si, K, Ti, and Pb.

Table 4. *Individual absorption profiles of pigment standards were collected in advance to determine elution order and how it would be later identified (diode array or fluorescence) within a sediment sample. Excitation and emission wavelengths were set at 450 nm (4-nm bandwidth) and 666 nm (4-nm bandwidth), respectively, with DAD set to 450 nm excitation and collection at a rate of 20 Hz. All pigments were observable under the diode array detector at 450 nm, but if they were observable at 666 nm it is noted here.*

Pigment	Stock Concentration (mg/L)	Elution Order	Retention Time (min)	Diode Array – 666 nm	Fluorescence 450nm
Alloxanthin	0.948	7	29.9	Yes	Yes
Aphanizophyll	0.845	3	27.9	No	No
β-Carotene	0.832	15	39.3	No	Yes
Canthaxanthin	1.648	10	31.2	Yes	Yes
Chlorophyll-a	1.707	12	34.9	Yes	No
Chlorophyll-b	1.190	11	33.2	Yes	No
Diadinoxanthin	0.690	6	28.9	Yes	Yes
Diatoxanthin	0.641	8	30.1	No	Yes
Echinenone	0.923	13	34.4	No	Yes
Fucoxanthin	1.490	1	27.1	Yes	Yes
Myxoxanthophyll	0.764	5	28.9	No	Yes
Neoxanthin	0.751	2	27.8	No	Yes
Pheophytin-a	3.208	14	37.3	No	No
Violaxanthin	1.118	4	28.2	Yes	Yes
Zeaxanthin	0.782	9	30.5	Yes	Yes

2.3 Results

2.3.1 Sediment Age and Depositional Rates

Using two of the sediment cores from Siskiwit Bay a 5,400-year approximate timeline was constructed. The ^{210}Pb data suggests a sediment age of 80 cal year BP at a depth of 10 cm, with about 4.00 mm of sediment deposition each year. In correlation, the ^{137}Cs results indicate the age at 9 cm is 60 cal year BP. In conjunction with the ^{210}Pb and ^{137}Cs isotopes, the ^{14}C isotopes brought additional resolution of ages throughout the core to a depth of 89 cm down, where the age was determined to be 5,400 cal year BP, and a probable disconformity at 45 to 63 cm downcore that dated from 1,205 to 3,490 cal year BP. ^{14}C measurements provide ages for 26 cm at 360 cal year BP, 39 cm at 980 cal year BP, 42 cm at 1,155 cal year BP, 45 cm at 1,180 cal year BP, 60 cm at 3,045 cal year BP, 61 cm at 3,100 cal year BP, and 89 cm at 4,710 cal year BP (Figure 7).

Sedimentation rates from the surface to 4 cm were 4 mm yr^{-1}, which is the highest sedimentation rate in the core. Depth of 4 to 9 cm averaged 1 mm yr^{-1}, 9 to 47 cm averaged 0.3 mm yr^{-1}, 47 to 60 cm averaged 0.07 mm yr^{-1} (the lowest rate recorded), and 60 to 89 cm averaged 0.14 mm yr^{-1} (Table 5; Figure 7). These estimated values include any disconformities, degradation, mineralization, and/or compaction throughout the depositional history.

Above 45 cm, or prior to 1,200 cal year BP, the calculated median and mean sedimentation rates were 0.035 cm/yr and 0.072 cm/yr, respectively, while the minimum and maximum sedimentation rates were 0.021 cm/yr and 0.455 cm/yr, respectively. Below 63 cm, or after 3,490 cal year BP, compaction of the sediment is clear with the calculated median and mean sedimentation rates being 0.013 cm/yr and 0.014 cm/yr, respectively, while the minimum and maximum sedimentation rates were 0.013 cm/yr and 0.017 cm/yr, respectively.

Table 5. *Averaged sediment accumulation rates of Siskiwit Bay core sediment. Depths ranging from 0 to 9 cm were determined using lead-210 and cesium-137 isotopes, while depths of 10-89 cm were determined using carbon-14 dating and the plum model's range of uncertainties.*

Cal Year BP	Section Depth (cm)	Linear Sediment Accumulation Rate (mm/year)
0 - 11	0 - 4	4.00
11 - 58	4 - 9	1.00
58 – 1,269	9 - 47	0.30
1,269 – 3,254	47 - 60	0.07
3,254 – 5,405	60 - 89	0.14

2.3.2 Elemental Composition

The highest percent nitrogen (%N) of 0.3% was found at the surface (0 - 1 cm; Figure 8). The values ranged from 0.0% to 0.3%, with a general increase towards the surface, with a mean of 0.1% (Figure 8). Percent organic carbon (%OC) ranged from 0.1% to 2.3%, steadily increasing from mid-core to the surface, with a mean of 0.88% ± 0.04% (Figure 8). On the other hand, the lower portions of the core had an overall average of 0.685%. The highest %OC, 2.3%, was found at the surface, denoted at 1 cm (Figure 8). The C:N molar ratios (mole:mole) ranged from 10.5 to 15.5, with an average of 11.9 and a maximum of 15.5 at 14 cm. For most of the samples, the C:N molar ratio decreased systematically with increasing bulk density (Figure 10). Additionally, when C:N molar ratios are paired with the measured $\delta^{13}C$, from -27.9‰ to -24.4‰ (mean of -25.8‰ ± 0.02‰;

Figure 8), the primary source of organic matter was identified to be likely lacustrine algal matter with influential factors of C3 land plants (Figure 9).

From 5,400 to 3,400 cal year BP, %OC ranged from 0.174% to 0.905%, with a median and average of around 0.730% and 0.685%, respectfully. From 3,490 to 1,200 cal year BP, %OC varied widely, though the median and average %OC were around 0.296% and 0.321%, respectively (Figure 8). The disconformity, overall, had the lowest %OC concentrations, as well as the lowest recorded %OC measurement through the entire core, 0.01% at 56 cm (2,710 cal year BP) and 63 cm (3,490 cal year BP) (Figure 8). Finally, from 1,205 cal year BP to 2021, there is a steady increase in %OC, with a mean of 1.40% ± 0.04% (Figure 8), reflecting an increase in loading of organic matter compared to the rest of the core.

From 5,400 to 3,400 cal year BP, $\delta^{13}C$ ranged from -27 to -25‰ (Figure 8), within the lacustrine algae and C3 land plants ranges, while C:N in the lower core ranged from 10.5 to 13.4 (Figure 9). From 3,490 to 1,205 cal year BP, $\delta^{13}C$ ranged from -25.4 to -24.9‰ (Figure 8), also within the lacustrine algae and C3 land plant ranges, while C:N ranged from 11.8 to 14.2 (Figure 9). Finally, from 1,205 cal year BP to 2021, $\delta^{13}C$ ranged from -26.4 to -24.5‰ (Figure 8; Figure 9), also within the lacustrine algae and C3 land plant ranges, C:N ratios alternated within the range of 10.5 to 15.5 (Figure 9), above the known algal ratios of 4 to 10, but below the known vascular land plants ratios of greater than 20 (Figure 4; Meyers, 1994).

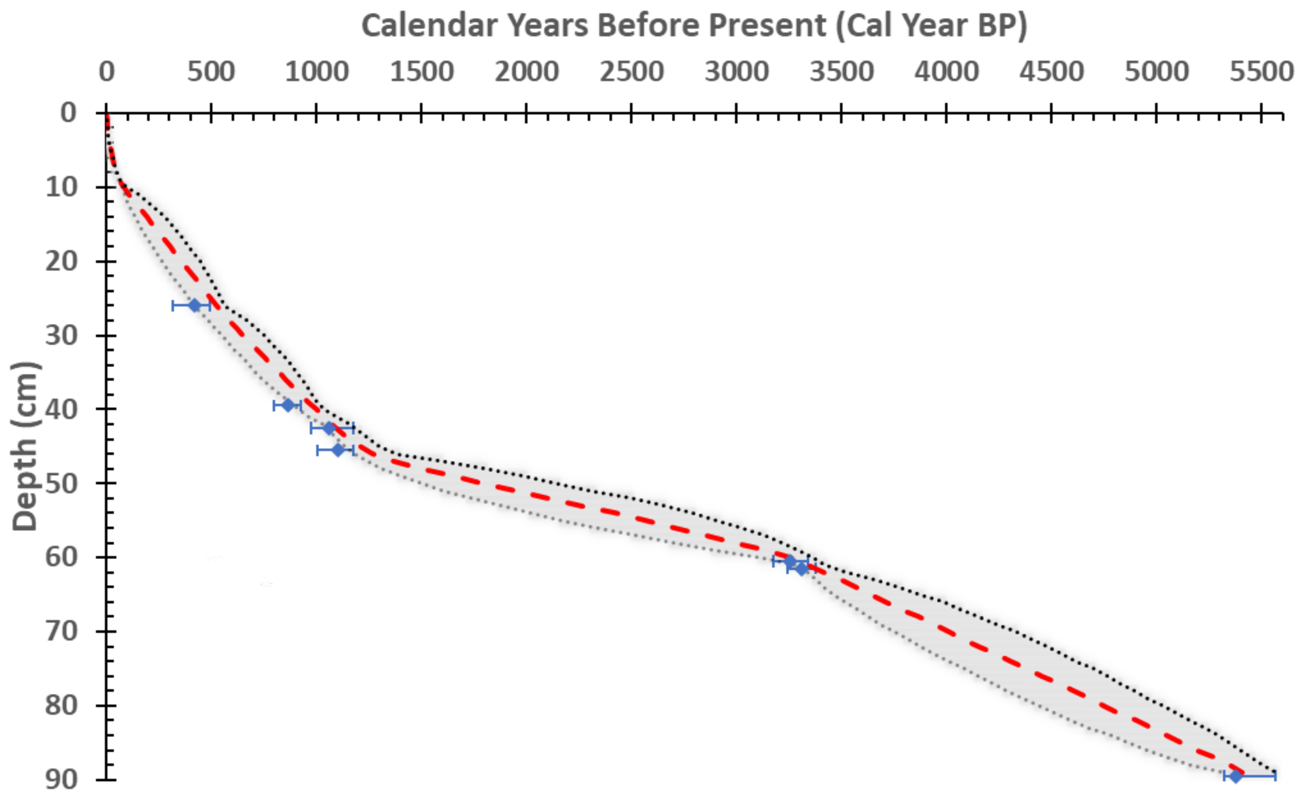

Figure 7. *PLUM age model program output (Aquino-Lopez et al., 2018, 2020). The blue points within the shaded region represent the depths at which carbon-14 was collected. Red dotted-lines are the median age correlations between each carbon-14 measurement. The grey-shaded region surrounding represents the error associated with the estimated ages.*

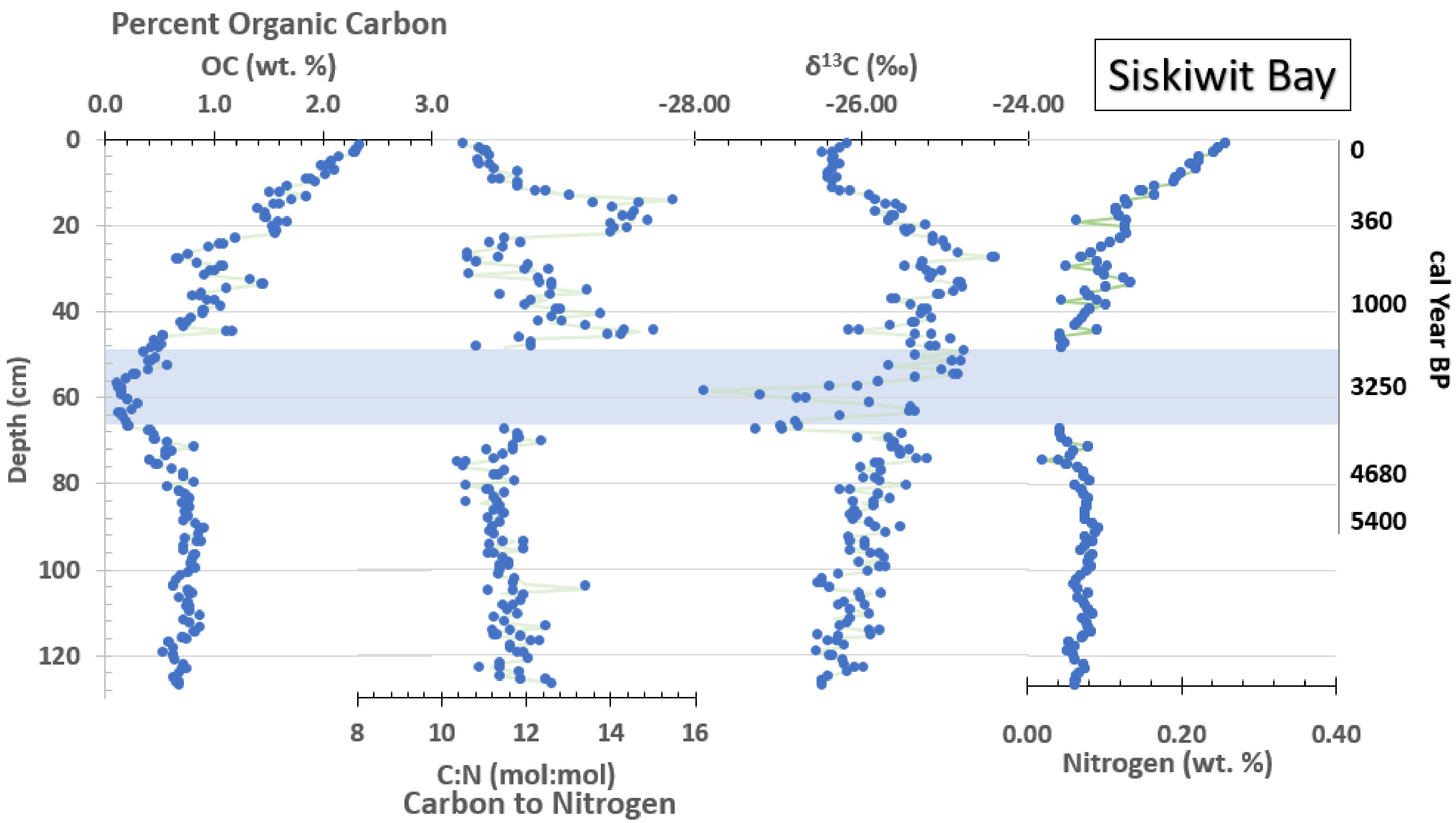

Figure 8. *Organic Carbon (left; wt. %), Carbon to Nitrogen ratio (middle-left; mol:mol), Isotopic Carbon ($\delta^{13}C$; middle-right; ‰), and Nitrogen (right; wt. %) plotted against depth (cm). The blue highlighted section correlates to peaks in pigment concentrations downcore and represents ages from 3,940 to 1,790 years old. Percent organic carbon (%OC) downcore is parallel to the percent nitrogen (%N) downcore, meaning they increase and decrease in similar manners at the same time intervals. The C:N Ratio has a break in the data due to nitrogen levels being outside the detection limit (LOD).*

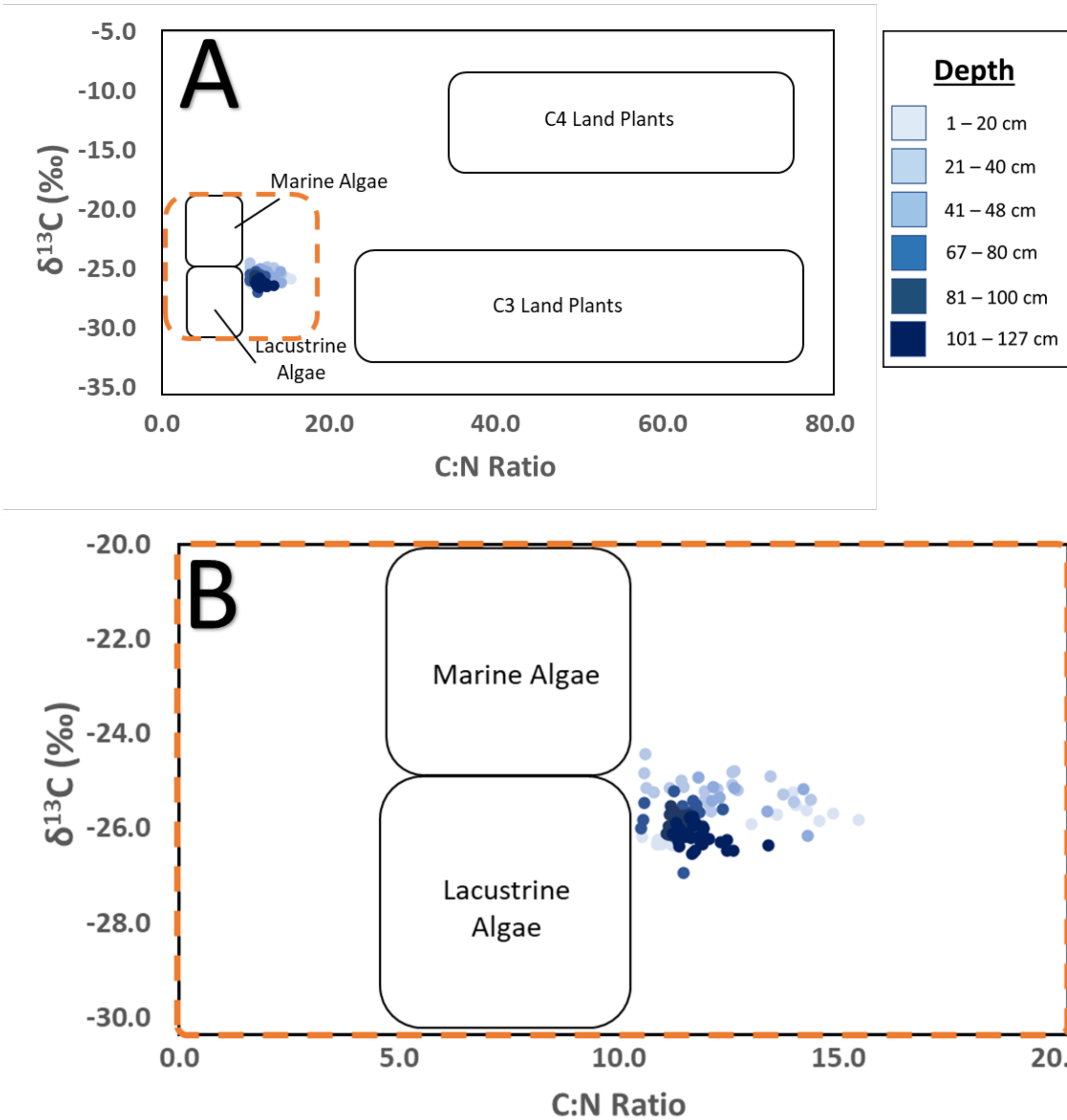

Figure 9. *The bulk identifier graph (A) related C:N ratios of Siskiwit Bay and the found stable isotope values to identify primary source of organic matter as lacustrine algal matter with an influence of C3 land plants. This graph is adapted from Meyers 1994. Within Figure 9A, is an orange outlined zone, this is correlated to Figure 9B.*

Organic matter includes components of organic compounds (hydrogen, nitrogen, oxygen, etc.), and is not limited to just carbon, like organic carbon content is. Within the deeper sediment, below 63 cm or prior to 3,490 cal year BP, organic matter content ranges from around 0.8% to 6.9% (Figure 10), with an average of approximately 4%. Coinciding at this time, carbonate ($CaCO_3$) weight percent (wt%) ranged from around 0.9% to 3.2% (Figure 10). The residual make-up of the sediment, in turn, ranged from 91.5% to 98.4% (Figure 10), with an average of 93.8%. Specifically, from 78 to 127 cm there are relatively stable values of organic matter content around 4% - 6% (Figure 10). Between 63 to 43 cm, or 3,490 to 1,200 cal year BP, organic matter content ranges from around 0.6% to 2.7% (Figure 10), with an average of approximately 1.4%. Coinciding at this time, $CaCO_3$ wt% ranged from around 0.7% to 1.8% (Figure 10), with an average of 1.2. The residual make-up of the sediment, in turn, ranged from 95.6% to 98.7% (Figure 10), with an average of 97.4%. Above 45 cm, or after 1,205 cal year BP, organic matter content ranges from around 2.5% to 7.5% (Figure 10), with an average of approximately 4.7%. Coinciding at this time, $CaCO_3$ wt% ranged from around 1.8% to 4.0% (Figure 10), with an average of 2.6%. The residual make-up of the sediment, in turn, ranged from 88.5% to 95.7% (Figure 10), with an average of 92.6%. Finally, present day organic matter content (0 cal year bp; 2021) is around 7.5% (Figure 10).

In addition, below 63 cm or prior to 3,490 cal year BP, organic matter mass accumulation rates (MAR) range from around 0.16 to 0.52 g/cm^2 ka yr (Figure 11), with an average of approximately 0.34 g/cm^2 ka yr. Coinciding at this time, $CaCO_3$ MAR ranged from around 0.14 to 0.33 g/cm^2 ka yr (Figure 11), with an average of about 0.23 g/cm^2 ka yr. The residual MAR of the sediment, in turn, ranged from 8.6 to 20.6 g/cm^2 ka yr (Figure

11), with an average of 11.5 g/cm^2 ka yr. Between 63 to 45 cm, or 3,490 to 1,200 cal year BP, organic matter MAR ranges from around 0.07 to 0.32 g/cm^2 ka yr (Figure 11), with an average of approximately 0.14 g/cm^2 ka yr. Moreover, $CaCO_3$ MAR ranged from around 0.08 to 0.25 g/cm^2 ka yr (Figure 11), with an average of 0.13 g/cm^2 ka yr. The residual MAR of the sediment, in turn, ranged from 6.0 to 20.7 g/cm^2 ka yr (Figure 11), with an average of 10.9 g/cm^2 ka yr. Above 45 cm, or after 1,205 cal year BP, organic matter MAR ranges from around 0.53 to 4.4 g/cm^2 ka yr (Figure 11), with an average of approximately 1.1 g/cm^2 ka yr. Additionally, $CaCO_3$ MAR ranged from around 0.33 to 2.2 g/cm^2 ka yr (Figure 11), with an average of 0.6 g/cm^2 ka yr. The residual MAR of the sediment, in turn, ranged from 12.1 to 53.6 g/cm^2 ka yr (Figure 11), with an average of 20.1 g/cm^2 ka yr.

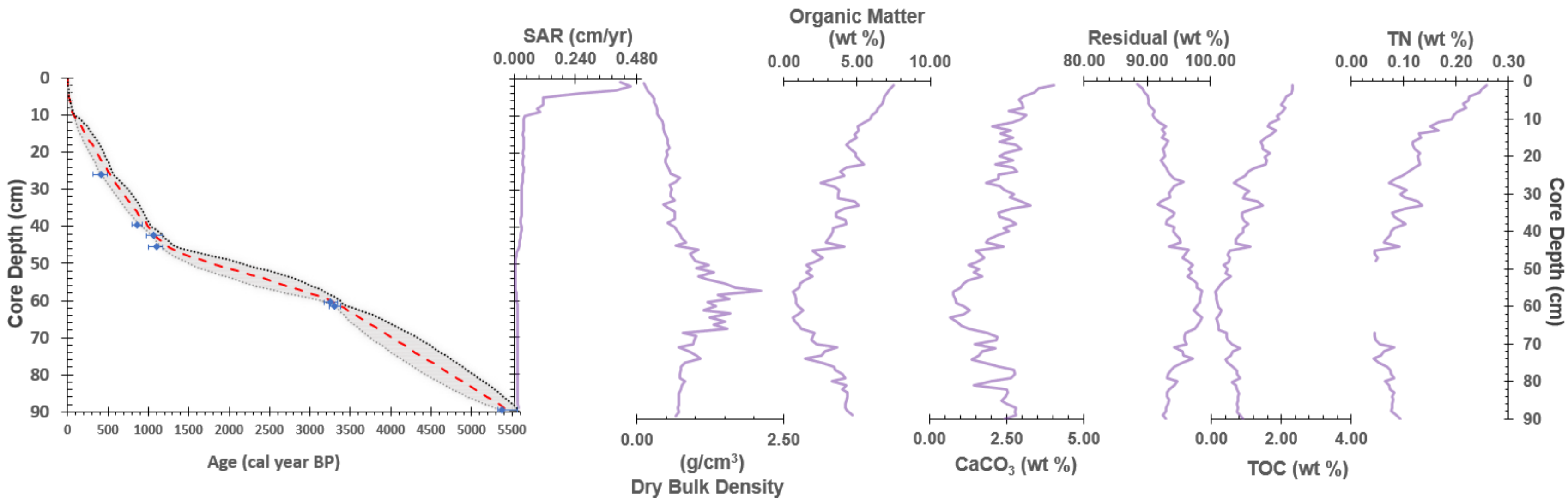

Figure 10. *Siskiwit Bay stratigraphic column and age model depicting the median (red-dotted line), 90% uncertainty range (grey lines), control points (blue circles), and 2σ uncertainty range (brackets) for each control point; sediment accumulation rate (SAR); dry bulk density (g/cm^3); % weight results for organic matter (LOI), carbonate (LOI), residual material (LOI), total organic carbon, and total nitrogen.*

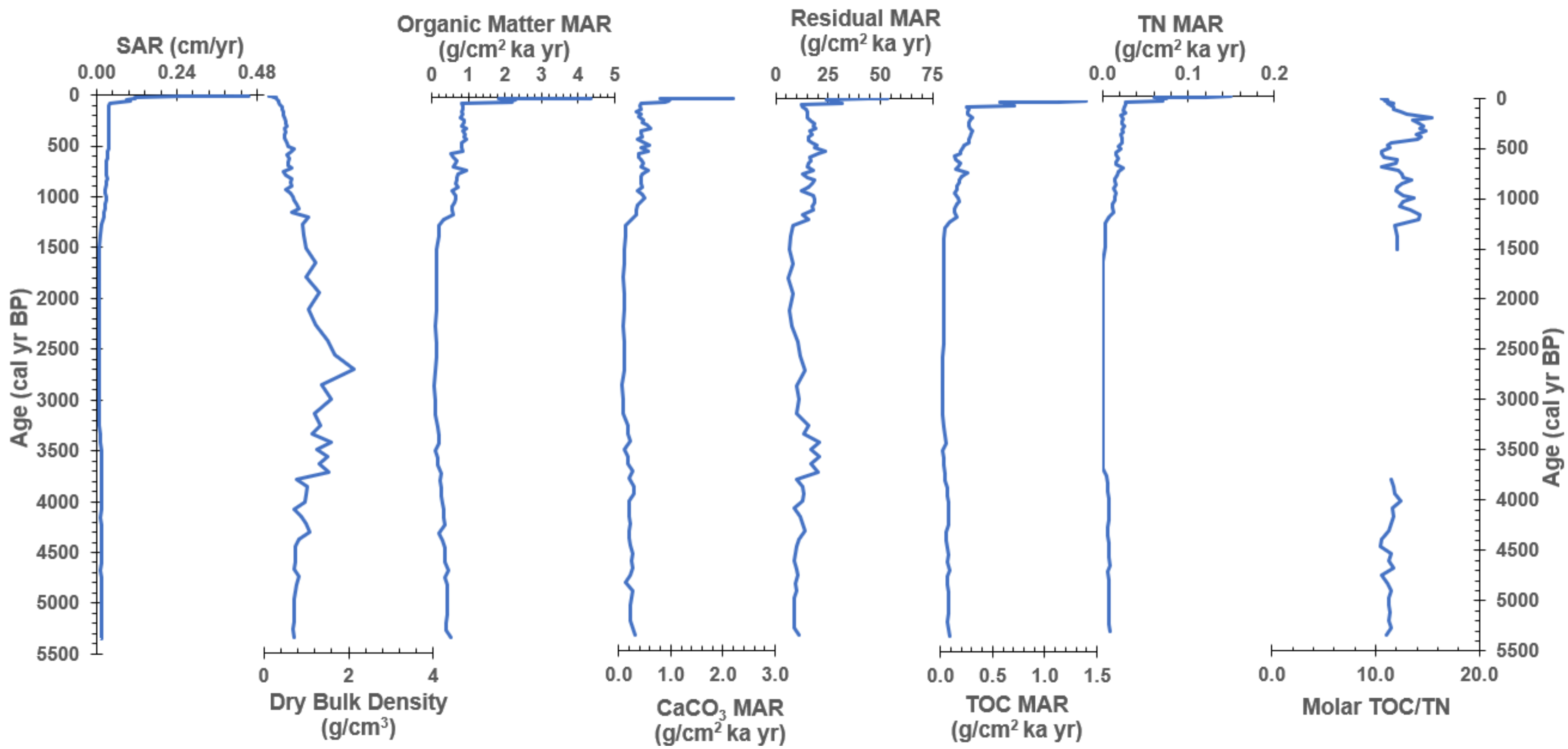

Figure 11. *Siskiwit Bay sediment accumulation rate (SAR), dry bulk density, organic matter mass accumulation rate (MAR), carbonate mineral MAR, residual material MAR, TOC MAR, TN MAR, and Molar TOC/TN data.*

2.3.3 Siskiwit Lake Bloom Phytoplankton Pigment Content

The 2021 Siskiwit Lake bloom showed predominantly cyanobacterial and chlorophyte pigments. The most abundant pigments were pheophytin-a (3.48 mg/gOC) and Chl-a (2.87 mg/gOC) (Table 6; Figure 12). Cyanobacteria pigments (aphanizophyll, canthaxanthin, echinenone, zeaxanthin, and myxoxanthophyll; Table 1; Table 6) constituted approximately 18.61% of the total pigment biomass, diatom pigments (diadinoxanthin, diatoxanthin, fucoxanthin, violaxanthin; Table 1; Table 6) represented 10.9%, and both notably higher than the 8.24% (Chl-b, neoxanthin, and violaxanthin; Table 1; Table 6) contributed by green algae and chlorophytes (Figure 12). The final component consisted of 62.24% (chlorophyll-a, pheophytin-a, and β-carotene; Table 1; Table 6; Figure 12).

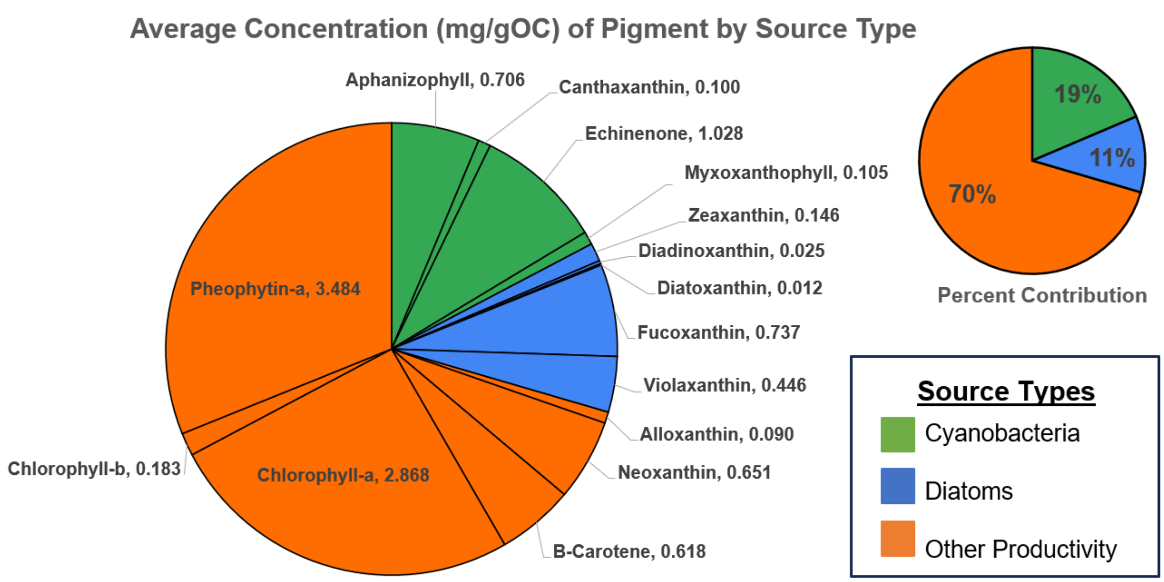

Figure 12. *Average pigment concentrations (mg/gOC) in water surface samples from Siskiwit Lake 2021 bloom. Pigments are grouped according to general source type, with diatoms in blue, cyanobacteria in green, and other/total productivity markers in orange. Percent composition of total organic biomass (%) per source type is shown in the upper left hand corner mini pie chart, which was grouped according to Table 6.*

Table 6. *Average individual phytoplankton pigment contributions in 2021 Siskiwit Lake bloom. Concentrations are listed in mg/gOC, along with their percentage of the total biomass present (%) and source type. See Table 1 for relevant citations.*

Pigment	**Average Concentration** (mg/gOC)	**Percent of Total Biomass** (%)	**Source**
Aphanizophyll	0.706	6.30	*Cyanobacteria*
Canthaxanthin	0.100	0.89	*Cyanobacteria*
Echinenone	1.028	9.18	*Cyanobacteria*
Myxoxanthophyll	0.105	0.94	*Cyanobacteria*
Zeaxanthin	0.146	1.30	*Cyanobacteria; Higher Plants*
Fucoxanthin	0.737	6.58	*Diatoms; Dinoflagellates; Brown seaweed*
Diadinoxanthin	0.025	0.23	*Diatoms; Dinoflagellates*
Diatoxanthin	0.012	0.11	*Diatoms; Dinoflagellates*
Violaxanthin	0.446	3.98	*Diatoms; Green Algae*
Alloxanthin	0.090	0.80	*Cryptophytes*
Neoxanthin	0.651	5.81	*Green Algae; Higher Plants*
Chlorophyll-*b*	0.183	1.63	*Green Algae*
Chlorophyll-*a*	2.868	25.61	*Photosynthetic Plants / Microalgae; Diatoms*
Pheophytin-*a*	3.484	31.11	*Degradation product of Chl-a; Zooplankton feces*
β-Carotene	0.618	5.52	*All Plants; Cyanobacteria; Diatoms*

2.3.4 Siskiwit Bay Bloom Phytoplankton Pigment Content

In current day deposits (surface: 0-1 cm) fucoxanthin, a diatom pigment, is the dominant carotenoid, while 5,400 years ago (oldest dated depth) canthaxanthin, a cyanobacteria pigment, is the dominant carotenoid. Siskiwit Bay surface sediments show an increase in overall pigment content (Figure 14) from 4 cm to 1 cm downcore of around 166.1 to 248.3 µg/g OC or 6,540 to 3,560 ng/g dry sediment, respectively, almost twice the total core average of 84.6 µg/g OC or 743 ng/g dry sediment (Figure 14). Diatom pigments increase from 32.8 µg/g OC or 702 ng/g sediment at 4 cm to 85.2 µg/g OC or 1,980 ng/g sediment at 1 cm, averaging 69.1 µg/g OC or 1,570 ng/g sediment, and shows the greatest ratio of that increase within present day deposits (Figure 13B). Cyanobacteria pigments are relatively higher in concentration than diatom pigments until around 790 cal year BP, the first instance where diatom concentrations surpassed those of cyanobacterial pigment concentrations (Figure 14). Of the pigments measured throughout the core, the overall cyanobacterial pigment concentration surpassed the overall diatom pigment concentration 82.8% of the time throughout the core. Total pigment concentrations were highest in 7.1 cal year BP sediment deposits at 286 µg/g OC or 356 ng/g dry sediment. The lowest concentrations of cyanobacteria pigments were measured at 110.1 cal year BP as 3.30 µg/gOC and at 2,860 cal year BP as 35.1 ng/g dry sediment. The lowest concentrations for diatom pigments were measured at 4,680 cal year BP as 2.1 µg/g OC and at 2,860 cal year BP at 16.8 ng/g dry sediment (Figure 14). Overall, all pigment concentrations have increased as deposits get closer to present day.

Below 63 cm, or prior to 3,490 cal year BP, the make-up of phytoplankton pigments was 76% phytoplankton pigment from general productivity, 16% from cyanobacteria-pigments, and 8% from diatom-pigments (Figure 15). Of the cyanobacteria-pigments, canthaxanthin has the highest concentration of 3.88 μg/gOC, while of the diatom-pigments, violaxanthin has the highest concentration of 1.69 μg/gOC. Around 4,700 cal year BP (Figure 14), the lowest concentration of diatom-indicating pigments was observed for the entirety of the sediment core. Additionally, an average of 78.5% of the chlorophyll-a deposited in this interval has since degraded.

Between 63 cm and 45 cm, or 1,200 to 3,490 to 1,200 cal year BP, the make-up of phytoplankton pigments was 80% phytoplankton pigment from general productivity, 13% from cyanobacteria-pigments, and 7% from diatom-pigments (Figure 15). Of the cyanobacteria-pigments, canthaxanthin has the highest concentration of 9.11 μg/gOC, while of the diatom-pigments, violaxanthin has the highest concentration of 4.89 μg/gOC.

Above 45 cm, or after 1,200 cal year BP, to the surface, 82% of the phytoplankton pigment concentrations came from general productivity, 6% from cyanobacteria-pigments, and 12% from diatom-pigments (Figure 15). Between 190 and 790 cal year BP, diatoms and cyanobacteria dominated blooms fairly equally (Figure 14). Prior to 790 cal year BP, the leading phytoplankton pigments suggest a cyanobacteria dominant environment. In relating each pigment's concentration to the overall content, violaxanthin (chlorophytes) and diadinoxanthin (diatoms) dominate overall percentages for a majority of the downcore values, except within present-day deposits, where fucoxanthin (8.61 μg/gOC; diatom) and canthaxanthin (2.23 μg/gOC; cyanobacteria) concentrations dominate (Figure 13). The lowest concentration of cyanobacteria pigments was at ~110 cal year BP (Figure 14). Cyanobacteria-indicating pigment concentrations were highest in present day sediment deposits.

In the upper layers of the Siskiwit Bay sediment core, 0 cm to 45 cm, there are peaks in pigment content at 7.1 and 470 cal year BP, or 3 cm and 24 cm downcore (Figure 14). At 7.1 cal year BP, 6% of pigments were cyanobacteria-sourced, 31% were diatom-sourced, and 63% were non-specific (Figure 15). At 470 cal year BP: 4% of pigments were cyanobacteria-sourced, 6% were diatom-sourced, and 90% were non-specific.

Additionally, pigment accumulation rates were calculated, from 5,400 to 3,490 cal year BP (89.5 to 63.5 cm), there is an average of 0.0086 µg/yr for overall pigments and no notable peaks in pigment concentrations here. In addition, from 3,490 to 1,200 cal year BP (63.5 to 45 cm), there is an average of 0.0079 µg/yr for overall pigments and no notable peaks in pigment concentrations here either. While from 1,200 cal year BP (45 cm) to present day, there is an average of 0.33 µg/yr and four notable peaks at 470 (24 cm), 160 (13 cm), 40 (7 cm), and 10 cal year BP (3 cm). At 470 cal year BP (24 cm) cyanobacteria-indicating pigments had a concentration of 0.010 µg/yr, diatom-indicating at 0.014 µg/yr, and other at 0.005 µg/yr. At 160 cal year BP (13 cm) cyanobacteria-indicating pigments had a concentration of 0.010 µg/yr, diatom-indicating at 0.012 µg/yr, and other at 0.008 µg/yr. At 40 cal year BP (7 cm) cyanobacteria-indicating pigments had a concentration of 0.031 µg/yr, diatom-indicating at 0.11 µg/yr, and other at 0.017 µg/yr. Finally, at 10 cal year BP (3 cm) cyanobacteria-indicating pigments had a concentration of 0.18 µg/yr, diatom-indicating at 1.05 µg/yr, and other at 0.098 µg/yr.

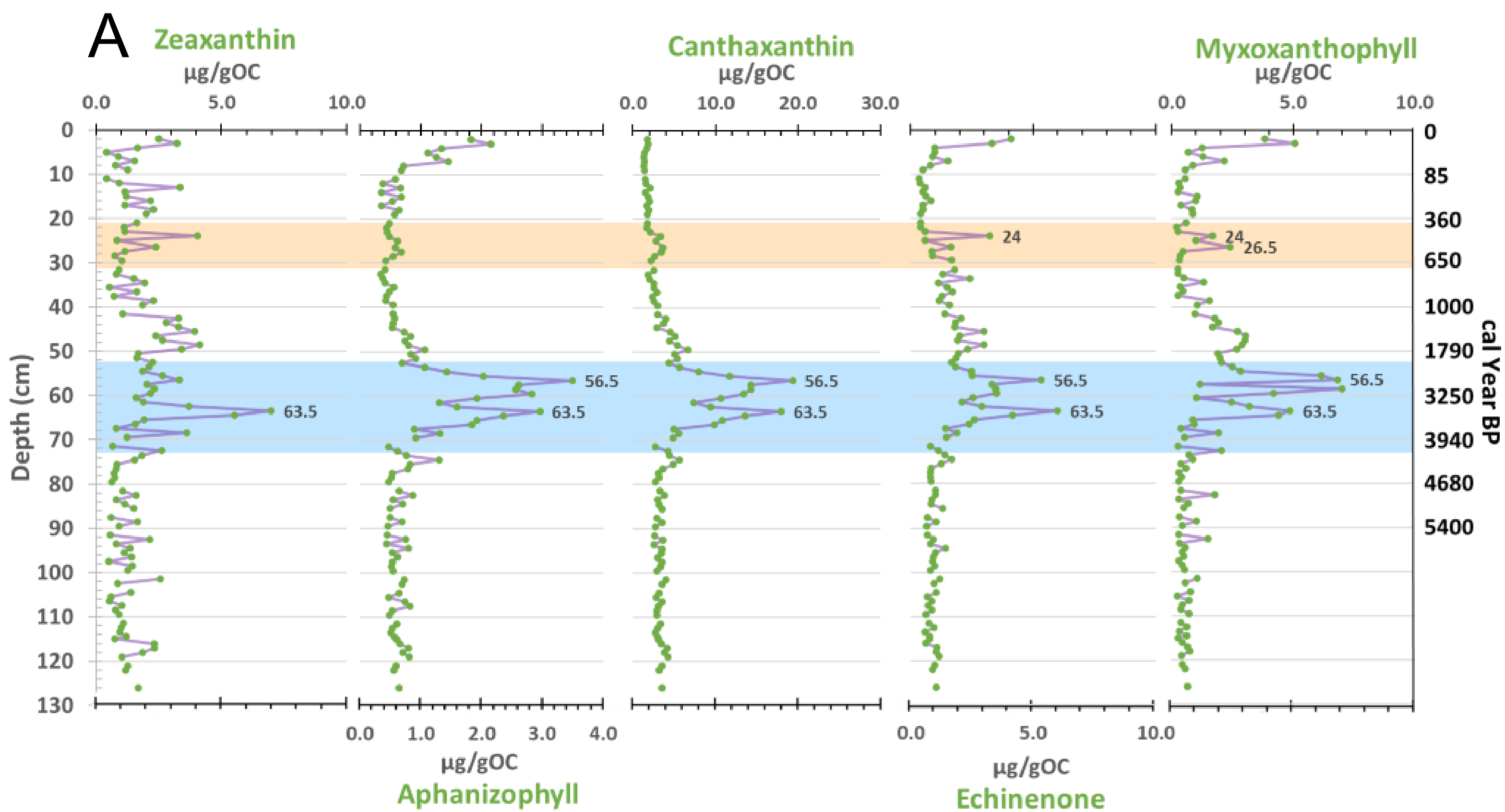

A
Zeaxanthin
µg/gOC
Canthaxanthin
µg/gOC
Myxoxanthophyll
µg/gOC
Depth (cm)
cal Year BP
Aphanizophyll
µg/gOC
Echinenone
µg/gOC
56.5
63.5
24
26.5

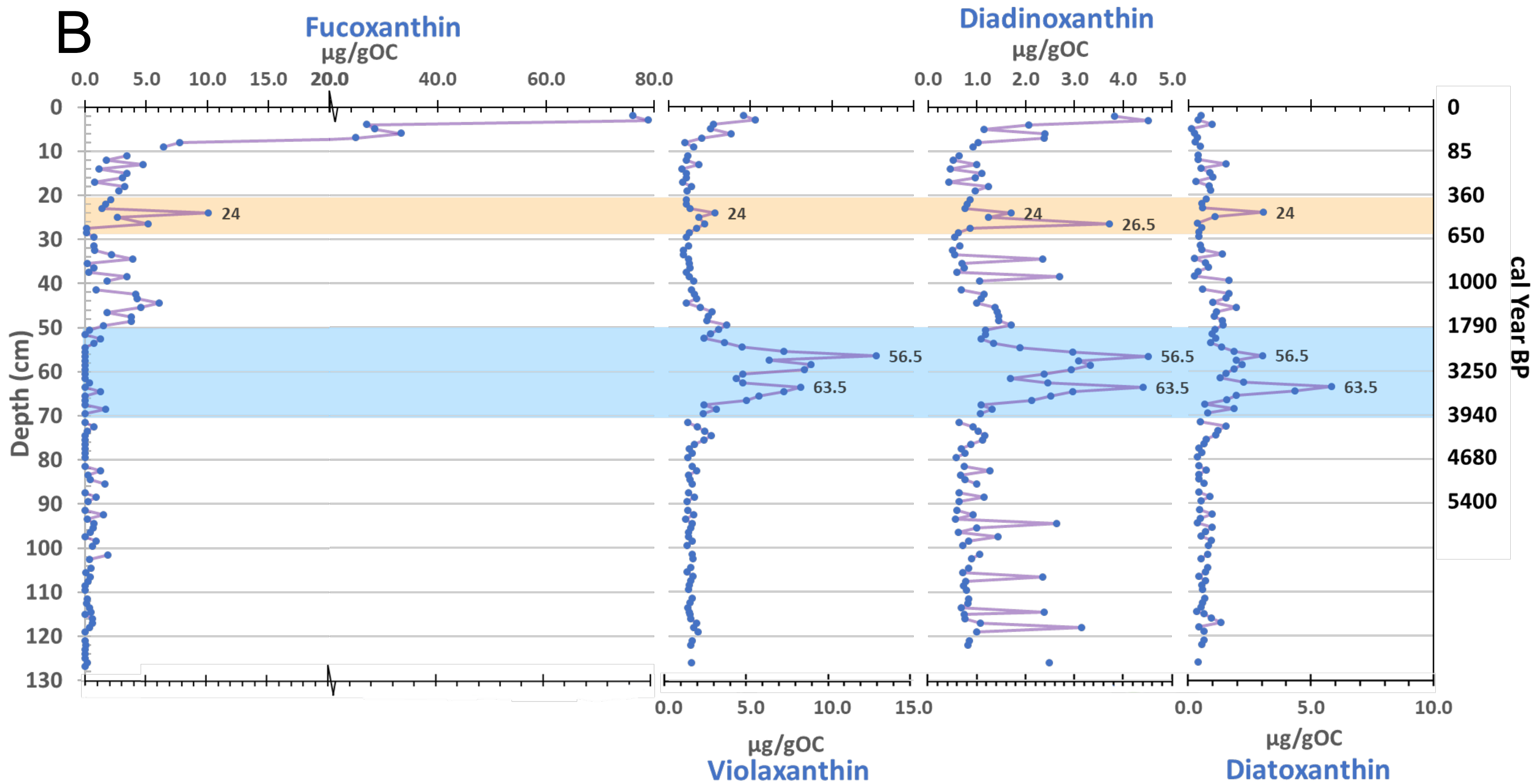

B
Fucoxanthin
µg/gOC
Diadinoxanthin
µg/gOC
Depth (cm)
cal Year BP
Violaxanthin
µg/gOC
Diatoxanthin
µg/gOC
24
26.5
56.5
63.5

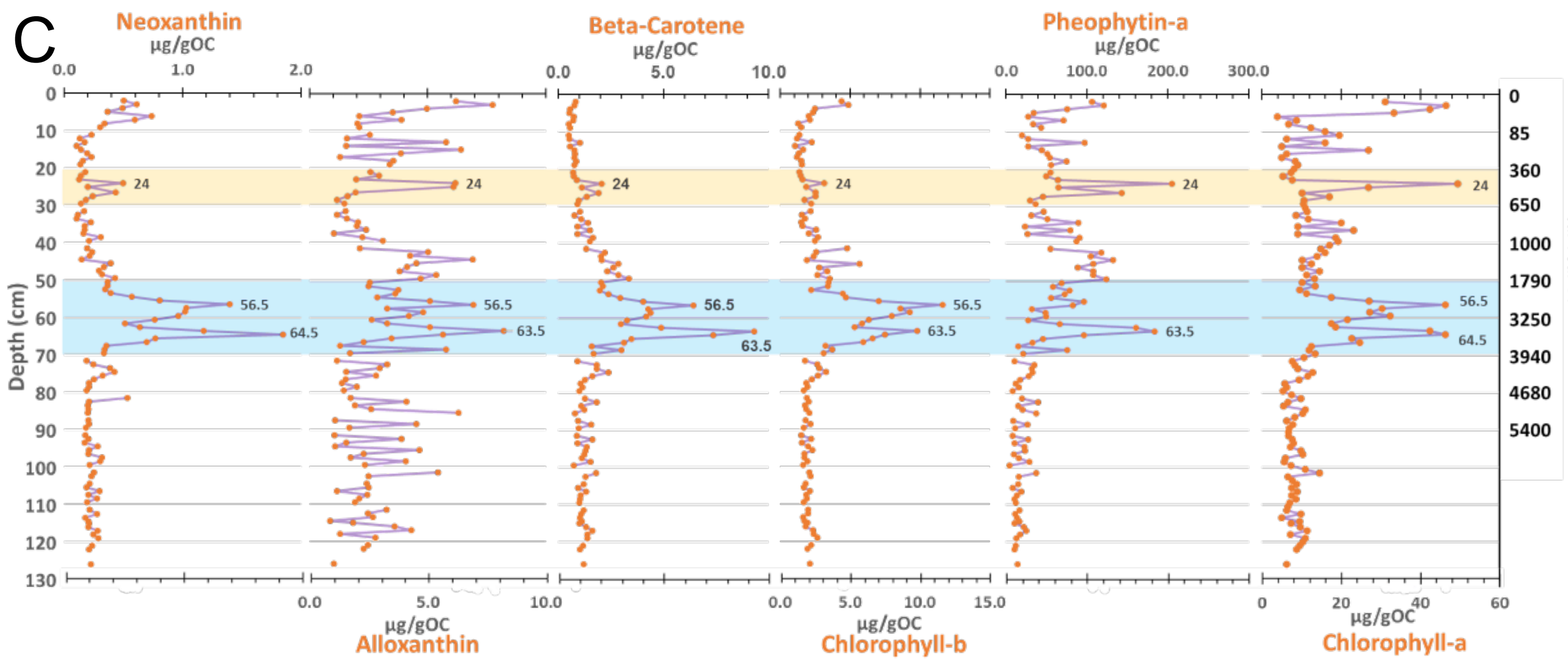

Figure 13. *Down-core concentrations (µg/gOC) of (**A; Green**) carotenoid pigments associated with cyanobacteria (Zeaxanthin, canthaxanthin, echinenone, myxoxanthophyll, and aphanizophyll), (**B; Blue**) diatom pigments (Fucoxanthin, diadinoxanthin, diatoxanthin, and violaxanthin), and (**C; Orange**) other pigments representing total productivity (Pheophytin-a, chlorophyll-a, chlorophyll-b, alloxanthin, neoxanthin, and beta-carotene) in sediments from Siskiwit Bay. Current day deposits (surface: 0-1 cm) show fucoxanthin is the dominant carotenoid, while 5,400 years ago (oldest dated depth) canthaxanthin, a cyanobacteria pigment, had the leading concentration. Common peaks are observable within the highlighted sections, orange represents ages from 360-650 years old and blue is 1,790-3,940 years old. **Note**: Fucoxanthin concentrations also include 19-but-fucoxanthin concentrations.*

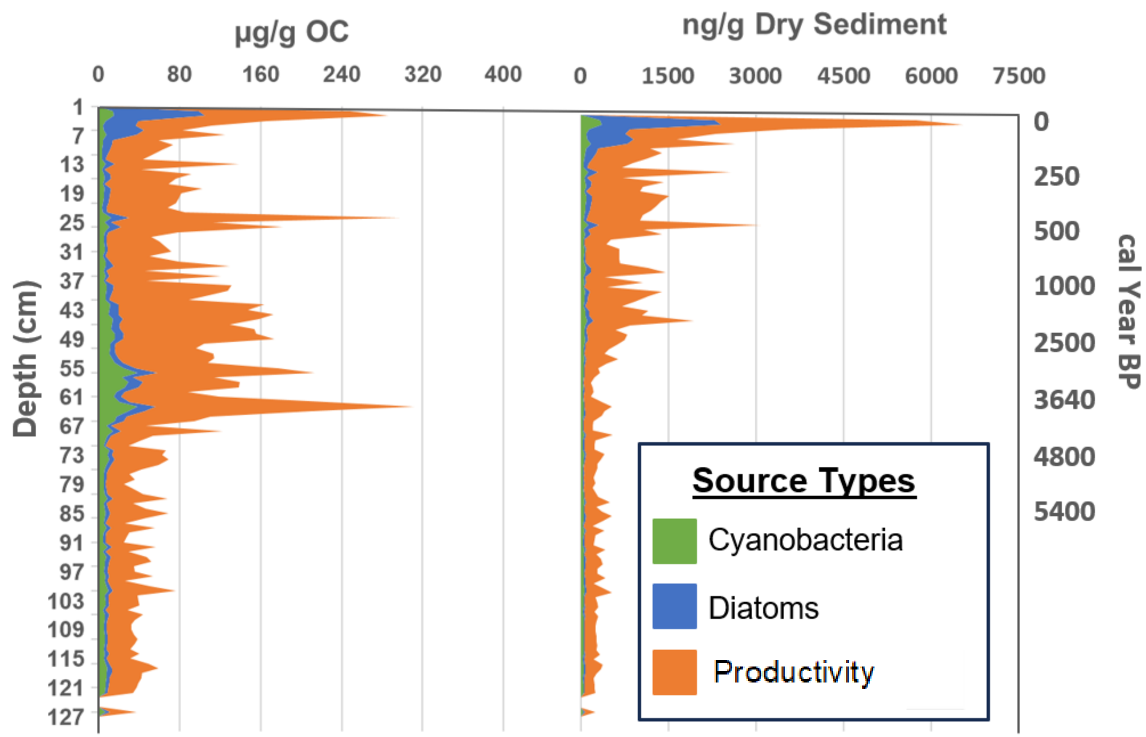

Figure 14. *Within the Siskiwit Bay sediment core, diatom (blue; sum of 19-but-fucoxanthin, fucoxanthin, violaxanthin, diatoxanthin, and diadinoxanthin) cyanobacteria (green; sum of zeaxanthin, aphanizophyll, canthaxanthin, echinenone, and myxoxanthophyll), and other non-specific productivity (orange; sum of pheophytin-a, chlorophyll-a, chlorophyll-b, alloxanthin, neoxanthin, and beta-carotene) pigment concentrations are depicted in micrograms (µg) of pigment per gram of organic carbon (left) and nanograms (ng) per gram of dry sediment (right). Depth (cm) is on the left y-axis, and age (cal year BP) is on the right y-axis.*

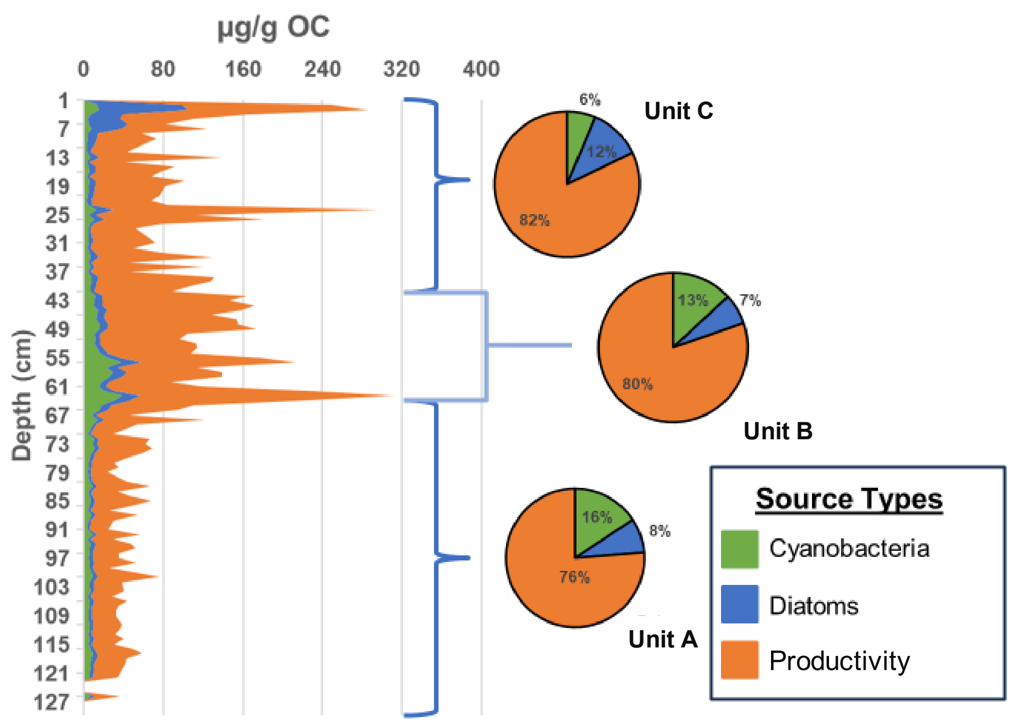

Figure 15. *A summary of the phytoplankton pigments found within Siskiwit Bay core, divided into the three sections: Unit C (top; 45 to 0 cm; 1,205 to 0 cal year BP), Unit B (middle; 63 to 46 cm; 3,490 to 1,205 cal year BP), and Unit A (bottom; 127 to 64 cm; beyond to 3,490 cal year BP). Diatom (19-but-fucoxanthin, fucoxanthin, violaxanthin, diatoxanthin, diadinoxanthin), cyanobacteria (Zeaxanthin, aphanizophyll, canthaxanthin, echinenone, and myxoxanthophyll) and other non-specific productivity pigment (pheophytin-a, chlorophyll-a, chlorophyll-b, alloxanthin, neoxanthin, and beta-carotene) concentrations are present in micrograms (µg) of pigment per gram of organic carbon (OC).*

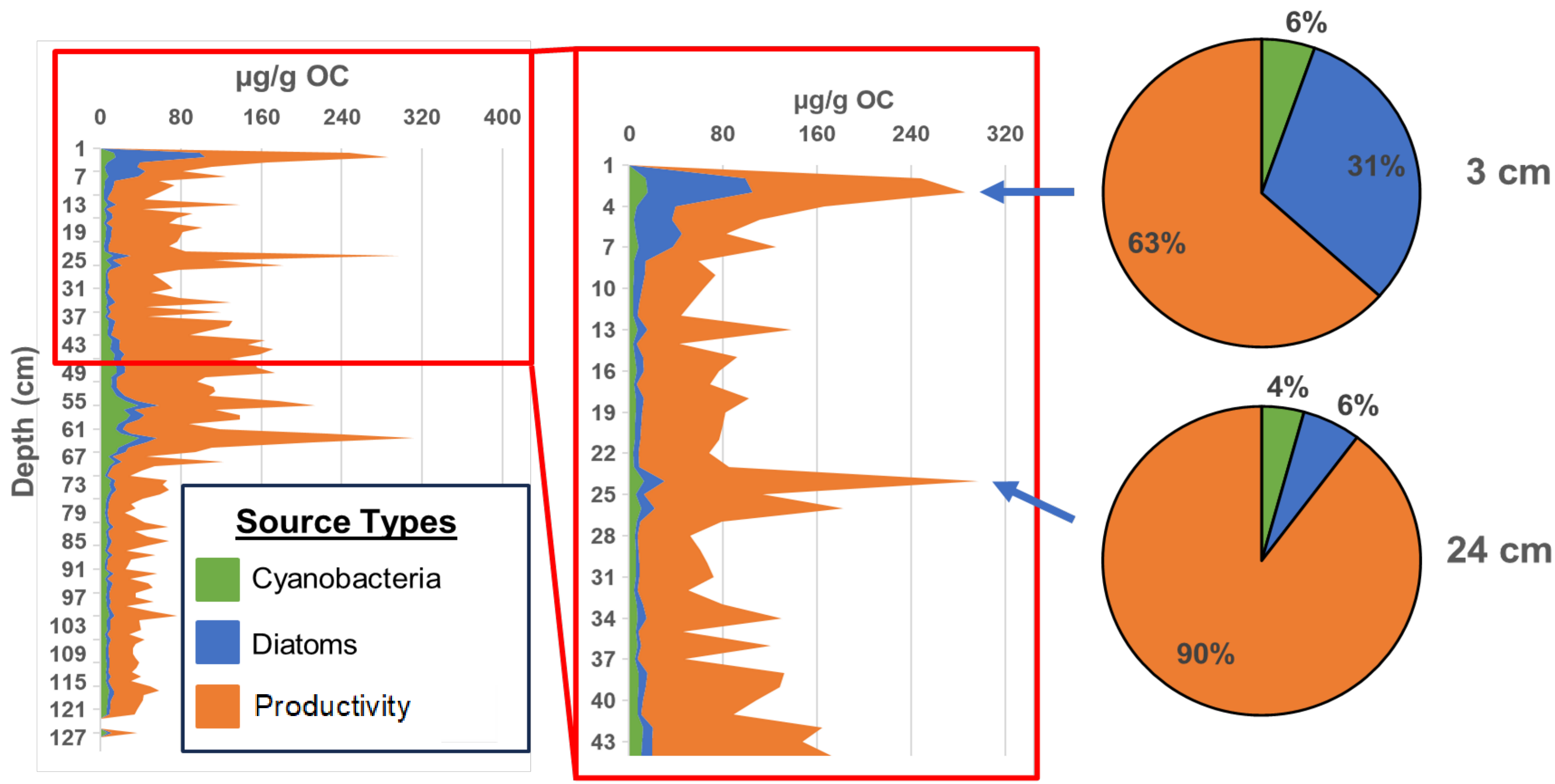

Figure 16. *The pie charts indicate the amount, as a percentage, of each source type out of the whole pigment content measured within the sediment samples at depths of 13 cm and 24 cm. Diatom (blue; sum of 19-but-fucoxanthin, fucoxanthin, violaxanthin, diatoxanthin, and diadinoxanthin) cyanobacteria (green; sum of zeaxanthin, aphanizophyll, canthaxanthin, echinenone, and myxoxanthophyll), and other non-specific productivity (orange; sum of pheophytin-a, chlorophyll-a, chlorophyll-b, alloxanthin, neoxanthin, and beta-carotene) pigment concentrations are depicted in micrograms (µg) of pigment per gram of organic carbon (OC).*

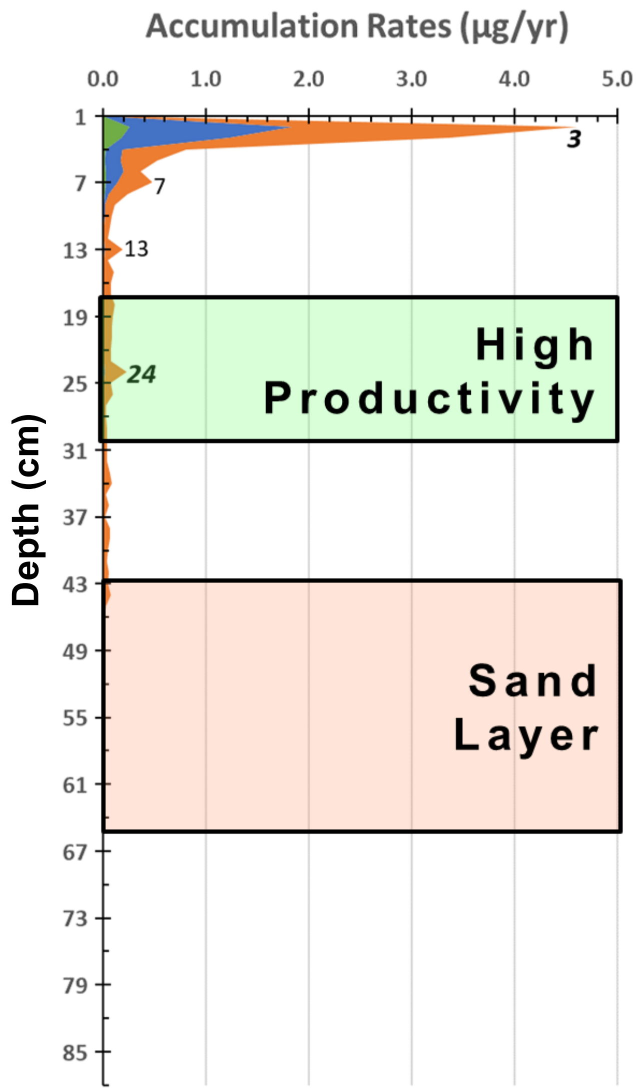

Figure 17. *Estimated pigment deposition in terms of micrograms (µg) per year (x-axis) versus sediment depth in centimeters (y-axis). The greater concentrations of pigments found within the upper regions of the core. This is likely due to accumulation rates not accounting for degradation. Four points of interest are labeled (3 cm, 7 cm, 13 cm, and 24 cm) where large changes in pigment deposition are observed.*

2.3.5 Mineral Elemental Content

Abundances of Titanium (Ti) have an overall decreasing trend towards the surface, with the additional and more significant drops in abundances around 1,205 cal year BP (45 cm downcore; Figure 18). Silicon (Si) also displays a general decreasing trend towards the surface, with a significant dip around 1,205 cal year BP, or 45 cm downcore, akin to the trend seen with Ti (Figure 18). Potassium (K) has similar characteristics to the other elements with its general decreasing trend towards the surface along with its decrease in abundance around 1,205 cal year BP (45 cm) (Figure 18). Pb content increases up core from the bottom, with the lowest value at 10 cm (Figure 18). The ratio of Si:Ti decreases towards the surface, with a more significant decrease at 810 cal year BP (35 cm downcore) and 1,180 cal year BP (44 cm) (Figure 19). These are accompanied by an increase in Si around 1,270 cal year BP (46 cm). There is also decreased K:Ti values from 2,710 cal year BP (53.6 cm) to 810 cal year BP (34.8 cm) (Figure 19). LOI and XRF analyses together confirm and identify dense sand layers at 52.5 to 45.5 cm, or 2,270 to 1,205 cal year BP, and 63.5 to 55.5 cm, or 3,490 to 2,560 cal year BP.

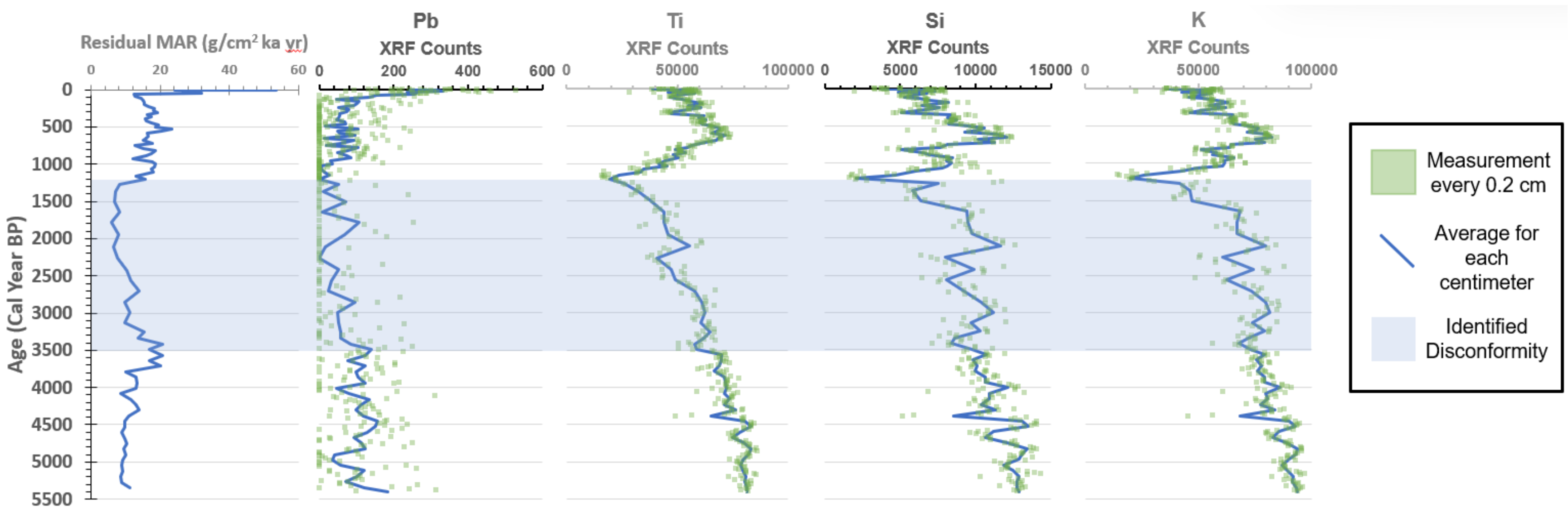

Figure 18. *Downcore plots of residual minerogenic content and elemental data produced from loss on ignition (LOI; far-left) and x-ray fluorescence (XRF). On the far-left graph residual mass accumulation rate in g/cm^2 ka yr is plotted against age in cal year BP. On the other graphs, the x-axis represents the number of XRF counts, while on the y-axis, age is represented in terms of calendar years before present (cal year BP). Each green square represents a data point, these occur every 0.2 cm. The solid blue line represents the 5-point running average, essentially representing each centimeter, between the raw data points. The blue-highlighted region (around 1,200 to 3,500 cal year BP) represents the identifiable disconformity, where a common dip in elemental composition is present.*

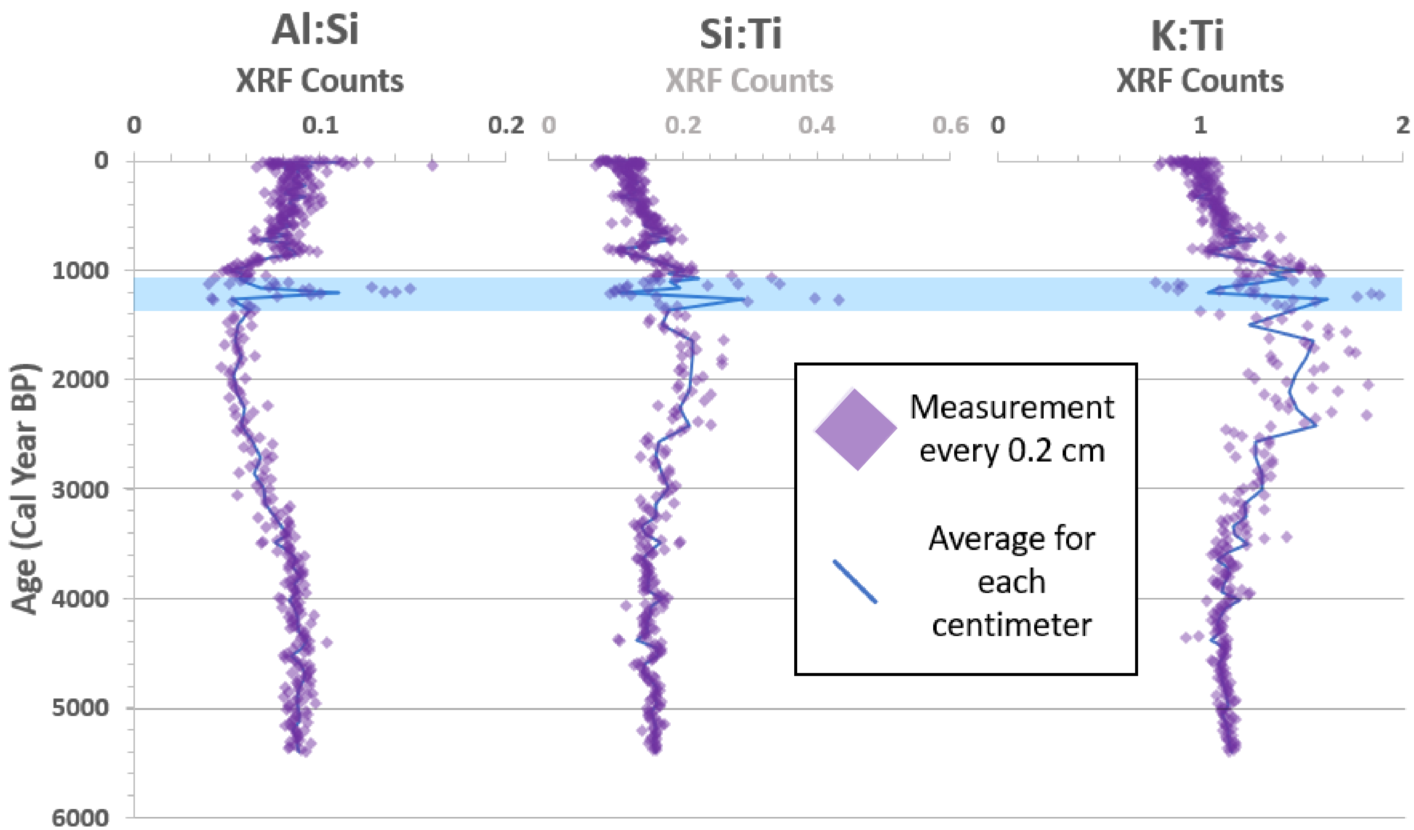

Figure 19. *Downcore plots of elemental ratio data produced from x-ray fluorescence (XRF). The x-axis represents the number of XRF counts, while the y-axis shows calendar years before present (cal year BP). Each purple diamond represents a data point; these occurred every 0.2 cm. The solid blue line represents the 5-point running average, essentially representing each centimeter, between the raw data points. The blue-highlighted region (around 1,200 cal year BP) represents the time of interest, where a common dip in elemental composition is present.*

2.4 Discussion

2.4.1 Overall Trends

Given Lake Superior's cold, oligotrophic system with fewer anthropogenic nutrient inputs relative to the other Laurentian Great Lakes (Kane et al., 2014), cyanobacterial blooms are an unusual phenomenon. There is a wealth of knowledge on drivers of cyanobacterial bloom from previous studies, highlighting the importance of increased water temperatures, the ensuing longer growing season, and major storm events (Reinl et al., 2020; Sterner et al., 2020). What is not well understood is if these blooms are "new" and how their frequency or intensity of today compares to the past. While other studies have used cyanobacterial akinetes to investigate similar questions (Favot et al., 2019), this study identified and measured pigments within the lakebed sediment and reconstructed an idea of the historical environment.

In general, Lake Superior has low sedimentation rates, as quantified from various stations across the lake (Evans et al., 1981). In summary of multiple surrounding aged-core locations, the Apostle Islands and the St. Louis Estuary median and mean sedimentation rates were calculated to be 0.04 cm/yr and 0.78 cm/yr, respectively, and minimum and maximum sedimentation rates of 0.01 cm/yr and 0.32 cm/yr, respectively, were identified (Evans et al., 1981; Sheik et al., 2022). Similarly, a sediment core taken in the St. Louis Estuary region had its deepest unsupported ^{210}Pb at 11.5 cm depth (Smalley, 2013), very similar to the Siskiwit Bay sediment core, in that it is shallow in depth, at 10 cm downcore. Compared to the rest of Lake Superior, the western shoreline adjacent to the Wisconsin coast, where Siskiwit Bay resides, has moderate to high sedimentation rates (0.072 cm/yr; 1,205 cal year BP to 2021) because of the high influx of sediment from shoreline erosion (Kemp et al., 1978; Evans et al., 1981) The sediment accumulates more rapidly within this region, though it is shallower than 100 m, because the sediment input rate surpasses the rate of removal, due to resuspension by storm waves (Evans et al., 1981). In comparison, inland *Spartina alterniflora* salt marsh in Louisiana and Airplane Lake, Mississippi, had sedimentation rates, measured strictly using ^{137}Cs, of 1.35 cm/yr and 1.1 cm/yr, respectfully (Delaune et al., 1978). Combined, these data suggest that the Siskiwit Bay sediment core site was not located in an area with a high rate of sediment accumulation.

Within the Siskiwit Bay sediment core, there is a definite break in the predominant sediment clast sizes, where a large deposition of thick sand lies between 63.5 to 45.5 cm, likely a disturbance in depositional time, also known as a “disconformity”, to be referred to as ‘Unit B’ within this study. This discussion will be fragmented into three sections: Unit A, 127 cm to 63.5 cm, or beyond 5,400 cal year BP to 3,490 cal year BP; Unit B, 63.5 cm to 45.5 cm, or 3,490 to 1,205 cal year BP; and Unit C, 45.5 cm to 0 cm, or 1,205 to 0 cal year BP.

A majority of organic carbon in Siskiwit Bay sediments is sourced from lacustrine algae with a supplementary minor source from terrestrial C3 land plants (Figure 9). Through time, lake level can naturally increase and decrease, which in turn can alter the core sites distance from shore. The distance from shore can impact the sediment composition as there could be more or less terrestrial organic sourcing (Breckenridge, 2013), additionally, resuspension could be a likely factor to consider with lower lake levels. As lake water levels lower, terrestrial organic sourcing can be located closer to the core location, increasing its influence on the depositional location. Additionally, given that production drives $\delta^{13}C$ signatures in Lake Superior (O'Beirne et al., 2017), the corresponding general increase in C:N ratios and %OC concentrations (Figure 8) towards the surface, could also correspond with increased productivity and thus nutrient inputs (O'Beirne et al., 2017; Shaw & Etterson, 2012).

The phytoplankton pigments found within the cyanobacteria bloom in Siskiwit Lake on June 8th, 2021, were predominately from cyanobacteria, chlorophyte, or green algae, matching the pigments typically found in the identified genus of this bloom, Dolichospermum and Microcystis (Egeland, 2016; Sheik et al., 2022). Meaning that though there was not an absence of diatom pigments, they were outnumbered by pigments more associated with the other types of phytoplankton. Siskiwit Lake eventually drains into the southwestern shoreline of Lake Superior, where similar water samples were taken in both 2017 and 2018 from nearby tributaries. These samples did not show dominance of cyanobacteria, but rather only comprising of approximately 1-5% of the total biomass (Reinl et al., 2020).

2.4.2 Unit A (3,490 to 5,400 cal year BP)

Sediment cores taken at Split Rock, MI (2002), Keweenaw, MI (2009), and Isle Royale, MI (2011) from Lake Superior (O'Beirne et al., 2017), measured C:N ratios of slightly under 8, around 6.5 to 7, and slightly under 8 again, respectfully, all had much lower C:N ratios compared to the lower portions of the Siskiwit Bay sediment core. In combination with the %OC in Siskiwit Bay, it is indicated that there is either less carbon input or more nitrogen input to Siskiwit Bay compared to the locations studied by O'Beirne et al.

Within the lower portion of the Siskiwit Bay sediment core, phytoplankton pigments indicate cyanobacteria is in greater abundance compared to diatoms, and to date no other studies are known to have investigated this deep into Lake Superior history using fossil pigments. Additionally, all photosynthetic pigments degrade with time and there are numerous studies that have examined the degradation in known sources of phytoplankton (Bianchi & Findlay, 1991; Jeffrey et al., 1997; Josefson et al., 2012; Leavitt, 1993),for example, chlorophyll-a tends to have low stability, noted by Leavitt & Hodgson, 2001. This natural degradation process is potentially indicative to the lower overall pigment content in Unit A (Figure 14), though this study notes recent increases in pigments with known reliability in long-term preservation in sedimentary records (pheophytin-a, fucoxanthin, diatoxanthin, aphanizophyll, myxoxanthophyll, and β-carotene; Alexson et al., 2018). Meaning that these pigments, diatom-, cyanobacteria-, and general productivity-indicating, may show as in higher concentration compared to other pigments.

2.4.3 Unit B (1,200 to 3,490 cal year BP)

The $\delta^{13}C$ concentrations are within the lacustrine algae and C3 land plant ranges, while the C:N ratios were above algal source ratios of 4 to 10, but below vascular land plant ratios of greater than 20 (Meyers, 1994). Additionally, with minimal change in organic matter MAR around 3500 cal yr BP, it suggests that a larger amount of inorganic material was deposited there, ultimately not reflecting any change in lake phytoplankton but rather just improving the environment for preservation. The decrease in the organic carbon content within the 3,940 to 1,790 cal year BP age range coincides with an increase in pigment content (Figure 8; Figure 13). Due to the low %OC content, the associated phytoplankton pigment concentrations were exaggerated within this region of the sediment core. To compensate for these factors, pigment amounts were correlated to mass of dry sediment per sample (*Appendix: Figure 24)*.

A commonality within the titanium (Ti), silicon (Si), potassium (K), and aluminum (Al) profiles measured using XRF was a decline in concentrations at 45 cm downcore, or 1,205 cal year BP. The significant dip in Si:Ti abundances at 1,205 cal year BP, or 45 cm depth, indicates the time at which the lowest sand deposition rates occurred within the timespan of the sediment core (Boës et al., 2011). High Si:Ti ratios prior to this section of core, suggests greater amounts of silica-rich sand relative to background lithogenic material (Boës et al., 2011). Keeping in mind that over 90% of Lake Superior sediment is lithogenic, glacial silts, some clays, and, in this case, sand. Providing evidence that almost all of the sediment is from catchment erosion (Boës et al., 2011). Additionally, the lowest amount of clay deposition, indicated by Al abundances, was observed at this same 1,205 cal year BP, or 45 cm depth period, meaning that glacial silts from inland erosion were likely deposited at this point (Davies et al., 2015). Lower K:Ti ratios can also be indicative of increased fluxes of clay minerals that are chemically weathered, while higher K:Ti can be a sign of greater erosion or less weathered soils (Brown et al., 2007). The sudden decrease in K:Ti 1,205 cal year BP (45 cm) suggests an increased flux of clay minerals (Figure 19; Boës et al., 2011; Davies et al., 2015). This corresponds to the Al:Si data where there is a peak at 1,205 cal year BP (45 cm) as well, suggesting an increase in clay minerals (Figure 18; Davies et al., 2015). The decrease increased K:Ti values from 2,710 cal year BP to 810 cal year BP (53.6 to 34.8 cm; Figure 19) suggests signs of deeper erosion or less weathered soil (Boës et al., 2011; Davies et al., 2015).

2.4.4 Unit C (2021 to 1,205 cal year BP)

Gradual, long-term increases in %OC and C:N in Siskiwit Bay suggest the possibility of increased terrestrial input to the lake basin or gradual breakdown with time (O'Beirne et al., 2017; Shaw & Etterson, 2012). The highest recorded %OC within the core, 2.3%, was at 1 cm downcore (3 cal year BP), correlating to the cyanobacteria bloom reported within Siskiwit Bay in 2018 (Sterner et al., 2020). The $\delta^{13}C$ concentrations identify a close resemblance to lacustrine algae with the additional influence of C3 land plant (Meyers, 1994). C:N ratios were above algal source ratios of 4 to 10, but below vascular land plant ratios of greater than 20 (Meyers, 1994). However, a cross-plot of C:N versus $\delta^{13}C$ (Figure 9) demonstrates that though autochthonous primary production is the dominant influence on the sedimentary organic record, it is also evident of influential allochthonous sources. Additionally, the increasing values of %OC, %N, and concentrations of pigments from green algae, cryptophytes, and cyanobacteria, seen within the Siskiwit Bay sediment are signs of lake eutrophication (Kane et al., 2014). Similar results were seen as the most consistent evidence of lake eutrophication (Ewing et al., 2020) across seven lakes in south-central Maine and New Hampshire, USA.

Unlike other sections of the core, diatom-indicating pigments have higher concentrations compared to cyanobacteria-indicating pigments since 170 cal year BP, which is supported by previous studies showing that diatoms are the dominating phytoplankton species in Lake Superior (Munawar & Munawar, 1978; Sterner et al., 2020). Despite diatom community dominance, peaks in cyanobacteria-associated pigments correlate with the 2012 bloom and possibly an earlier bloom around 470 cal year BP. This section of the core has the highest concentrations of overall phytoplankton pigment concentrations, providing a parallel that phytoplankton production has increased in present day deposits compared to historical values. This finding coincides with the pigment concentrations found in almost 60% of over 100 lakes studied in North America and Europe (Taranu et al., 2015). Taranu et al. reported that cyanobacterial pigments found within the studied lake's sediment have been increasing substantially since the industrial revolution (Taranu et al., 2015). Additionally, since 1945, cyanobacterial abundance had increased disproportionately relative to the other phytoplankton (Taranu et al., 2015) and it is likely to continue moving forward (Huisman et al., 2018).

In comparison, algal pigments measured in sediment cores from the St. Louis River estuary, the largest water source to the western part Lake Superior, revealed increases in two cyanobacterial pigments, aphanizophyll and myxoxanthophyll, beginning in 1970, with high concentrations since 2000 (Alexson et al., 2018; Sterner et al., 2020). In Siskiwit Bay, fucoxanthin, a diatom-indicating pigment, is the dominant carotenoid with a concentration of around 70 µg/g OC (Figure 13). In a similar study, fucoxanthin was also found to have the highest concentration of the studies of phytoplankton pigments within upper levels of its sediment core, taken in Billings Park, Wisconsin (Alexson et al., 2018).

In correlation to other studies, DNA from three cyanobacterial species were found within the upper 10 cm of a sediment core taken near Isle Royale, MI, about 130 miles northeast of Siskiwit Bay (Sheik et al., 2022). These matched the phytoplankton species and timing of the cyanobacterial bloom suspected in 2012 (Sheik et al., 2022). However, Lake Superior is a dynamic system and different phytoplankton communities are evident in diverse locations (Munawar & Munawar, 1978; Reavie et al., 2018; Sheik et al., 2022), though Siskiwit Bay is likely dominated by diatoms, as it neighbors confirmed diatom-dominated locations, such as the St. Louis Estuary (west) and the Apostle Islands (east), through DNA analysis (Reavie et al., 2014; Sheik et al., 2022; Alexson et al., 2018). For example, Alexson et al. found four embayment's of Lake Superior to be mainly dominated by planktonic centric diatom species. Other studies also confirm that diatoms are the main overall phytoplankton of Lake Superior (Munawar & Munawar, 1978; O'Beirne et al., 2017; Reavie et al., 2014; Sheik et al., 2022). Though, it should be noted that Lake Superior's phytoplankton communities also change seasonally, as conditions affect certain types of phytoplankton (Reavie et al., 2018), such as how cyanobacteria species can adapt more readily to warmer water temperatures and thus anoxic and hypoxic zones, than compared to diatoms (Panigrahi et al., 2013). In general, because of cyanobacteria's ability to adapt to the environment more readily, they can thrive throughout the year (Reavie et al., 2018). In terms of phytoplankton by volume, diatoms, chrysophytes, cryptophytes, and dinoflagellates thrive in the spring, while in the summer, diatoms are the more dominating phytoplankton (Reavie et al., 2018). The resolution of which phytoplankton pigments are measured within the sediment does not necessarily depict the seasonal changes in each phytoplankton species production, but rather a summary snapshot of production within that depositional interval.

2.5 Conclusions

As one of the first studies of sedimentary pigments within the southwestern region of Lake Superior, alongside Alexson et al., this work provides historical context that informs the understanding of modern-day cyanobacteria presence. Pigment biomarkers from cyanobacteria (aphanizophyll, canthaxanthin, echinenone, myxoxanthophyll, and zeaxanthin), diatoms (fucoxanthin, diadinoxanthin, diatoxanthin, and violaxanthin), and non-specific productivity (alloxanthin, neoxanthin, chlorophyll-a, chlorophyll-b, pheophytin-a, and beta-carotene) can be correlated measured as far back as 5,400 years. The largest concentration of cyanobacterial pigments found within the sediment core correlated to the 2012 bloom. Another similar concentration of pigments was found in sediment aging 470 cal year BP, or 1551 AD, suggesting the possibility of high productivity but with uncertainty born by preservation biases which cannot be resolved.

The make-up of the phytoplankton community in Siskiwit Bay, Lake Superior now is primarily dominated by diatoms. Cyanobacteria were in probable higher abundance compared to diatoms, as seen in fossil pigment concentrations downcore. Overall, all phytoplankton productivity has been increasing towards the present day.

Potential future research includes using HPLC to identify cyanobacteria species presence by relating carotenoid content found in a water sample to the carotenoids typically found within certain species. By creating a standard from DNA-sequenced cyanobacteria and its carotenoid content, an unknown cyanobacteria sample can be identified more readily. For example, if the carotenoid content of Microcystis, a toxin-producing cyanobacteria species, was standardized, a water sample with unknown cyanobacteria content can be analyzed for the pigments it contains, and matched or related closely to the standard. This process, though it not a guarantee, could then be used to assist in predicting the presence of toxin-producing cyanobacteria species.

Chapter 3. Appendix

3.1 The Organic Geochemical Record of Siskiwit Lake, Wisconsin, USA

3.1.1 Sample Collection

One core was collected from Siskiwit Lake on July 29th, 2021 (Figure 20), using an Aquatic Instruments Piston Corer and a 2-5/8 in diameter polycarbonate core barrel, in the deepest portions of the lake (3.55 meters). The core's length was 81 cm and was studied for its bulk elemental and isotopic concentrations through depth. Additionally, the core's surface sediment was visually inspected and deemed undisturbed.

3.1.2 Sample Processing

The core was completely extruded into 1 cm samples down the entire length (81 cm) and stored in 24 oz polyethylene Nasco WHIRL-PAKs. Between each centimeter section, the extruder set up and spatula were wiped dry with paper towel to prevent contamination between samples. All extruded samples were frozen at -20°C within 12 hours of collection and then lyophilized to dryness with a LABCONCO Freezone-6 System. After lyophilization, samples were inspected visually for terrestrial organic matter such as leaves and sticks to be used later for carbon-14 (^{14}C) analysis. Then samples were ground and homogenized with a mortar and pestle, weighed, and kept in pre-combusted scintillation vials, and then stored at -20°C until further processing and analysis.

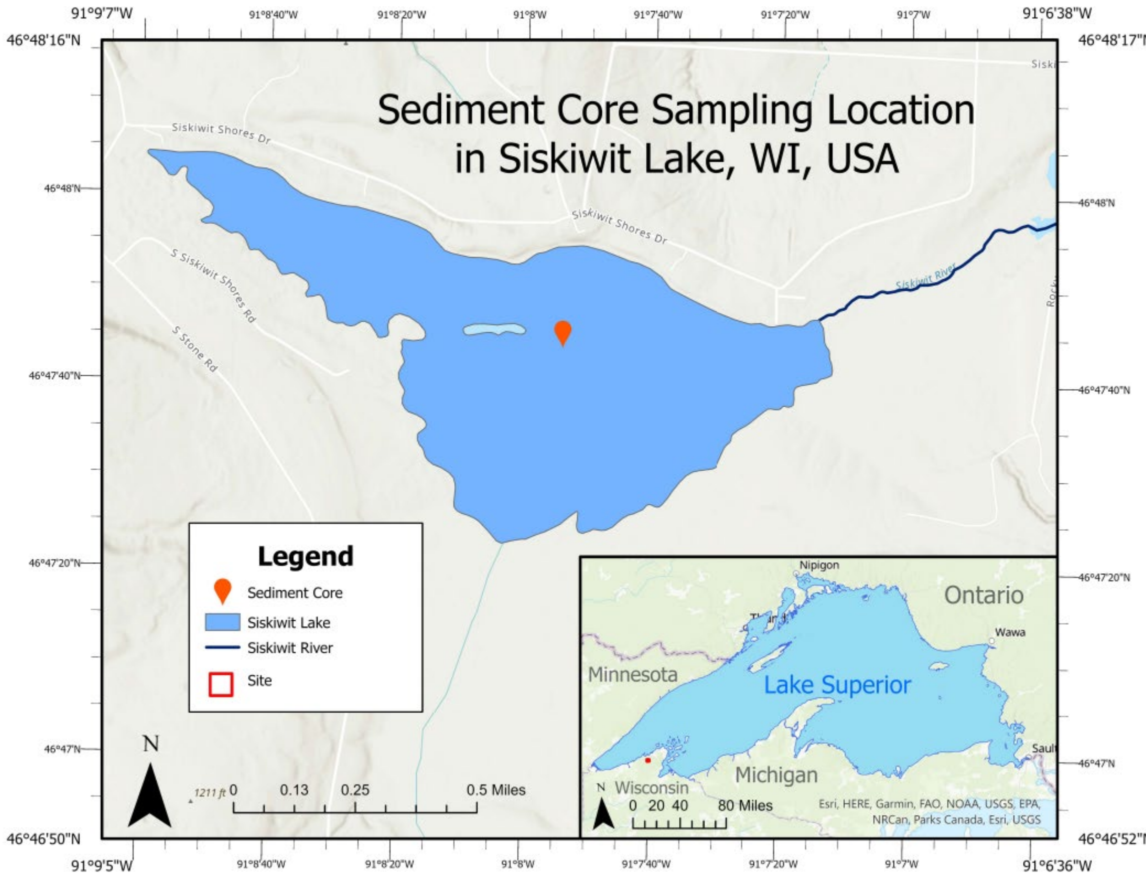

Figure 20. *Sediment core sampling location on Siskiwit Lake at Cornucopia, Wisconsin, USA, on July 29th, 2021. The orange pinpoint displays the exact location (N46.79392°, W91.12994°). Siskiwit Lake, as a potential source of cyanobacteria to Lake Superior, is hydrologically connected to Siskiwit Bay by the waterway highlighted in dark blue (Siskiwit River). The sediment core location was at the deepest point within the lake.*

3.1.3 Bulk Element and Isotope Analysis

Bulk elemental characteristics such as carbon (%OC) and nitrogen (%N) content, were analyzed using a Costech 4010 Elemental Analyzer coupled to a Thermo Fisher Scientific - Finnigan Delta Plus XP isotope ratio mass spectrometer at the Large Lakes Observatory at University of Minnesota, Duluth. For %OC and its associated isotopes ($\delta^{13}C$), carbonates were removed from freeze-dried sediments using the HCl vaporization method (Harris et al., 2001). Stable carbon isotope values are reported in delta notation (Equation 2) relative to the Vienna Pee Dee Belemnite (VPDB) isotopic standard. Samples for N concentration (%N) analysis did not undergo fumigation and were weighed directly into 2x5 mm tin capsules and stored in a desiccator until analysis.

Standards were analyzed every 10 samples to calculate instrument drift. The set of standards used were acetanilide, low-organic content soil (B-2153), and caffeine (Table 3). Precision (1σ) of the internal lab standards was approximately 0.755%OC, 0.218%N, and 0.257‰ for $\delta^{13}C$. Selected samples run in duplicate had measurements within this standard error.

3.1.4 Results

Percent Nitrogen (N) (with precision (1σ) of 0.2% N) is presented in Figure 20. The highest N by weight (wt. %) is 1.4% found at 30 cm. The values were relatively stable throughout the sediment and ranged from 1.1% to 1.4%, with a mean of 1.2% ± 0.08% (Figure 21).

Percent Organic Carbon (%OC) (with precision (1σ) of 0.8%), percent of total OC (by mass), and C:N ratios are presented in Figure 21. Siskiwit Lake %OC by weight (wt %) ranges in total from 16.94% to 22.02% with an average of 19.42% ± 0.04% (Figure 21). There was no apparent trend downcore, though the largest percentages of carbon by weight, ca. 21%, reside relatively at depths ranging from 25 cm to 40 cm, with the maximum of 22.02% at 28 cm depth. Siskiwit Lake exhibited a high variability between the surface, middle, and bottom of the core in C:N molar ratios throughout the sediment record

(Figure 21). The C:N molar ratio ranged from 16.6 to 20.9, with an average of 19.0, and a standard deviation of 0.8.

Stable carbon isotope signatures in Siskiwit Lake identified freshwater or lacustrine organic matter as the primary source, and then with the addition of the C:N ratios, it indicated more C3 Land Plant origin, with influence of Lacustrine Algae organic matter deposits. The $\delta^{13}C$ of these sediment samples range from -28.2‰ to -29.9‰ with an average of -29.0‰ ± 0.4‰ (Figure 21). These values (Figure 22) implied slightly higher allochthonous sourcing, or a higher input of terrestrial particulate organic carbon as compared to Siskiwit Bay (Figure 9). This could be attributed to more direct interactions between the lake water and surrounding land plant establishments, which are introduced to the lake in high concentrations relative to its size, compared to Siskiwit Bay.

3.1.5 Discussion and Conclusion

Elemental and isotopic data obtained from Siskiwit Lake sediment deposits exhibited general signals of dominant aquatic and terrestrial-influenced organic matter sources. $\delta^{13}C$ signatures identified freshwater or lacustrine organic matter as the primary source. With the addition of the C:N ratios, it is indicative of algal sources. Fluctuating deposits of organic matter were found within Siskiwit Lake (Figure 22). Siskiwit Lake showed variation in C:N molar ratios downcore, though when paired with isotopic carbon signatures, organic matter sources were predictably C3 Land Plant in source, though they were slightly less enriched and influenced by Lacustrine Algae sources in Siskiwit Lake (Figure 22).

Construction of an age model on Siskiwit Lake's sediment core was unsuccessful due to the ^{137}Cs peak not being visible, which suggests the loss of some quantity of surface sediments.

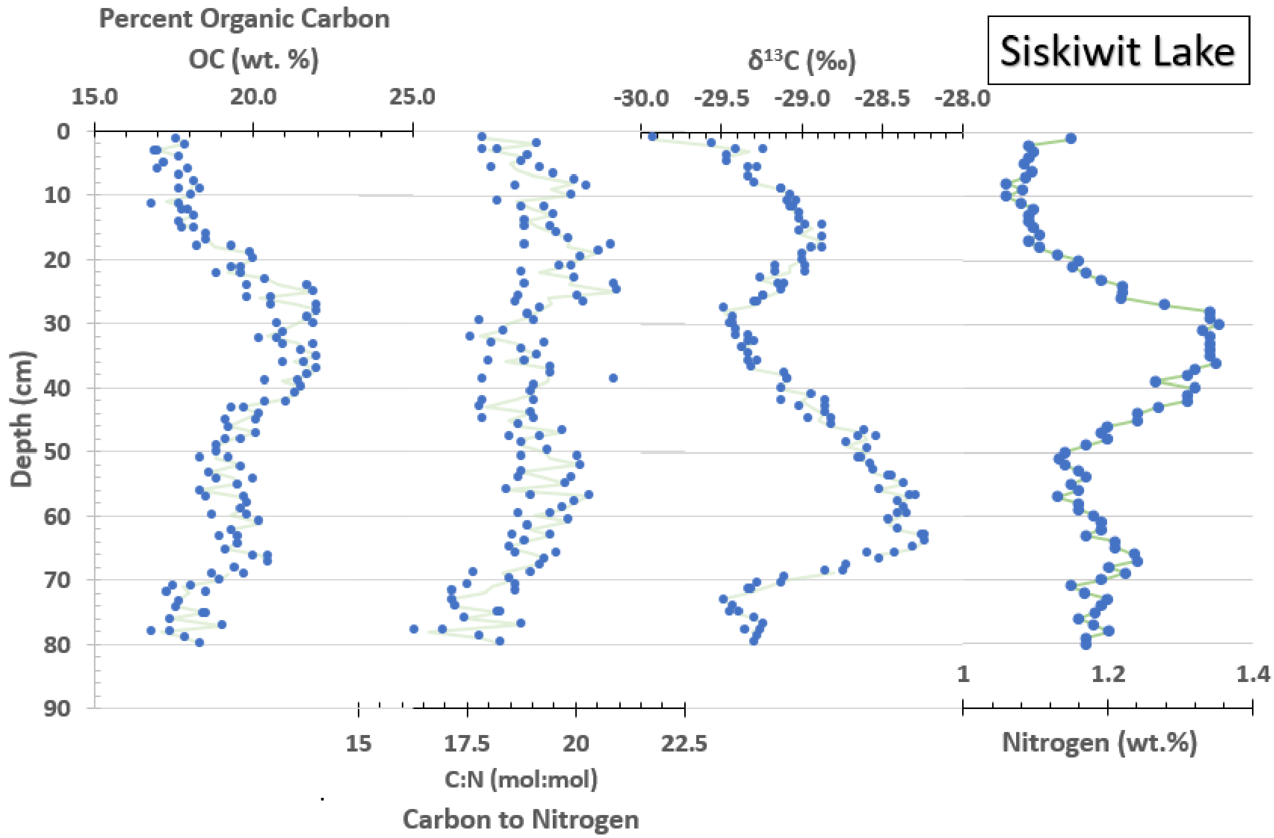

Figure 21. *Organic Carbon (left; wt. %), Carbon to Nitrogen ratio (middle-left; mol:mol), Isotopic Carbon (δ^{13}C; middle-right; ‰), and Nitrogen (right; wt. %) plotted against depth (cm). OC (wt. %) increases between 20 and 40 cm and has its lowest amounts at both the surface and at 80 cm. C:N is steady and relatively unchanging throughout the entire depth. Isotopic Carbon has its highest values between 60 and 70 cm and its lowest values are observed at the surface. N (wt. %) increases between 20 and 30 cm, and decreases between 40 and 50 cm.*

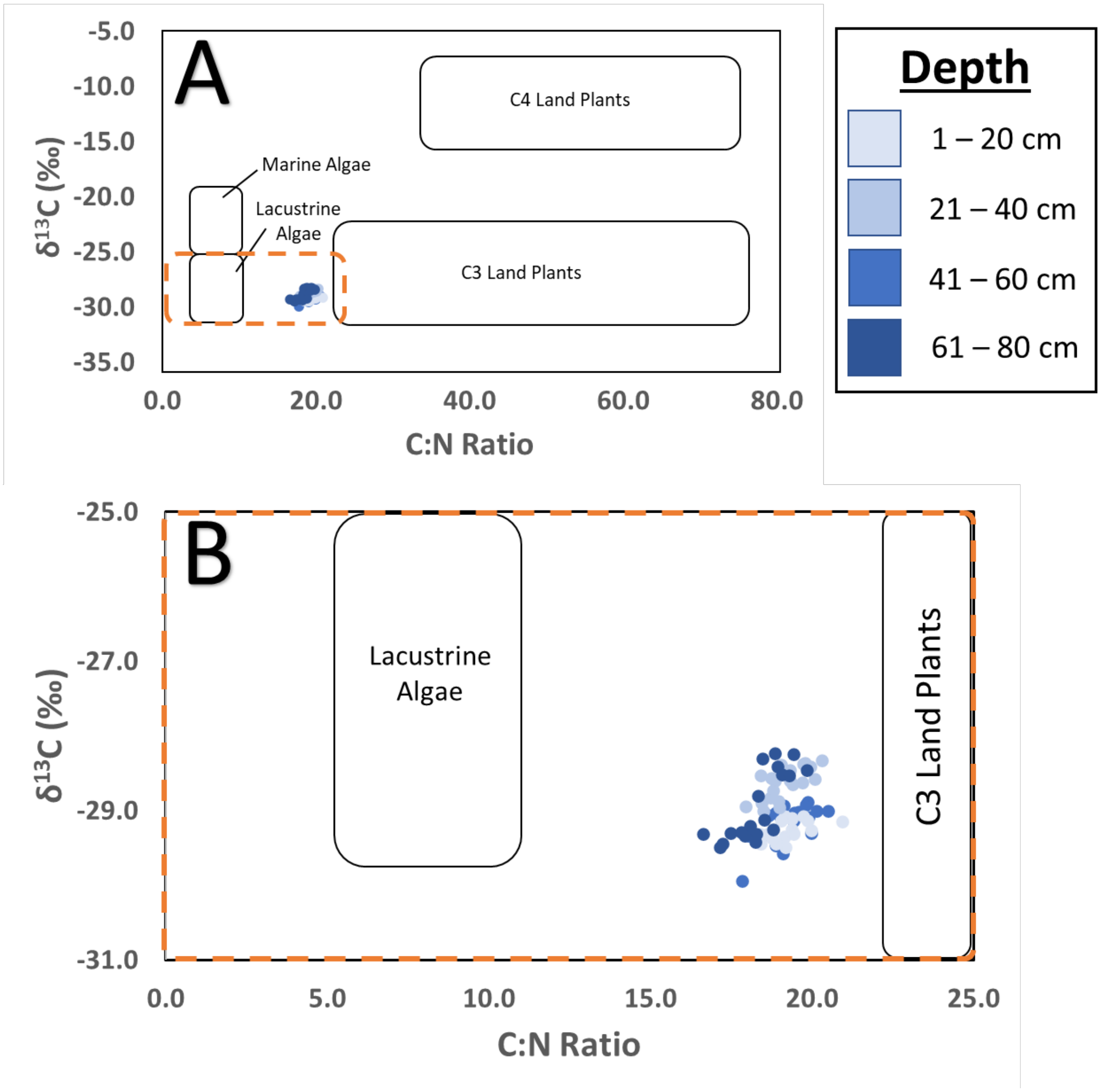

Figure 22. *Carbon to nitrogen (C:N) ratios of Siskiwit Lake correlated with stable isotope ($\delta^{13}C$) values. The C:N molar ratio ranged from 16.6 to 20.9, with an average of 19.0 ± 0.8, exhibiting varying C:N values throughout the core. The $\delta^{13}C$ of these sediment samples range from -28.2‰ to -29.9‰ with an average of -29.0‰ ± 0.4‰ (Figure 17). The bulk identifier graph is adapted from Meyers 1994, revealed a dominance of C3 Land Plants with influence from Lacustrine algal input.*

3.2 Supplementary Data

3.2.1 Sample Collection

Table 7. *Name of each core, their sample date, location and method, their approximate lengths, and the examinations executed on the core.*

Name	Collection Date	Sample Location	Sampling Method	Length (cm)	Examined for
Siskiwit Lake Core A	07/29/2021	N46.793920°, W91.129940°	Aquatic Instruments Piston Corer	81	^{210}Pb, ^{14}C, $\delta^{13}C$, C, N
Siskiwit Bay Core A	09/27/2021	N46.877930°, W091.11308°	Aquatic Instruments Gravity Corer	15	Back-up Surface Sediment
Siskiwit Bay Core B	09/27/2021	N46.877930°, W091.11308°	Aquatic Instruments Gravity Corer	17	Back-up Surface Sediment
Siskiwit Bay Core C	09/28/2021	N46.877250°, W091.11320°	Aquatic Instruments Hammer Corer	89	XRF
Siskiwit Bay Core D	09/28/2021	N46.877250°, W091.11320°	Aquatic Instruments Hammer Corer	65	^{210}Pb, ^{14}C
Siskiwit Bay Core E	09/28/2021	N46.877250°, W091.11320°	Aquatic Instruments Hammer Corer	126	^{14}C, $\delta^{13}C$, C, N, Pigments

3.2.2 Phytoplankton Pigments Standard Curves

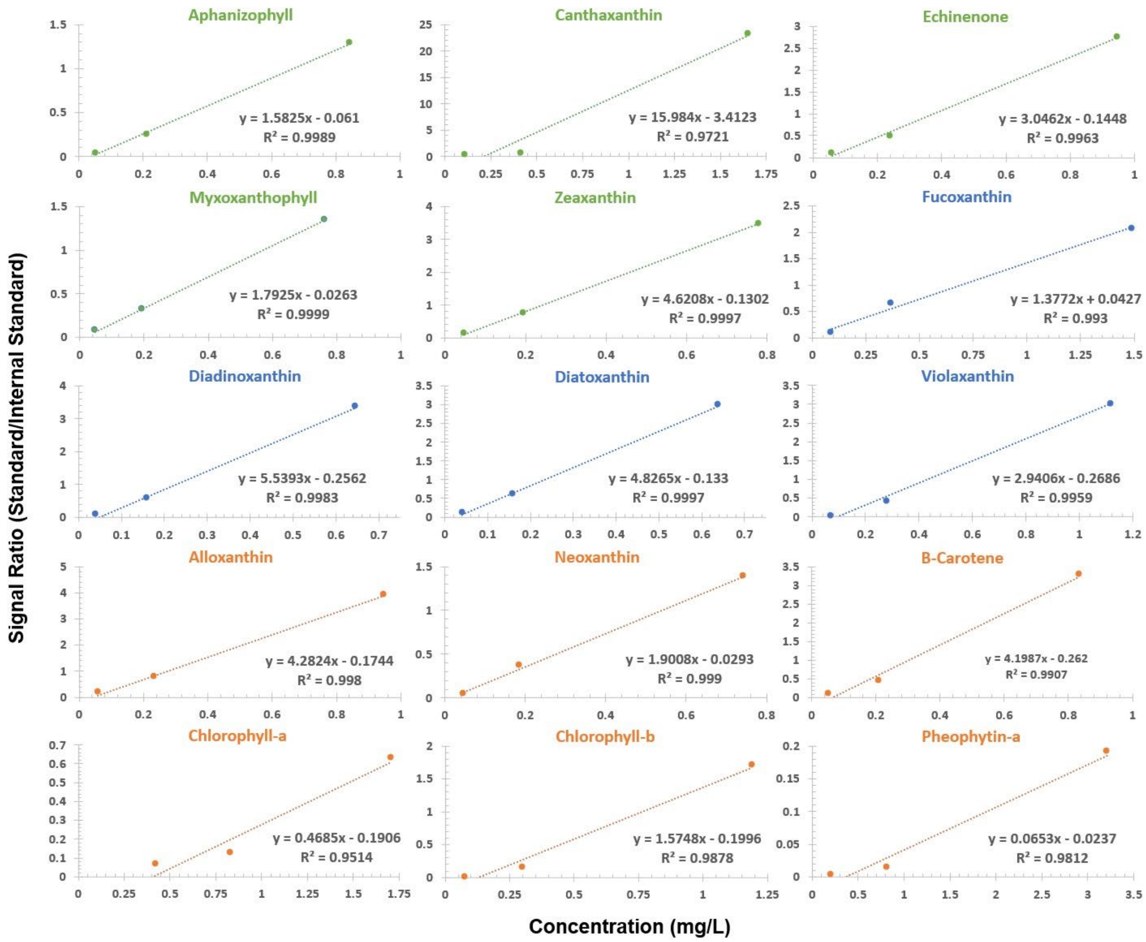

Figure 23. *Concentration curves of the studied pigments. Concentration (mg/L) is on the x-axes and signal ratio between the Pigment standard's signal versus the Internal standard's signal on the y-axes.*

3.2.3 Siskiwit Bay Phytoplankton Pigments

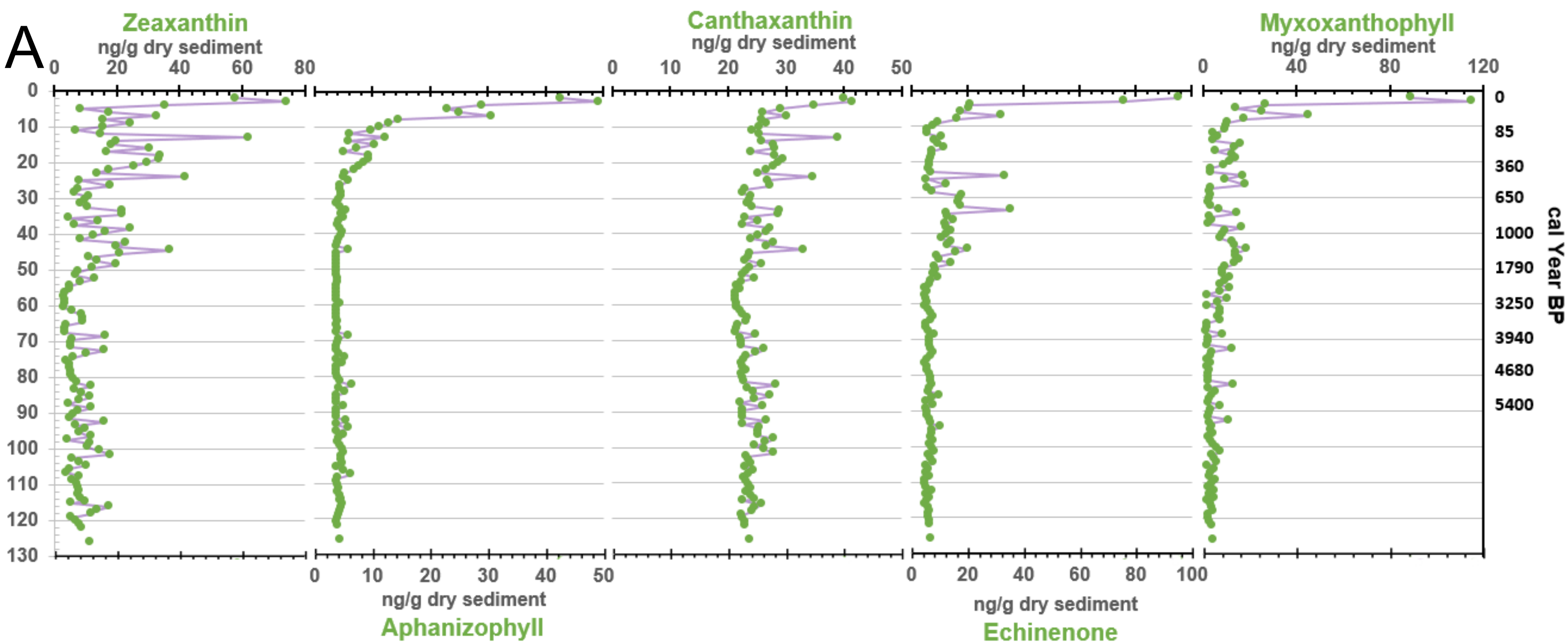

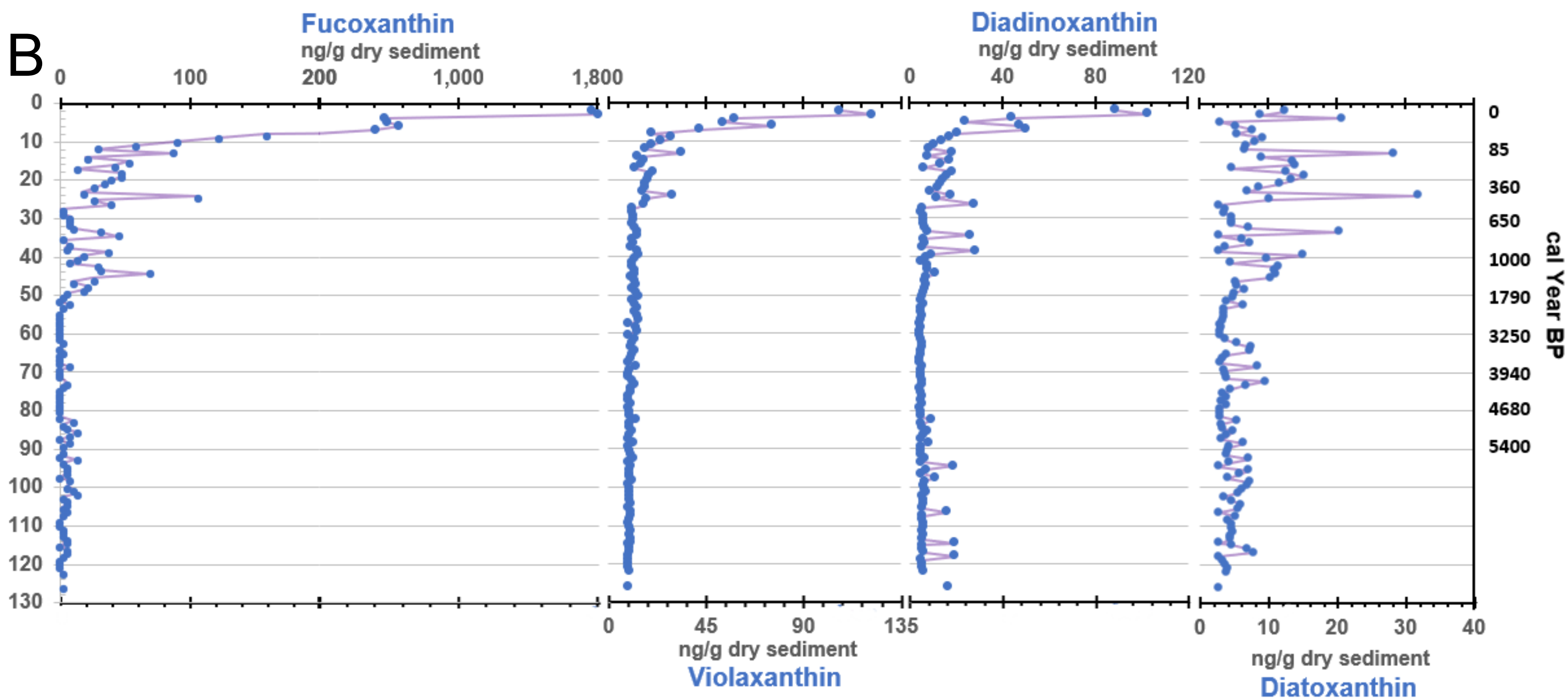
B
Fucoxanthin
ng/g dry sediment
0
100
200
1,000
1,800
Diadinoxanthin
ng/g dry sediment
0
40
80
120
0
10
20
30
40
50
60
70
80
90
100
110
120
130
0
45
90
135
ng/g dry sediment
Violaxanthin
0
10
20
30
40
ng/g dry sediment
Diatoxanthin
0
85
360
650
1000
1790
3250
3940
4680
5400
cal Year BP

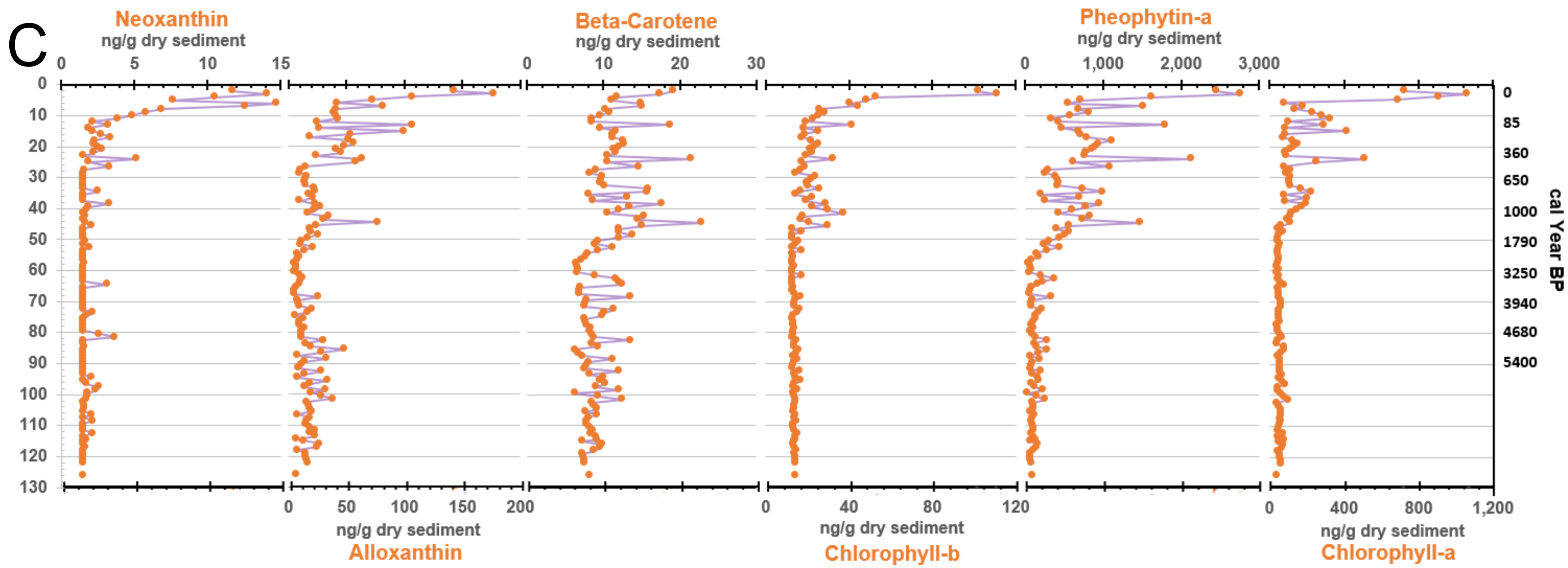

Figure 24. *Down-core concentrations (ng/g Dry sediment) of (**A; Green**) carotenoid pigments associated with cyanobacteria (Zeaxanthin, canthaxanthin, echinenone, myxoxanthophyll, and aphanizophyll), (**B; Blue**) diatom pigments (Fucoxanthin, diadinoxanthin, diatoxanthin, and violaxanthin), and (**C; Orange**) other pigments representing total productivity (Pheophytin-a, chlorophyll-a, chlorophyll-b, alloxanthin, neoxanthin, and beta-carotene) in sediments from Siskiwit Bay, collected in September 2021. **Note**: Fucoxanthin concentrations also include 19-but-fucoxanthin concentrations.*

3.3 Standard Operating Procedures

3.3.1 Sediment Core Sampling

Purpose:

To collect lakebed sediment to do further analysis on its content.

Materials:

- Aquatic Instruments Hammer Corer
- Aquatic Instruments Piston Corer
    - Aquatic Instruments Piston Corer Rods
- Aquatic Instruments Gravity Corer
- 2-5/8 Diameter polycarbonate core barrels
- Core Caps
- Rope (at least 100ft; with markups for measurements)
- Measuring tape
- Duct Tape
- Sharpee

Procedure:

1. Locate the sediment sample location(s). Record the geographical coordinates.
2. Measure the depth from the surface of the water to the surface of the lakebed sediment.
3. Attach the core barrel to the sediment coring device of choice.
4. Measure the length of the barrel and corer head to get an estimated length of how deep to drive the barrel into the sediment to retrieve a core.
5. Mark on the rope or piston rod for the approximated length needed for the desired sediment core length.
6. Slowly lower the corer into the water until it hits lake bottom, then:
    a. Push the piston corer into the sediment until the marked length on the rod
    b. OR hammer into the sediment until the desired sediment core length
    c. OR lift the Gravity corer enough to let it fall far enough to capture a core of the desired length.
7. Proceed by pulling the sediment core back to the surface. Be sure to keep the sediment core in the upright position the whole time.
8. Before leaving the surface of the water, cap the end of the core barrel so sediment is not lost.
9. Reinforce the cap to the core barrel using duct tape to ensure sediment is not lost. Again, be sure to keep the sediment core as upright as possible, until it is fully extruded.
10. Record the length of the recovered sediment.

11. Take detailed records of the sediment characteristics, as a function of depth (i.e. undisturbed surface), as well as a notion of any unusual properties (i.e. large wood chips) if obviously observable.

NOTES: A back-up core is taken in case of unexpected problems in analyzing the first core or if an interest in analysis of additional material develops. Sorbitol can be used on the surface of cores if unable to extrude the same day as sampling.

3.3.2 Sediment Core Extrusion

Purpose:

To divide the core into equal parts downcore in order to correlate depth to the factors to be analyzed and measured.

Materials:

- Aquatic Instruments Core Extruder
    - Piston Rod
    - Extension Rods
    - Funnel
- 1 cm block
- Putty Knife (1¼" wide blade)
- 24 oz polyethylene Nasco WHIRL-PAKs
- Sharpie
- Absorbent Paper Towels
- Latex gloves
- Razor blade

Procedure:

1. All materials used for core sectioning are cleaned carefully prior to removing the frozen core from the freezer.
2. Label WhirlPaks prior to removing the sediment core from the freezer as well.
3. Mount the core barrel into the core extruder apparatus.
    a. Remove the bottom cap first using a razor blade.
4. Place the extrusion funnel on top of the core barrel. To ensure no loss of sample, make sure it is flush with the core barrel.
5. If applicable, remove the water from the sediment core barrel by lowering the apparatus until the sediment is flush to the extrusion funnel.
6. To start extruding samples, lower the extruder assembly by 1 cm, quality checking with the 1 cm block, by loosening the "depth" bolts and pushing the core bottom towards the extrusion piston.
    a. By pushing the core barrel downwards, the piston will push against the rubber stopper, pushing 1 cm of sediment out at the top of the extruder onto the Core Extruding Funnel.
7. Scrape the extruding sediment from funnel to the sample container, or WhirlPak.
8. Between each sample, use an absorbent paper towel to clean all surfaces to minimize any contamination between samples. Deionized water can be used to help clean the surfaces.

A detailed record of the sediment characteristics, as a function of depth, as well as a notation of any unusual properties (i.e. large wood chips) were recorded.

3.3.3 Freeze-drying Sediment

Purpose:

Freeze-drying is mandatory for the sediment samples to be properly prepared for pigment extraction and analysis because it slows degradation and preserves the sample.

Materials:

- LABCONCO Freezone 6 Freeze-Dry System
- Lint-free KimWipes
- Mortar and Pestle
- Pre-weighed, pre-combusted, labelled scintillation vials
- Methanol (MeOH)

Procedure:

1. Place the ajar sediment-filled WhirlPaks into the Labconco Freezone 6 freeze dry system at -45°C; ≤ 70 mbar for ca. 2-4 days, or until all water is removed.
2. Once samples are dry, sift through the sediment to remove any terrestrial organic matter found and store them in a separate pre-weighed, pre-combusted, and labeled scintillation vial.
    a. Optimal: Identify the terrestrial organic matter and separate the types if more than one type is extracted from the sample.
        i. Examples include: Woody Debris and Grass/Leaf Fibers
3. Grind sediment until it becomes a homogeneous mixture.
4. Transfer sediment from mortar to pre-weighed, pre-combusted, and labeled scintillation vial.
5. Wash mortar and pestle first with deionized water, then wipe with a lint-free KimWipe, then rinse with methanol to ensure zero contamination between samples.
6. Allow to fully dry.
7. Repeat with remaining samples.

3.3.4 Loss on Ignition (LOI)

Purpose:

Lake sediment organic matter and carbonate content can be estimated by weight loss measurements in sediment samples subjected to sequential heating (Dean, 1974; Heiri et al., 2001; Santisteban et al., 2004).

Background:

"Organic matter is oxidized to carbon dioxide and ash at temperatures between ~200 and 500ºC. Further evolution of carbon dioxide from carbonate mineral forms occurs at temperatures between approximately 700 and 900ºC. Weight losses associated with water and carbon dioxide evolutions are easily quantified by recording sample weights before and after controlled heating (ignition at 550 and 1000ºC) and, in turn, may be correlated to water content, and organic matter and carbonate content." (Rosenmeier, 2005)

Materials:

- Crucibles
- Mass Balance
- Drying Oven
- Cole-Parmer Muffle Furnace

Safety Considerations:

- Tongs should be used to handle sample vessels (individual crucibles and crucible trays) heated to temperatures greater than ~70ºC.
- High-temperature gloves should be used when handling samples heated to temperatures between 550 and 1000ºC. Note, however, that most gloves offer protection only at temperatures less than ~350ºC.
- The muffle furnace door should be opened, and considerable quantities of heat should be dissipated before any samples are removed. Do not be positioned in front of the furnace when opening the door.
- Provide all other laboratory personnel with fair warning before opening the muffle furnace, and never leave the muffle furnace unattended when cooling.
- Post the two-hour 1000ºC ignition, set the muffle furnace to 600ºC or lower for approximately an hour to allow the sediment filled crucibles to cool down steadily. Rapid cooling may lead to cracking of the crucibles and loss of sample.

Procedure:

1. Record the weight of each empty and labeled crucible. There will be one crucible per sediment sample.
2. Add about one gram per cubic centimeter of pre-freeze-dried sediment to its designated crucible.
3. Transfer the sediment-filled crucibles to the drying-oven. To ensure complete dryness, allow the samples to dry in the oven at 60ºC overnight.
4. Once dried, measure and record the weight of dry sediment + crucible. The samples must remain in the drying oven (when not in use) and therefore should be weighed "one-at-a-time".
5. Transfer the crucibles to the muffle furnace, seal the door, and set the temperature to 550ºC.
6. When the temperature stabilizes at 550ºC, start a timer for exactly four hours of heating.
7. Once the four hours is reached, turn off the muffle furnace and allow it to cool enough to transfer the hot samples to the 60ºC drying oven for cooling. Allow at least one hour for sample cooling.
8. When the post-550ºC ignition samples have cooled enough for safe handling, begin recording the new sediment and crucible weight.
9. After recording all post-550ºC sediment and crucible weights, the samples should be returned to the muffle furnace and subjected to the two-hour ignition at 1000º C. Again, timing of the two-hour ignition should be measured relative to the point at which the oven achieves a 1000ºC temperature following sample placement.
10. Following exactly two hours of heating at 1000ºC, carefully remove the crucibles from the muffle furnace and transfer the ignited samples to the 60ºC drying oven for at least two hours of cooling.
11. When the post-1000ºC ignition samples have cooled enough for safe handling, measure and record the final crucible and sediment weight. After recording all values, discard the remaining ignited sample and wash the crucibles for additional usage.

Calculations:

To determine the sample's dry weight, the following equation was utilized:

Organic matter content is calculated as the difference in weight between the sediment dried at 60ºC and the sediment post-550ºC ignition:

Organic matter content can be multiplied by a constant to estimate the organic matter concentration of the sediment samples. This multiplicative factor, though not exact, stems from:

Results will be documented as losses by weight percent (Weight % LOI, 550°C).

The difference in weight between the 550 ºC and 1000ºC sediment may (to first approximation) be assumed to result from loss of carbon dioxide during carbonate mineral break-down. However, loss on ignition techniques cannot indicate which carbonate minerals may be present within any given sample. Because calcium carbonate is generally the dominant form of carbonate in most lake sediments, weight losses at 1000ºC will be used to estimate calcium carbonate content :

It should be noted that clay minerals may contain significant quantities of lattice-bound hydroxide (as much as five percent by weight) and these ions may be liberated (as water) at high temperatures. Calcium carbonate content estimates from weight losses at 1000ºC may therefore contain errors as great as five percent and (as such) data results are most appropriately reported as losses by weight percent (Weight % LOI, 1000°C).

References Cited:

Dean, W.E. (1974). *Determination of carbonate and organic matter in calcareous sediments and sedimentary rocks by loss on ignition: comparison with other methods.* Journal of Sedimentary Petrology 44: 242-248.

Heiri, O., A.F. Lotter, and G. Lemcke (2001). *Loss on ignition as a method for estimating organic and carbonate content in sediments: reproducibility and comparability of results.* Journal of Paleolimnology 25: 101-110.

Santisteban, J.I., R. Mediavilla, E. López-Pamo, C.J. Dabrio, M.B.R. Zapata, M.J.G. García, S. Castaño, and P.E. Martínez-Alfaro (2004). *Loss on ignition: a qualitative or quantitative method for organic matter and carbonate mineral content in sediments?* Journal of Paleolimnology 32: 287-299.

[Adapted from: Abbott Rosenmeier at the University of Pittsburg, 2005]

3.3.5 Fumigation (for EA-IRMS Analysis)

Purpose:

To measure organic carbon (OC) content and $\delta^{13}C$ within the sediment to determine the dominating source of organic matter in the depositional location. Additionally, this analysis will assist in reporting pigment concentrations in relation to the amount of OC within the sediment.

Materials:

- Fumigation chamber
- Fresh 12 M HCl (straight from the stock HCl bottle)
- 125 ml glass beaker
- Silver 2x5 mm capsules (for fumigation)
- Tin 2x5 mm capsules (for encapsulating silver fumigated sample)
- Yellow acid-resistant microtiter tray
- Lid for microtiter tray
- Pre-ground sediment samples
- Sartorius microbalance, tools
- Barnstead Thermolyne Cimarec Hot plate
- Thermometer
- Syringe to deliver 50 µL MQ aliquots
- Deionized water (MiliQ)
- Desiccator

Procedure:

1. Use the Sartorius microbalance and transfer enough sample to provide at least 50 µg N to a silver capsule, leave the capsule OPEN.
2. Place the capsule in a yellow microtiter tray; record ID, wt. (mg) and capsule location.
3. Repeat 1-4 for all samples.
4. Add 50 µL MQ water to capsules using the syringe.
5. Place the microtiter tray in the fumigation chamber.
6. DO NOT use any form of grease on the ground glass of the lid or base.
7. DO NOT use desiccant.
8. Place a beaker containing ca. 50 mL fresh 12 M HCl in the fumigation chamber with sample tray.
9. Allow carbonate release ca. 16 hrs. (Do not leave in fumes 24 hours)
10. Remove the tray from the fumigation chamber and allow acid fumes to dissipate 48 hours; cover the tray loosely with a tent of aluminum foil in the hood – no contact between foil and top of tray.
11. Place a microtiter tray on a hotplate in a hood at 50 °C to dry for ca. 6 hours.

12. Enclose each silver capsule in a tin 2x5 mm capsule and carefully close silver and tin capsules on each other. (Make sure that capsules are completely closed and not ruptured)
13. Place the samples in desiccator until ready to run.

[Adapted from: Acid Fumigation of Soils to Remove Carbonates Prior to Total Organic Carbon or Carbon-13 Isotopic Analysis, D.Harris, W.R. Horwath, and C.Van Kessel, Soil Sci. Soc. Am. J. 65:1853-1856 (2001).]

3.3.6 Sample Preparation for EA-IRMS Analysis

Purpose:

To measure dry, homogenized sediment for elemental percentages (%OC and %N) and light stable isotope ratios ($\delta^{13}C$ and $\delta^{15}N$) via elemental analysis – isotope ratio mass spectrometry (EA-IRMS). This process can be in conjunction to fumigation (*3.3.5 Fumigation (for EA-IRMS Analysis))* when measuring for %OC and $\delta^{13}C$.

Materials:

- Tin 2x5 mm capsules
- Microtiter tray
- Lid for microtiter tray
- Pre-ground sediment samples
- Sartorius Microbalance
- Sartorius Microbalance tools

Standards:

A suite of working standards is run every ten samples, and the slope and intercept of the individual sets are then used to calculate drift of the samples throughout the run. All standard $\delta^{13}C$ values have been confirmed via periodic runs against the international $\delta^{13}C$ standard, Vienna PeeDee Belemnite (VPDB). This standard is run approximately every two to three years against working standards and laboratory CO_2 (g) standards to confirm literature values. According to convention, all standard and sample delta values are calculated against VPDB.

Standards	%OC	‰ $\delta^{13}C$	%N
Acetanilide	71.1	-33.8	10.4
Low-Organic Content Soil [B-2153]	1.9	-22.9	0.1
Caffeine	41.6	-13.7	28.9

Procedure:

1. Using the microbalance, weigh out samples into tin capsules and record sample ID, weight, and capsule location.
2. Gently fold the tin capsules into a ball.
3. Store in desiccation until analysis.

3.3.7 Pigment Extraction from Sediment

Purpose: To extract phytoplankton pigments from the sediment for further analysis.

Materials:

- Optima-grade Acetone
- Falcon Centrifuge Tubes (15 mL) [Two per sample]
- 20 mL Disposable Syringes
- Syringe Filters
- LC Vials
- LC Vial 200 µL Inserts
- Pasteur Pipettes with Bulb
- Vortex Mixer
- Sonicator Bath
- Centrifuge
- Drying Apparatus - Nitrogen Gas

Procedure:

1. Weigh out ca. 2 grams of sediment and place it in a centrifuge tube (record the weight to the nearest 0.001 grams).
2. Add 3-5 mL of optima-acetone to the sediment-filled centrifuge tube.
3. Shake the tube in the vortex mixer until the sediment is thoroughly saturated.
4. Create an ice bath within the sonicator bath (to prevent pigment breakdown) and then sonicate the sediment-acetone solution (this breaks down cell membranes and releases pigments).
5. Sonicate sample for 50-60 seconds. [Make sure the water bath level is below the liquid level in the centrifuge tube.]
6. Store sample in freezer (ca. 4 °C) overnight (ca. 12 hrs).
7. If the temperature is too low (less than -20 °C), the extraction speed will be slowed down.
8. If the temperature is too high (greater than 20 °C), the pigments will degrade during the extraction; if the extraction duration is too long, some labile pigments will degrade.
9. When taking the tube out from the freezer, let it sit at room temperature for ca. 2 min.
10. Centrifuge at 2000 rpm for 5 minutes. [Make sure the centrifuge is balanced, no odd numbers.]
11. Drain acetone/pigment solution from sediment into a new 20 mL disposable syringe (with a syringe filter attached) and squeeze it into a new centrifuge tube. [Rinse/ prime all parts with acetone!]

12. Can repeat adding acetone, vortexing, and centrifuging the sediment to make sure all pigments are extracted thoroughly. (Keep in mind that when repeating these steps, the more acetone there is used, the longer it will take to dry.)
13. Blow new centrifuge mixture to complete dryness using N_2. While drying, keep the tube covered in tinfoil or in the dark.
14. Add tiny drops of acetone using a pasteur pipette to help transfer this mixture into an LC insert.
15. Transfer the mixture to a LC vial using a pasteur pipette, making sure to rinse the centrifuge tube with another few drops of optima-grade acetone.
16. Make sure LC vials have inserts before adding the solution.
17. Blow the mixture to dryness using N_2.
18. Store in the refrigerator until ready for analysis.
19. Just before injection add 100 μL of optima-grade acetone to resolve the pigments.
20. Additionally, spike the solution using 100 μL of internal standard. (trans-β-Apo-8'-carotenal)
21. Pigment solution is ready for HPLC injection.

NOTE: All procedures should be done in dark or dim light. In reality this is hard to do, but nonetheless try to keep the pigment sample from being exposed to light when at all possible.

3.3.8 HPLC and Analysis

Purpose:

To quantify unknown concentrations of phytoplankton pigments, using known standards and an internal standard.

Apparatus:

- HPLC System:
    - ThermoScientific Dionex UltiMate 3000
    - Dionex HPLC Pump
    - Rheodyne 7125 injector with 5 µL loop
    - HPLC column, 2.1 x 100 mm, Agilent - Zorbax Eclipse Plus C8, 95Å, 1.8-µm, (1200 bar pressure limit).
    - HPLC guard column, 2.1 x 5 mm, VanGuard - Acquity UPLC BEH C8, 1.7-µm.
    - Linear UV-Visible detector, model UVIS 200 (variable wavelength, adjustable range and rise time, 1 V/AU integrator output). Flow cell is 316 stainless steel, 6-mm path length, and 9 µL volume.
    - HPLC column heater, Eppendorf CH-30.
- Data System:
    - SRI Instruments PeakSimple model 333 single channel chromatography data system with 20-bit high resolution A/D board. USB 2.0 for Windows PC
    - Chromeleon Software, Version 7.2

Chemicals:

- Mobile phase:
    - 70:30 (v:v) Methanol : tetrabutylammonium acetate (TbAA)
    - Optima-grade Methanol

- Pigment Standards (DHI Laboratory Products, DHI A/S Group, Denmark):
    - Single Pigment Standards:
        - Alloxanthin (0.948 mg/L)
        - Aphanizophyll (0.845 mg/L)
        - B-carotene (0.832 mg/L)
        - Canthaxanthin (1.648 mg/L)
        - Chlorophyll-a (1.707 mg/L)
        - Chlorophyll-b (1.190 mg/L)
        - Chlorophyllide-a (0.802 mg/L)
        - Diadinoxanthin (0.690 mg/L)
        - Diatoxanthin (0.641 mg/L)
        - Divinyl protochlorophyllide (Mg-DVP) (0.474 mg/L)
        - Echinenone (0.923 mg/L)
        - Fucoxanthin (1.490 mg/L)

- Myxoxanthophyll (0.764 mg/L)
- Neoxanthin (0.751 mg/L)
- Pheophorbide-a (1.835 mg/L)
- Pheophytin-a (3.208 mg/L)
- Violaxanthin (1.118 mg/L)
- Zeaxanthin (0.782 mg/L)

- Mixed Pigments Standards
  - MIX-1 (3.317mg/L Total Chl-a)
  - MIX-2 (0.243 mg/L Total Chl-a)

- Internal Standard
  - Trans-B-Apo-8'-carotenal

<u>Making Internal Standard:</u>

Materials:

- Trans-B-Apo-8'-carotenal
- HPLC-grade Acetone
- 200 mL Volumetric Flask
- 250 mL Glass or Amber bottle
- Sartorius Microbalance

Procedure:

1. Weigh out around 0.2 mg of Trans-B-Apo-8'-carotenal and place it in a beaker. (Record weight)
2. Dissolve it using 200 mL of HPLC-grade Acetone.
3. Keep the stock solution in a dark fridge.

This will make around a 1 mg/L concentration, be sure to calculate and note the actual concentration according to the weight in step 1. By adding 100uL just before injection to every sample, this will be used as a Spike.

<u>Making Mobile Phases:</u>

Materials:

- Graduated Cylinder
- 500 mL Beaker (for TbAA solution)
- 30- or 50-mL Beaker for stock acetic acid
- 100 mL Beaker for diluted acetic acid
- Barnstead Thermolyne Cimarec Stir Plate

- Stir Bar
- Mettler Toledo pH Probe
- Eppendorf Pipette (50 µL)
- Two 1000 mL Amber or dark (tinfoil) glass corning bottles
- 0.4 M Tetrabutylammonium hydrate titrant (TbA)
- Acetic Acid (OPTIMA grade)
- Methanol (OPTIMA grade)

Prior to Solvent A – *0.028 M Tetrabutylammonium acid (TbAA)**

1. Create 300 mL of a 0.028 M TbA solution by measuring out 21 mL of stock 0.4 M TbA solution and mixing it with 279 mL of MQ DI water.
   [Be careful! TbA is <u>very</u> basic! ~12.60 pH]
2. Place the solution on a stir plate and add in a stir bar.
3. Insert the pH probe and observe the pH carefully.
4. Add Acetic Acid (OPTIMA-grade) dropwise with a pasteur pipette until the pH is nearing 10.
5. As the pH nears 10, dilute the acetic acid 1000-fold (Ex. 50 µL diluted to 50 mL).
6. Once the pH is about 10, it will decrease more than 1 unit with 1-2 drops. Continue to dilute the acetic acid if the pH is dropping too quickly.
7. Be sure not to overshoot 6.5 pH.
8. Reagent is stable for about 1 month at room temperature in the dark.

**Adapted from* NMS Work Element, 2014.

Solvent A – *70:30: Optima-grade Methanol: 0.028M Tetrabutylammonium Acetate (TbAA), pH = 6.5*

1. Add the 300 mL solution of TbAA and 700 mL of Optima-grade Methanol to a 1000 mL amber or dark (tinfoil) glass corning bottle.
2. This will be stable for around 1 month at room temperature.
3. Should be filtered weekly or anytime a noticeable precipitate is present. Batches can be mixed, as long as they are filtered.

Solvent B – *100% Optima-grade Methanol*

<u>Equilibration:</u>

Equilibration is performed prior to each batch of injections run to ensure the system is at peak performance. If pressures within the UHPLC exceeded 7,500 psi, the system must be purged and equilibration must be started over. This process is a total of 40 minutes.

1. 10 minutes of 0% Solvent A and 100% Solvent B.
2. 10 minutes of 50% Solvent A and 50% Solvent B.
3. 10 minutes of 100% Solvent A and 0% Solvent B.

4. 10 minutes of 95% Solvent A and 5% Solvent B.

Each Injection:

1. Constant flow rate of 0.200 mL/min.
2. Once sample or standard is injected, the flow gradient will start holding Solvent A at 95% and Solvent B at 5% for 11.5 minutes.
3. Then for 15 minutes, gradual ramping to 5% Solvent A and 95% Solvent B.
4. Hold for 11.5 minutes.
5. 7 minutes of gradual ramping to 95% Solvent A and 5% Solvent B.
6. Hold for 6 minutes.

Samples were analyzed via Ultra High-Performance Liquid Chromatography (UHPLC/HPLC) using a ThermoScientific Dionex UltiMate 3000. Included apparatus were a Dionex HPLC pump, Rheodyne 7125 injector, Agilent - Zorbax Eclipse Plus C8 HPLC column, VanGuard - Acquity UPLC BEH C8 HPLC guard column, UVIS 200 linear UV-Visible detector, and Eppendorf CH-30 HPLC column heater. The data was recorded using Chromeleon Version 7.2 via an SRI Instruments PeakSimple 333 single-channel chromatography data system.

To determine elution order and how the certain pigments would be captured and identified (via photodiode array or fluorescence), prior to samples, individual absorption profiles of standards were collected in advance (Table 3). Additionally, to correlate the measured signal from the instrument to the concentration of pigment found within a sample, concentration curves were created. Each pigment standard's trendline was used to correlate the relationship of signal to the calculated concentration within samples. The R^2 values, and their distance from 1.00, correlate to the reliability between the standards created. These range from 1.00 (Chl-a, Myxoxanthophyll, Diatoxanthin, and Zeaxanthin) to 0.972 (Canthaxanthin), with an average of 0.994.

References

Abbott, M. B., & Stafford, T. W. (1996). Radiocarbon Geochemistry of Modern and Ancient Arctic Lake Systems, Baffin Island, Canada. In *QUATERNARY RESEARCH* (Vol. 45).

Alexson, E. E., Reavie, E. D., Axler, R. P., Yemets, S. V., Krasutsky, P. A., Edlund, M. B., Pillsbury, R. W., & Desotelle, D. (2018). Paleolimnology of a freshwater estuary to inform Area of Concern nutrient delisting efforts. *Journal of Paleolimnology*, *59*(3), 373–395. https://doi.org/10.1007/s10933-017-0014-8

Andersson, A., Meier, H. E. M., Ripszam, M., Rowe, O., Wikner, J., Haglund, P., Eilola, K., Legrand, C., Figueroa, D., Paczkowska, J., Lindehoff, E., Tysklind, M., & Elmgren, R. (2015). Projected future climate change and Baltic Sea ecosystem management. *AMBIO*, *44*, S345–S356. https://doi.org/10.1007/s13280-015-0654-8

Appleby, P. G. (1998). *Dating Recent Sediments by 210Pb: Problems and Solutions*.

Appleby, P. G. (2001). Chronostratigraphic Techniques in Recent Sediments. In *Tracking Environmental Change Using Lake Sediments* (pp. 171–203). Kluwer Academic Publishers. https://doi.org/10.1007/0-306-47669-X_9

Appleby, P. G., & Oldfield, F. (1983). *The assessment of 210 Pb data from sites with varying sediment accumulation rates*.

Aquino-López, M. A., Blaauw, M., Christen, J. A., & Sanderson, N. K. (2018). Bayesian Analysis of 210 Pb Dating. *Journal of Agricultural, Biological, and Environmental Statistics*, *23*(3), 317–333. https://doi.org/10.1007/s13253-018-0328-7

Aquino-López, M. A., Ruiz-Fernández, A. C., Blaauw, M., & Sanchez-Cabeza, J. A. (2020). Comparing classical and Bayesian 210Pb dating models in human-impacted aquatic environments. *Quaternary Geochronology*, *60*. https://doi.org/10.1016/j.quageo.2020.101106

Austin, J. A., & Colman, S. M. (2007). Lake Superior summer water temperatures are increasing more rapidly than regional temperatures: A positive ice-albedo feedback. *Geophysical Research Letters*, *34*(6). https://doi.org/10.1029/2006GL029021

Basen, T., Gergs, R., Rothhaupt, K. O., & Martin-Creuzburg, D. (2013). Phytoplankton food quality effects on Gammarids: Benthic-pelagic coupling mediated by an invasive freshwater clam. *Canadian Journal of Fisheries and Aquatic Sciences*, *70*(2), 198–207. https://doi.org/10.1139/cjfas-2012-0188

Basen, T., Martin-Creuzburg, D., & Rothhaupt, K. O. (2011). Role of essential lipids in determining food quality for the invasive freshwater clam Corbicula fluminea. *Journal of the North American Benthological Society*, *30*(3), 653–664. https://doi.org/10.1899/10-087.1

Basen, T., Rothhaupt, K. O., & Martin-Creuzburg, D. (2012). Absence of sterols constrains food quality of cyanobacteria for an invasive freshwater bivalve. *Oecologia*, *170*(1), 57–64. https://doi.org/10.1007/s00442-012-2294-z

Baustian, M. M., Brooks, Y. M., Baskaran, M., Leavitt, P. R., Liu, B., Ostrom, N., Stevenson, R. J., & Rose, J. B. (2020). Paleo-environmental evidence of ecosystem change in Lake St. Clair region of Laurentian Great Lakes basin: contrasting responses to land-use change and invasive mussels. *Journal of Paleolimnology*, *63*(3), 177–193. https://doi.org/10.1007/s10933-019-00108-x

Bengtsson, L., & Enell, M. (1986). Chemical analysis. *Handbook of Holocene Palaeoecology and Palaeohydrology*, 423–451. https://cir.nii.ac.jp/crid/1571980074944568320.bib?lang=en

Bianchi, T. S., Baskaran, M., Delord, J., & Ravichandran, M. (1997). *Carbon Cycling in a Shallow Turbid Estuary of Southeast Texas: The Use of Plant Pigment Biomarkers and Water Quality Parameters* (Vol. 20, Issue 2).

Bianchi, T. S., & Canuel, E. A. (2011). *Chemical Biomarkers in Aquatic Ecosystems*. Princeton University Press. https://doi.org/10.1515/9781400839100

Bianchi, T. S., Engelhaupt, E., Westman, P., Andrén, T., Rolff, C., & Elmgren, R. (2000). Cyanobacterial blooms in the Baltic Sea: Natural or human-induced? *Limnology and Oceanography*, *45*(3), 716–726. https://doi.org/10.4319/lo.2000.45.3.0716

Bianchi, T. S., & Findlay, S. (1991). Decomposition of Hudson estuary macrophytes: Photosynthetic pigment transformations and decay constants. *Estuaries*, *14*(1), 65–73. https://doi.org/10.2307/1351983

Bianchi, T. S., Wysocki, L. A., Schreiner, K. M., Filley, T. R., Corbett, D. R., & Kolker, A. S. (2011). Sources of Terrestrial Organic Carbon in the Mississippi Plume Region: Evidence for the Importance of Coastal Marsh Inputs. *Aquatic Geochemistry*, *17*(4), 431–456. https://doi.org/10.1007/s10498-010-9110-3

Boës, X., Rydberg, J., Martinez-Cortizas, A., Bindler, R., & Renberg, I. (2011). Evaluation of conservative lithogenic elements (Ti, Zr, Al, and Rb) to study anthropogenic element enrichments in lake sediments. *Journal of Paleolimnology*, *46*(1), 75–87. https://doi.org/10.1007/s10933-011-9515-z

Breckenridge, A. (2013). An analysis of the late glacial lake levels within the western Lake Superior basin based on digital elevation models. *Quaternary Research*, *80*(3), 383–395. https://doi.org/10.1016/j.yqres.2013.09.001

Brocks, J. J., Love, G. D., Summons, R. E., Knoll, A. H., Logan, G. A., & Bowden, S. A. (2005). *Biomarker evidence for green and purple sulphur bacteria in a stratified Palaeoproterozoic sea*. https://doi.org/10.1038/nature04068

Brown, E. T., Johnson, T. C., Scholz, C. A., Cohen, A. S., & King, J. W. (2007). Abrupt change in tropical African climate linked to the bipolar seesaw over the past 55,000 years. *Geophysical Research Letters*, *34*(20). https://doi.org/10.1029/2007GL031240

Chen, N., Bianchi, T. S., McKee, B. A., & Bland, J. M. (2001). Historical trends of hypoxia on the Louisiana shelf: application of pigments as biomarkers. *Organic Geochemistry*, *32*, 543–561. www.elsevier.nl/locate/orggeochem

Chen, X., Lim, X., Bouin, A., Lautier, T., & Zhang, C. (2021). High-level de novo biosynthesis of glycosylated zeaxanthin and astaxanthin in Escherichia coli. *Bioresources and Bioprocessing*, *8*(1). https://doi.org/10.1186/s40643-021-00415-0

Cohen, A. S. (2003). *Paleolimnology: The History and Evolution of Lake Systems* (1st ed.). Oxford University Press.

Conroy, J. D., Kane, D. D., Briland, R. D., & Culver, D. A. (2014). Systemic, early-season Microcystis blooms in western Lake Erie and two of its major agricultural tributaries (Maumee and Sandusky rivers). *Journal of Great Lakes Research*, *40*(3), 518–523. https://doi.org/10.1016/j.jglr.2014.04.015

Cooney, E. M., Mckinney, P., Sterner, R., Small, G. E., & Minor, E. C. (2016). *Tale of Two Storms: Impact of Extreme Rain Events on the Biogeochemistry of Lake Superior*. https://doi.org/10.1029/2017JG004216

Cutshall, N. H., Larsen, I. L., & Olsen, C. R. (1983). Direct Analysis of "Pb in Sediment Samples: Self-Absorption Corrections." In *Nuclear Instruments andMethods* (Vol. 206).

Davies, S. J., Lamb, H. F., & Roberts, S. J. (2015). *Micro-XRF Core Scanning in Palaeolimnology: Recent Developments* (pp. 189–226). https://doi.org/10.1007/978-94-017-9849-5_7

Dean, W. E. Jr. (1974). Determination of Carbonate and Organic Matter in Calcareous Sediments and Sedimentary Rocks by Loss on Ignition: Comparison With Other Methods. *SEPM Journal of Sedimentary Research*, *Vol. 44*. https://doi.org/10.1306/74D729D2-2B21-11D7-8648000102C1865D

Delaune, R. D. , Patrick Jr., W. H., & Buresh, R. J. (1978). Sedimentation rates determined by 137 Cs dating in a rapidly accreting salt marsh. *Nature*, *2*(275), 532–533.

Egeland, E. S. (2016). Carotenoids. In *The Physiology of Microalgae* (pp. 507–563). Springer International Publishing. https://doi.org/10.1007/978-3-319-24945-2_20

Evans, J. E., Johnson, T. C., Alexander, E. C., Lively, R. S., & Eisenreich, S. J. (1981). Sedimentation Rates and Depositional Processes in Lake Superior from 210Pb

Geochronology. *Journal of Great Lakes Research*, *7*(3), 299–310. https://doi.org/10.1016/S0380-1330(81)72058-6

Ewing, H. A., Weathers, K. C., Cottingham, K. L., Leavitt, P. R., Greer, M. L., Carey, C. C., Steele, B. G., Fiorillo, A. U., & Sowles, J. P. (2020). “New” cyanobacterial blooms are not new: two centuries of lake production are related to ice cover and land use. *Ecosphere*, *11*(6). https://doi.org/10.1002/ecs2.3170

Fahnenstiel, G. L., Sicko-Goad, L., Scavia, D., & Stoermer, E. F. (1986). Importance of Picoplankton in Lake Superior. *Canadian Journal of Fisheries and Aquatic Sciences*, *43*, 235–240.

Favot, E. J., Rühland, K. M., DeSellas, A. M., Ingram, R., Paterson, A. M., & Smol, J. P. (2019). Climate variability promotes unprecedented cyanobacterial blooms in a remote, oligotrophic Ontario lake: evidence from paleolimnology. *Journal of Paleolimnology*. https://doi.org/10.1007/s10933-019-00074-4

Foerster, V., Junginger, A., Langkamp, O., Gebru, T., Asrat, A., Umer, M., Lamb, H. F., Wennrich, V., Rethemeyer, J., Nowaczyk, N., Trauth, M. H., & Schaebitz, F. (2012). Climatic change recorded in the sediments of the Chew Bahir basin, southern Ethiopia, during the last 45,000 years. *Quaternary International*, *274*, 25–37. https://doi.org/10.1016/j.quaint.2012.06.028

Granado-Lorencio, F., Blanco-Navarro, I., Pérez-Sacristán, B., & Hernández-Álvarez, E. (2017). Biomarkers of carotenoid bioavailability. In *Food Research International* (Vol. 99, pp. 902–916). Elsevier Ltd. https://doi.org/10.1016/j.foodres.2017.03.036

Guidi, L., Tattini, M., & Landi, M. (2017). How Does Chloroplast Protect Chlorophyll Against Excessive Light? In *Chlorophyll*. InTech. https://doi.org/10.5772/67887

Harris, D., Horwáth, W. R., & van Kessel, C. (2001). Acid fumigation of soils to remove carbonates prior to total organic carbon or CARBON-13 isotopic analysis. *Soil Science Society of America Journal*, *65*(6), 1853–1856. https://doi.org/10.2136/sssaj2001.1853

Heathcote, A. J., Taranu, Z. E., Tromas, N., MacIntyre-Newell, M., Leavitt, P. R., & Pick, F. R. (2023). Sedimentary DNA and pigments show increasing abundance and toxicity of cyanoHABs during the Anthropocene. *Freshwater Biology*, *68*(11), 1859–1874. https://doi.org/10.1111/fwb.14069

Hedberg, P., Albert, S., Nascimento, F. J. A., & Winder, M. (2021). Effects of changing phytoplankton species composition on carbon and nitrogen uptake in benthic invertebrates. *Limnology and Oceanography*, *66*(2), 469–480. https://doi.org/10.1002/lno.11617

Heiri, O., Lotter, A. F., & Lemcke, G. (2001). Loss on ignition as a method for estimating organic and carbonate content in sediments: reproducibility and comparability of results. In *Journal of Paleolimnology* (Vol. 25).

Hertzberg, S., & Liaaen-jensen, S. (1971). The Constitution of Aphanizophyll. In *Z. Physiol. Chem. Hoppe-Seyler's* (Vol. 10). Pergamon Press.

Hertzberg, S., Liaaen-Jensen, S., & Siegelman, H. W. (1971). The carotenoids of blue-green algae. *Phytochemistry*, *10*, 3121–3127.

Hirschberg, J., & Chamovitz, D. (1994). Carotenoids in Cyanobacteria. In *The Molecular Biology of Cyanobacteria* (pp. 559–579). Springer Netherlands. https://doi.org/10.1007/978-94-011-0227-8_18

Hobbs, W. O., Dreher, T. W., Davis, E. W., Vinebrooke, R. D., Wong, S., Weissman, T., & Dawson, M. (2021). Using a lake sediment record to infer the long-term history of cyanobacteria and the recent rise of an anatoxin producing Dolichospermum sp. *Harmful Algae*, *101*. https://doi.org/10.1016/j.hal.2020.101971

Hollenhorst, T., Johnson, L. B., & Ciborowski, J. (2011). Monitoring Land Cover Change in the Lake Superior Basin. *Aquatic Ecosystem Health and Management*, *4*(14), 433–442.

Huisman, J., Codd, G. A., Paerl, H. W., Ibelings, B. W., Verspagen, J. M. H., & Visser, P. M. (2018). Cyanobacterial blooms. *Nature Reviews: Microbiology*, *16*(8), 471–483. https://doi.org/10.1038/s41579-018-0040-1

Jeffrey, S. W., Mantoura, R. F. C., & Wright, S. W. (1997). *Phytoplankton pigments in oceanography : guidelines to modern methods*. UNESCO Pub.,.

Josefson, A. B., Norkko, J., & Norkko, A. (2012). Burial and decomposition of plant pigments in surface sediments of the Baltic Sea: Role of oxygen and benthic fauna. *Marine Ecology Progress Series*, *455*, 33–49. https://doi.org/10.3354/meps09661

Kane, D. D., Conroy, J. D., Peter, R. R., Baker, D. B., & Culver, D. A. (2014). Re-eutrophication of Lake Erie: Correlations between tributary nutrient loads and phytoplankton biomass. *Journal of Great Lakes Research*, *40*(3), 496–501. https://doi.org/10.1016/j.jglr.2014.04.004

Kemp, A. L. W., Dell, C. I., & Harper, N. S. (1978). Sedimentation Rates and a Sediment Budget for Lake Superior. *Journal of Great Lakes Research*, *4*(3–4), 276–287. https://doi.org/10.1016/S0380-1330(78)72198-2

Klump, J. V., Paddock, R., Remsen, C. C., Fitzgerald, S., Boraas, M., & Anderson, P. (1989). Variations in Sediment Accumulation Rates and the Flux of Labile Organic Matter in Eastern Lake Superior Basins. *Journal of Great Lakes Research*, *15*(1), 104–122. https://doi.org/10.1016/S0380-1330(89)71465-9

Lafrancois, B., & Reinl, K. L. (2024). Lake Superior cyanobacterial bloom reports, 2012 - present. In *Environmental Data Initiative*. EDI Data Portal.

Leavitt, P. R. (1993). A review of factors that regulate carotenoid and chlorophyll deposition and fossil pigment abundance. In *Journal of Paleolimnology* (Vol. 9, Issue 2, pp. 109–127). Kluwer Academic Publishers. https://doi.org/10.1007/BF00677513

Leavitt, P. R., & Hodgson, D. A. (2001). Sedimentary Pigments. In *Tracking Environmental Change Using Lake Sediments* (Vol. 3, pp. 295–325). Kluwer Academic.

Lenters, J. D. (2004). Trends in the lake superior water budget since 1948: A weakening seasonal cycle. *Journal of Great Lakes Research*, *30*(SUPPL. 1), 20–40. https://doi.org/10.1016/S0380-1330(04)70375-5

McKindles, K., Frenken, T., McKay, R. M. L., & Bullerjahn, G. S. (2020). Binational efforts addressing cyanobacterial harmful algal blooms in the great lakes. In *Handbook of Environmental Chemistry* (Vol. 101, pp. 109–133). Springer Science and Business Media Deutschland GmbH. https://doi.org/10.1007/698_2020_513

Meyers, P. A. (1994). Preservation of elemental and isotopic source identification of sedimentary organic matter. In *Chemical Geology* (Vol. 114).

Meyers, P. A. (2003). *Applications of organic geochemistry to paleolimnological reconstructions: a summary of examples from the Laurentian Great Lakes*. www.elsevier.com/locate/orggeochem

Meyers, P. A., & Ishiwatari, R. (1993). Lacustrine organic geochemistry - an overview of indicators of organic matter sources and diagenesis in lake sediments. In *Org. Geochem* (Vol. 20, Issue 7).

Munawar, M., & Munawar, I. F. (1978). Phytoplankton of Lake Superior 1973. *Journal of Great Lakes Research*, *4*(3–4), 415–442. https://doi.org/10.1016/S0380-1330(78)72212-4

National Oceanic and Atmospheric Administration (NOAA). (2010). *Great Lakes Regional Land Cover Change Report*. www.coast.noaa.gov.

O'Beirne, M. D., Werne, J. P., Hecky, R. E., Johnson, T. C., Katsev, S., & Reavie, E. D. (2017). Anthropogenic climate change has altered primary productivity in Lake Superior. *Nature Communications*, *8*(1), 15713. https://doi.org/10.1038/ncomms15713

O'Reilly, C. M., Sharma, S., Gray, D. K., Hampton, S. E., Read, J. S., Rowley, R. J., Schneider, P., Lenters, J. D., McIntyre, P. B., Kraemer, B. M., Weyhenmeyer, G. A., Straile, D., Dong, B., Adrian, R., Allan, M. G., Anneville, O., Arvola, L., Austin, J., Bailey, J. L., … Zhang, G. (2015). Rapid and highly variable warming of lake surface waters around the globe. *Geophysical Research Letters*, *42*(24). https://doi.org/10.1002/2015GL066235

Paerl, H. W. (1996). A comparison of cyanobacterial bloom dynamics in freshwater, estuarine and marine environments. In *Phycologia* (Vol. 35, Issue SUPPL., pp. 25–35). International Phycological Society. https://doi.org/10.2216/i0031-8884-35-6s-25.1

Paerl, H. W. (2017). Controlling cyanobacterial harmful blooms in freshwater ecosystems. *Microbial Biotechnology*, *10*(5), 1106–1110. https://doi.org/10.1111/1751-7915.12725

Panigrahi, S., Nydahl, A., Anton, P., & Wikner, J. (2013). Strong seasonal effect of moderate experimental warming on plankton respiration in a temperate estuarine plankton community. *Estuarine, Coastal and Shelf Science*, *135*, 269–279. https://doi.org/10.1016/j.ecss.2013.10.029

Perri, K. A., Sullivan, J. M., & Boyer, G. L. (2015). Harmful algal blooms in Sodus Bay, Lake Ontario: A comparison of nutrients, marina presence, and cyanobacterial toxins. *Journal of Great Lakes Research*, *41*(2), 326–337. https://doi.org/10.1016/j.jglr.2015.03.022

Picard, M., Wood, S. A., Pochon, X., Vandergoes, M. J., Reyes, L., Howarth, J. D., Hawes, I., & Puddick, J. (2022). Molecular and Pigment Analyses Provide Comparative Results When Reconstructing Historic Cyanobacterial Abundances from Lake Sediment Cores. *Microorganisms*, *10*(2). https://doi.org/10.3390/microorganisms10020279

Prahl, F. G., Bennett, J. T., & Carpenter, R. (1980). The early diagenesis of aliphatic hydrocarbons and organic matter in sedimentary particulates from Dabob Bay, Washington. In *Geochunica et Cosmochmucu Acra* (Vol. 44). Pergamon Press Lfd.

Quinn, F. H. (1992). Hydraulic Residence Times for the Laurentian Great Lakes. *Journal of Great Lakes Research*, *18*(1), 22–28. https://doi.org/10.1016/S0380-1330(92)71271-4

Reavie, E. D., Barbiero, R. P., Allinger, L. E., & Warren, G. J. (2014). Phytoplankton trends in the Great Lakes, 2001-2011. *Journal of Great Lakes Research*, *40*(3), 618–639. https://doi.org/10.1016/j.jglr.2014.04.013

Reavie, E. D., Cai, M., & Brown, T. N. (2018). Historical watershed stressors for the Laurentian Great Lakes Title: Historical watershed stressors for the Laurentian Great Lakes. *Geoscience Data*. https://doi.org/10.1002/gdj3.53

Reinl, K. L., Sterner, R. W., Lafrancois, B. M., & Brovold, S. (2020). Fluvial seeding of cyanobacterial blooms in oligotrophic Lake Superior. *Harmful Algae*, *100*. https://doi.org/10.1016/j.hal.2020.101941

Rigosi, A., Carey, C. C., Ibelings, B. W., & Brookes, J. D. (2014). The interaction between climate warming and eutrophication to promote cyanobacteria is dependent on trophic state and varies among taxa. *Limnology. Oceanography*, *59*(1), 99–114. https://doi.org/10.4319/lo.2014.59.01.0099

Robbins, J. A., & Ed, D. N. (1975). *Determination of recent sedimentation rates in Lake Michigan using Pb-210 ad Cs-137* (Vol. 39). Pergamon Press.

Rosenmeier, A. (2005). *Loss on Ignition (LOI) Procedure*. University of Pittsburg. https://sites.pitt.edu/~mabbott1/climate/mark/Teaching/GEOL_3931_PaleoAnalysis/0909LOIProtocol.pdf

Salmaso, N., Capelli, C., Shams, S., & Cerasino, L. (2015). Expansion of bloom-forming Dolichospermum lemmermannii (Nostocales, Cyanobacteria) to the deep lakes south of the Alps: Colonization patterns, driving forces and implications for water use. *Harmful Algae*, *50*, 76–87. https://doi.org/10.1016/j.hal.2015.09.008

Santisteban, J. I., Mediavilla, R., Lo´pezlo´pez-Pamo, E., Dabrio, C. J., Blanca, M., Zapata, R., Jose´gil, M., Garcıá, J., Castanõ, S., & Martı´nezmartı´nez-Alfaro, P. E. (2004). *Loss on ignition: a qualitative or quantitative method for organic matter and carbonate mineral content in sediments?*

Schlüter, L., David, G. S., Jørgensen, N. O. G., Podduturi, R., Tucci, A., Dias, A. S., & da Silva, R. J. (2018). Characterization of phytoplankton by pigment analysis and the detection of toxic cyanobacteria in reservoirs with aquaculture production. *Aquaculture Environment Interactions*, *10*, 35–48. https://doi.org/10.3354/AEI00256

Schnurrenberger, D., Russell, J., & Kelts, K. (2003). Classification of lacustrine sediments based on sedimentary components. In *Journal of Paleolimnology* (Vol. 29).

Schreiner, K. M., Bianchi, T. S., Eglinton, T. I., Allison, M. A., & Hanna, A. J. M. (2013). Sources of terrigenous inputs to surface sediments of the Colville River Delta and Simpson's Lagoon, Beaufort Sea, Alaska. *Journal of Geophysical Research: Biogeosciences*, *118*(2), 808–824. https://doi.org/10.1002/jgrg.20065

Shaw, R. G., & Etterson, J. R. (2012). Rapid climate change and the rate of adaptation: Insight from experimental quantitative genetics. In *New Phytologist* (Vol. 195, Issue 4, pp. 752–765). https://doi.org/10.1111/j.1469-8137.2012.04230.x

Sheik, C. S., Natwora, K. E., Alexson, E. E., Callaghan, J. D., Sailer, A., Schreiner, K. M., Steinman, B. A., Finkenbinder, M. S., Filstrup, C. T., & Bramburger, A. J. (2022). Dolichospermum blooms in Lake Superior: DNA-based approach provides insight to the past, present and future of blooms. *Journal of Great Lakes Research*, *48*(5), 1191–1205. https://doi.org/10.1016/j.jglr.2022.08.002

Smalley, C. C. (2013). *Radioisotope Geochronology of Lake Superior Sediments*.

State of the Great Lakes. (2022). *Technical Report Sub-Indicator: Land Cover*.

Sterner, R. W., Anagnostou, E., Brovold, S., Bullerjahn, G. S., Finlay, J. C., Kumar, S., McKay, M. L., & Sherrell, R. M. (2007). Increasing stoichiometric imbalance in North America's largest lake: Nitrification in Lake Superior. *Geophysical Research Letters*, *34*(10). https://doi.org/10.1029/2006GL028861

Sterner, R. W., Reinl, K. L., Lafrancois, B. M., Brovold, S., & Miller, T. R. (2020). A first assessment of cyanobacterial blooms in oligotrophic Lake Superior. *Limnol. Oceanogr*, *65*, 2984–2998. https://doi.org/10.1002/lno.11569

Streli, C., Wobrauschek, P., & Kregsamer, P. (1999). *X-Ray Fluorescence Spectroscopy, Applications*.

The Nature Conservancy. (2005). *A Practitioner's Guide to Freshwater Biodiversity Conservation* (N. Silk & K. Ciruna, Eds.). The Nature Conservancy.

Tóth, T. N., Chukhutsina, V., Domonkos, I., Knoppová, J., Komenda, J., Kis, M., Lénárt, Z., Garab, G., Kovács, L., Gombos, Z., & Van Amerongen, H. (2015). Carotenoids are essential for the assembly of cyanobacterial photosynthetic complexes. *Biochimica et Biophysica Acta - Bioenergetics*, *1847*(10), 1153–1165. https://doi.org/10.1016/j.bbabio.2015.05.020

Trees, C. C., Clark, D. K., Bidigare, R. R., Ondrusek, M. E., & Mueller, J. L. (2000). Accessory pigments versus chlorophyll a concentrations within the euphoric zone: A ubiquitous relationship. *Limnology and Oceanography*, *45*(5), 1130–1143. https://doi.org/10.4319/lo.2000.45.5.1130

Tromas, N., Fortin, N., Bedrani, L., Terrat, Y., Cardoso, P., Bird, D., Greer, C. W., & Shapiro, B. J. (2017). Characterising and predicting cyanobacterial blooms in an 8-year amplicon sequencing time course. *The ISME Journal*, *11*(8), 1746–1763. https://doi.org/10.1038/ismej.2017.58

Vallentyne, J. R. (1957). Carotenoids in a 20,000-year-old sediment from Searles Lake, California. *Archives of Biochemistry and Biophysics*, *70*(1), 29–34. https://doi.org/10.1016/0003-9861(57)90076-0

Van Cleave, K., Lenters, J. D., Wang, J., & Verhamme, E. M. (2014). A regime shift in lake superior ice cover, Evaporation, And water temperature following the warm el niño winter of 1997–1998. *Limnology and Oceanography*, *59*(6), 1889–1898. https://doi.org/10.4319/lo.2014.59.6.1889

Van Leeuwe, M. A., Villerius, L. A., Roggeveld, J., Visser, R. J. W., & Stefels, J. (2006). An optimized method for automated analysis of algal pigments by HPLC. *Marine Chemistry*, *102*(3–4), 267–275. https://doi.org/10.1016/j.marchem.2006.05.003

Walsh, J., Wuebbles, D., Hayhoe, K., Kossin, J., Kunkel, K., Stephens, G., Thorne, P., Vose, R., Wehner, M., Willis, J., Anderson, D., Doney, S., Feely, R., Hennon, P., Kharin, V., Knutson, T., Landerer, F., Lenton, T., Kennedy, J., & Somerville, R. (2014). *Ch. 2: Our Changing Climate. Climate Change Impacts in the United States: The Third National Climate Assessment*. https://doi.org/10.7930/J0KW5CXT

Watts, C. D., & Maxwell, J. R. (1977). *Carotenoid diagenesis in a marine sediment* (Vol. 41). Pergamon Press. Pruned m Greal Bntam. https://doi.org/10.1016/0016-7037(77)90287-3

Whitton, B. A., & Potts, M. (2012). Introduction to the Cyanobacteria. In *Ecology of Cyanobacteria II* (pp. 1–13). Springer Netherlands. https://doi.org/10.1007/978-94-007-3855-3_1

Wilkinson, G. M., Walter, J. A., Buelo, C. D., & Pace, M. L. (2022). No evidence of widespread algal bloom intensification in hundreds of lakes. *Frontiers in Ecology and the Environment*, *20*(1), 16–21. https://doi.org/10.1002/fee.2421

Zhang, L., Zhao, Y., Hein-Griggs, D., Janes, T., Tucker, S., & Ciborowski, J. J. H. (2020). Climate change projections of temperature and precipitation for the great lakes basin using the PRECIS regional climate model. *Journal of Great Lakes Research*, *46*(2), 255–266. https://doi.org/10.1016/j.jglr.2020.01.013